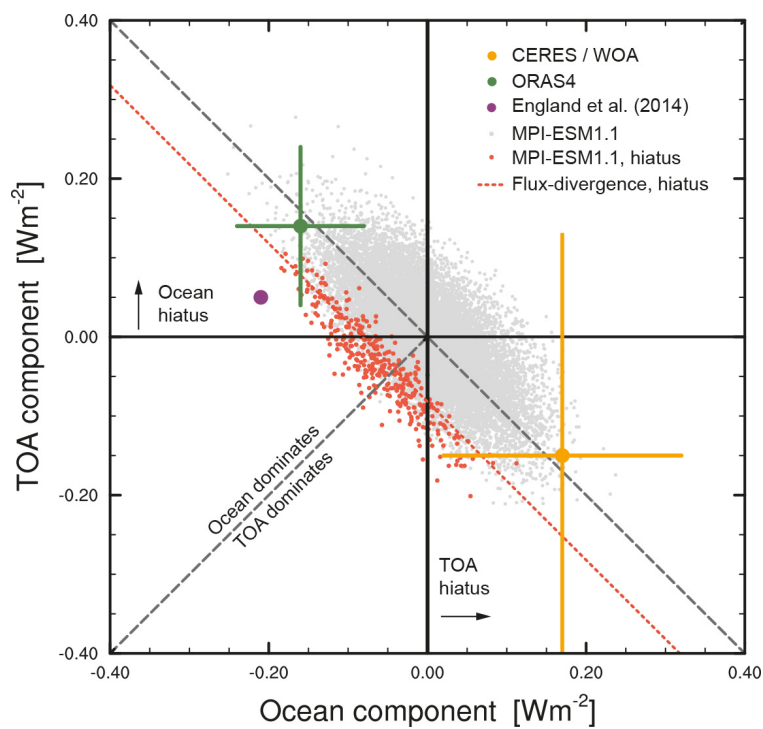


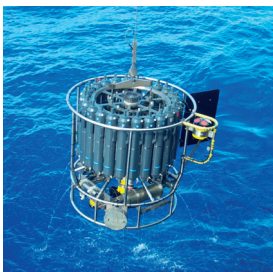


Conflicting Expectations of Global Surface Warming



Christopher Hedemann

Hamburg 2017



Hinweis

Die Berichte zur Erdsystemforschung werden vom Max-Planck-Institut für Meteorologie in Hamburg in unregelmäßiger Abfolge herausgegeben.

Sie enthalten wissenschaftliche und technische Beiträge, inklusive Dissertationen.

Die Beiträge geben nicht notwendigerweise die Auffassung des Instituts wieder.

Die "Berichte zur Erdsystemforschung" führen die vorherigen Reihen "Reports" und "Examensarbeiten" weiter.

Anschrift / Address

Max-Planck-Institut für Meteorologie
Bundesstrasse 53
20146 Hamburg
Deutschland

Tel./Phone: +49 (0)40 4 11 73 - 0
Fax: +49 (0)40 4 11 73 - 298

name.surname@mpimet.mpg.de
www.mpimet.mpg.de

Notice

The Reports on Earth System Science are published by the Max Planck Institute for Meteorology in Hamburg. They appear in irregular intervals.

They contain scientific and technical contributions, including Ph. D. theses.

The Reports do not necessarily reflect the opinion of the Institute.

The "Reports on Earth System Science" continue the former "Reports" and "Examensarbeiten" of the Max Planck Institute.

Layout

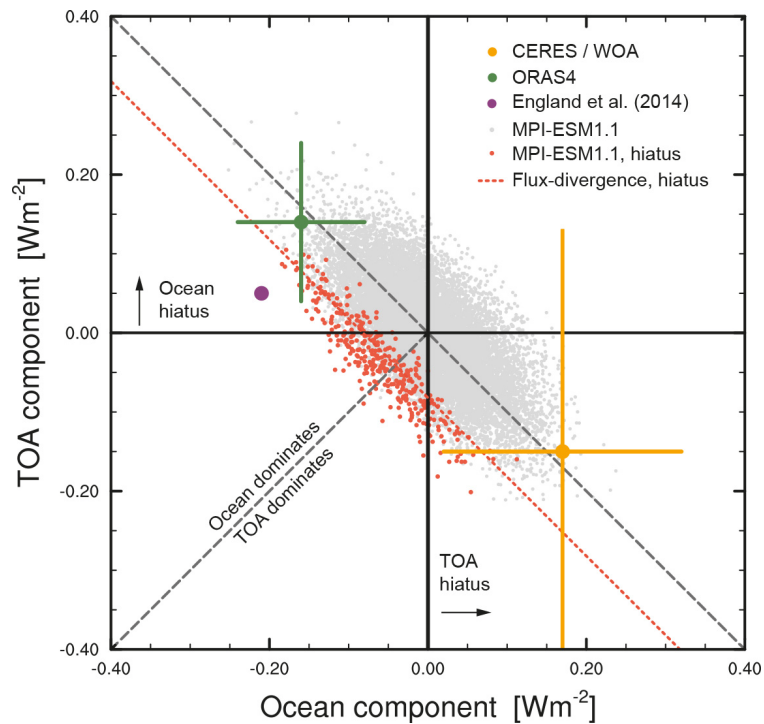
Bettina Diallo and Norbert P. Noreiks
Communication

Copyright

Photos below: ©MPI-M
Photos on the back from left to right:
Christian Klepp, Jochem Marotzke,
Christian Klepp, Clotilde Dubois,
Christian Klepp, Katsumasa Tanaka



Conflicting Expectations of Global Surface Warming



Dissertation with the aim of achieving a doctoral degree
at the Faculty of Mathematics, Informatics and Natural Sciences
Department of Earth Sciences of Universität Hamburg

submitted by

Christopher James Hedemann

Hamburg 2017

Christopher Hedemann

Max-Planck-Institut für Meteorologie
Bundesstrasse 53
20146 Hamburg

Tag der Disputation: 14.07.2017

Folgende Gutachter empfehlen die Annahme der Dissertation:

Prof. Dr. Jochem Marotzke
Prof. Dr. Johanna Baehr
Prof. Dr. Gabriele Hegerl

For Maree
1954-2013

ABSTRACT

In this dissertation I examine processes that cause Earth's surface warming to deviate from what we might expect. Using frameworks that incorporate regional and global energy exchange, I scrutinise previous theories for why these deviations occur.

The first part of this thesis examines the 1998–2012 surface-warming hiatus, in which the surface warmed more slowly than might be expected from examining model simulations or the long-term trend in observations. The preferred explanation for the hiatus is that internal variability in regional ocean heat uptake caused the surface warming to slow. However, observational analyses disagree about the ocean basin in which the definitive heat uptake occurred. Energy budgeting for the ocean surface layer, over a 100-member historical ensemble of simulations, reveals that variability in the top-of-atmosphere balance could also have caused the hiatus. Although previous studies have attributed the hiatus to fluctuations as large as 0.5 Wm^{-2} , I show that as little as 0.08 Wm^{-2} could be necessary. The sensitivity of these flux deviations to the observational dataset and to energy budget choices helps explain why previous studies conflict, and suggests that the origin of the recent hiatus may never be identified.

The second part of this thesis examines how climate sensitivity in model simulations grows with surface warming. The 'pattern effect' theory attributes this phenomenon to changing spatial patterns of warming, but previous accounts of the pattern effect disagree. I propose a new framework to unite theories about how regional processes affect climate sensitivity, and apply the framework to 1000-year simulations with a coupled climate model, exposed to abrupt CO_2 increases up to sixteen-times pre-industrial concentrations. Applying the assumptions of previous studies to the model output leads to misdiagnosis of radiative forcing. Furthermore, the fact that past studies find different critical regions for the pattern effect may result from their assumptions and not divergent model behaviour. The pattern effect in the four simulations depends partly on the time elapsed since the forcing increase, and not merely the surface temperature, suggesting that current observations could underestimate climate sensitivity.

Both parts of this thesis represent areas of tension in climate science between different perspectives and tools. Normative understandings may presume the superiority of empirical measurement over model simulation, or the superiority of the detailed regional perspective over the general global perspective. However, the findings presented in this thesis serve to highlight the pitfalls of restricting ourselves to one tool or view in the endeavour to understand climate.

ZUSAMMENFASSUNG

In dieser Dissertation untersuche ich, warum die tatsächliche Erwärmung der globalen Oberfläche von der zu erwartenden abweicht. Anhand von Ansätzen, die sowohl den regionalen wie auch den globalen Energieaustausch berücksichtigen, untersuche ich bisherige Erklärungen für diese Unregelmäßigkeiten in der Erwärmung.

Der erste Teil der Dissertation untersucht den Hiatus der Oberflächenerwärmung zwischen 1998 und 2012, ein Zeitraum, in dem die Oberfläche sich langsamer erwärmte als durch die Berücksichtigung von Modellsimulationen oder des beobachteten Langfristtrends zu vermuten wäre. Die gängigste Erklärung des Hiatus geht davon aus, dass die geringere Oberflächenerwärmung von der internen Variabilität der regionalen Wärmeaufnahme des Ozeans verursacht wurde. Jedoch stimmen Analysen der Beobachtungen über die ausschlaggebende Region des Ozeans nicht überein. Hier wird anhand eines Energiehaushalts der oberflächennahen Ozeanschichten und eines Ensembles von 100 gekoppelten Klimamodellsimulationen gezeigt, dass der Hiatus ebenfalls durch die Variabilität der Energiebilanz am Oberrand der Atmosphäre hätte verursacht werden können. Obwohl frühere Studien dem Hiatus Fluktuationen bis zu 0.5 Wm^{-2} zugeschrieben haben, zeige ich, dass bereits eine Abweichung von 0.08 Wm^{-2} einen Hiatus verursachen könnte. Die Sensibilität dieser Flussabweichungen gegenüber dem benutzten Datensatz und den Annahmen bezüglich des Energiehaushalts legt nahe, dass der Ursprung des Hiatus wohl niemals bestimmt werden kann.

Der zweite Teil der Ausarbeitung analysiert, wie die Klimasensitivität von Modellsimulationen mit der Erderwärmung steigt. Die Theorie des ‚Mustereffekts‘ führt dieses Phänomen auf sich verändernde räumliche Muster der Erwärmung zurück. Allerdings sind sich bisherige Erklärungsansätze des Mustereffekts nicht einig. Ich schlage einen neuen Theorierahmen vor, um verschiedene Erklärungen für die Auswirkungen der regionalen Ebene auf die Klimasensitivität miteinander in Einklang zu bringen. Der Theorierahmen wird auf vier 1000-jährige Simulationen angewandt, die einem abrupten Anstieg an CO_2 Konzentration ausgesetzt werden, die bis zu 16-fach den prä-industriellen Stand übersteigt. Wenn die Annahmen früherer Studien auf die Modellergebnisse angewandt werden, kommt es zu einer Fehleinschätzung des externen Antriebs. Ferner kann die Auswahl unterschiedlicher Regionen, denen die Studien eine entscheidende Rolle in der Änderung der Klimasensitivität beimessen, durch die eigenen Annahmen und nicht durch abweichende Modellergebnisse erklärt werden. Da der Mustereffekt in den vier Simulationen teilweise vom Zeitraum seit Beginn des Antriebanstiegs und nicht nur von

der Temperatur abhängig ist, könnten die Beobachtungen des heutigen Klimas die Klimasensitivität unterschätzen.

Die beiden in der Dissertation untersuchten Aspekte stellen Bereiche der Klimawissenschaft dar, in welchen Unstimmigkeiten zwischen verschiedenen Sichtweisen und Methoden bestehen. Ein normatives Verständnis könnte die Überlegenheit empirischer Messungen gegenüber Modellsimulationen annehmen oder die Überlegenheit der detailreichen regionalen Perspektive gegenüber der allgemeinen globalen. Gleichwohl unterstreichen die Ergebnisse dieser Arbeit, wie irreführend es für unser Verständnis des Klimas sein kann, sich auf eine Perspektive oder ein Werkzeug zu beschränken.

TEILVERÖFFENTLICHUNGEN DIESER DISSERTATION

Pre-published work related to this dissertation

Hedemann, Christopher, Thorsten Mauritsen, Johann Jungclaus and Jochem Marotzke (2017). "The subtle origins of surface-warming hiatuses". *Nature Climate Change* 7.5, pp. 336-339. doi:[10.1038/nclimate3274](https://doi.org/10.1038/nclimate3274)

ACKNOWLEDGMENTS

I could only write this dissertation because of the incredible support I have received from others. More important than ever has been the love and support of my witty, wise and wonderful family, Peter and Elise, who have always believed in me. Miriam González and Josiane Salameh: your friendship here at the coal face has been an indispensable source of strength and resilience.

Writing this thesis has meant becoming the scientist (and writer) who is capable of such a feat. Jochem Marotzke has been my mentor in that process and I am incredibly grateful for his unfailing support and guidance over the last four years. I also owe much to Johann Jungclaus and Thorsten Mauritsen for their invaluable supervision, and for smiling when ‘just a quick question’ inevitably turned into time-consuming discussions. I am also grateful to Johanna Baehr for lending her fresh sense of perspective and welcome wisdom in the crucial final stages.

I have received help in other ways from many people, because they are great at what they do. Thanks again to Elise and to Miriam for proof-reading parts of this thesis and for your valuable suggestions. The technical support at MPI-M is unparalleled, but Helmuth Haak deserves special thanks for his attentive assistance with all things model. Thank you to Antje Weitz, Cornelia Kampmann and Wiebke Böhm, for smoothing the way and for caring, to Bettina Diallo for graphical assistance, to Anne Patricia Wiedl, for making Hamburg’s grey skies brighter, Hans Figueroa for keeping me in form, and to the friendly team at Elbgold, for providing me with mental strength in shiny, white cups.

Other special people have been important lifelines for me over the last four years. Genevieve Mortimer, thank you for the much-needed laughs and much-needed dinners. Thank you also to my friends afar – especially Mareike Rehl, Haley Middler, Joanna Woods, Ross Neilson and Pam Christie – for bridging the distance and being there for me. To my partner Patrick, who shared my burden and kept me going: I am extraordinarily lucky to have you!

Finally, this dissertation is dedicated with utmost love to my mother Maree Hedemann, who inspired me and continues to inspire me. In many ways Mum, I wrote this for you.

CONTENTS

1	CONFLICTING EXPECTATIONS OF SURFACE WARMING	1
1.1	Introduction	1
1.2	The surface-warming hiatus	3
1.3	Climate sensitivity and the pattern effect	7
2	THE SUBTLE ORIGINS OF SURFACE-WARMING HIATUSES	13
2.1	Summary	13
2.2	Introduction	13
2.3	Hiatuses in the large ensemble	14
2.4	Energy budgeting for the surface layer	16
2.4.1	The flux-divergence combination	17
2.4.2	The surface-layer depth	20
2.5	The energetic origins of hiatuses in the large ensemble	21
2.5.1	How much flux-divergence causes a hiatus?	21
2.5.2	Which ocean regions can provide the flux-divergence?	21
2.6	The origin of the hiatus in observations	22
2.6.1	Constructing observation-based budgets	24
2.6.2	What the budgets imply	26
2.7	Resolving conflicts in previous studies	26
2.8	The true hiatus dilemma	28
3	HOW THE PATTERN EFFECT CHANGES CLIMATE SENSITIVITY	31
3.1	Summary	31
3.2	Introduction	31
3.3	Model integrations and diagnostics	34
3.4	Estimating the global feedback parameter	34
3.5	Isolating the components of the pattern effect	36
3.5.1	The temperature component	38
3.5.2	The feedback component	38
3.5.3	The combined pattern effect	39
3.6	A simple two-region example	42
3.7	Reconstructing the energy imbalance	44
3.8	The changing global feedback parameter	47
3.9	Discussion	52
3.9.1	Reconciling interpretations of the pattern effect	52
3.9.2	Time- and state-dependence of climate feedbacks	53
4	CONCLUSIONS	57
4.1	The surface-warming hiatus	57
4.2	Climate sensitivity and the pattern effect	58
4.3	Knowledge conflicts and knowledge production	59
4.3.1	The forest or the trees?	59
4.3.2	Fairy-tale or fact?	61

APPENDICES	65
A APPENDIX TO CHAPTER 1	67
B APPENDIX TO CHAPTER 2	69
B.1 Data availability	69
B.2 Extended Figures	69
C APPENDIX TO CHAPTER 3	73
C.1 Data availability	73
BIBLIOGRAPHY	75

LIST OF FIGURES

Figure 1.1	The surface-warming hiatus.	4
Figure 1.2	Estimates of climate sensitivity.	10
Figure 2.1	Distribution of 15-year trends in GMST in the 100-member ensemble.	15
Figure 2.2	The surface energy budget in the large ensemble.	17
Figure 2.3	Regression of ocean surface-layer heat content with flux-divergence.	18
Figure 2.4	Regression of global mean surface temperature (GMST) trends with flux-divergence.	19
Figure 2.5	Results from surface budgets determined by increasingly deeper definitions of the ocean surface layer.	20
Figure 2.6	Heat fluxes and their predictive power for GMST trends.	22
Figure 2.7	Example illustrating the energetic origin of a hiatus.	23
Figure 2.8	Hiatuses and their origins in models and observations.	27
Figure 2.9	Energy budgets that only consider upper-level ocean heat content fail to predict GMST variability.	28
Figure 2.10	Variability in top-of-atmosphere (TOA) fluxes in observations, reconstructions and MPI-ESM1.1.	30
Figure 3.1	The non-linear relationship between energy imbalance and surface warming.	37
Figure 3.2	A two-region example of the pattern effect.	40
Figure 3.3	Components of the pattern effect in the two-region example.	41
Figure 3.4	Components of the pattern effect misrepresent the initial response to forcing.	44
Figure 3.5	Components of the pattern effect misdiagnose the effective climate feedback parameter.	46
Figure 3.6	Temperature component diagnoses near-constant global feedback parameter.	48
Figure 3.7	Regional contributions to the pattern effect.	49
Figure 3.8	Individual radiative feedbacks in 16xCO ₂ .	50
Figure 3.9	Initial rapid warming in the upper troposphere causes negative feedbacks over the Southern Ocean.	51

Figure 3.10	The changing global feedback parameter with time and with surface warming.	52
Figure A.1	FAQ3.1, IPCC Assessment Report 4	67
Figure B.1	Poor correlation between ensemble anomalies in GMST trends and heat-content trends.	70
Figure B.2	Both TOA-only hiatuses and ocean-only hiatuses can present sub-surface warming.	71

LIST OF TABLES

Table 2.1	Observational estimates for the ocean component over 2000–2010 in Wm^{-2} .	25
Table 2.2	Observational estimates for TOA component over 2000–2010 in Wm^{-2} .	25
Table B.1	Number of hiatuses sorted by origin and start-year in the 100-member historical ensemble.	72

ACRONYMS

CMIP5	Coupled Model Intercomparison Project Phase 5
ECS	equilibrium climate sensitivity
GMST	global mean surface temperature
IPCC	Intergovernmental Panel on Climate Change
IPO	Interdecadal Pacific Oscillation
PRP	partial radiative perturbation
SST	sea surface temperature
TOA	top-of-atmosphere

CONFLICTING EXPECTATIONS OF SURFACE WARMING

We have no right to measure these [Joule-Thomson] heating and cooling effects on any scale of temperature, as we have not yet formed a thermometric scale.

— William Thomson, "Heat", 1880; cited in Chang (2008)

1.1 INTRODUCTION

This dissertation is about the surface temperature of the Earth and its evolution under global warming. In particular, I consider processes that change that evolution, bringing the surface temperature away from the path we might expect. Surface temperature can deviate from our expectations only temporarily, such as during the 1998–2012 surface-warming hiatus. But it can also deviate systematically, when changing radiative feedbacks alter the very relationship between forcing from CO₂ emissions and the amount that the surface must warm to compensate.

Our knowledge of surface temperature on Earth is shaped primarily by two tools: observations and computational simulations of climate. These tools represent the culmination of centuries of hard-won scientific advances. Consider the above quote from William Thomson, perhaps better known as Lord Kelvin. Even in the mid- to late nineteenth century, when humankind's influence on the Earth's surface was already under way, the theories of what temperature is and how it should be measured were still not settled (Chang 2008). We have since developed a vast observational network measuring temperature on land, in the ocean and circling the planet in space. We now have the computational power to simulate the temperature in past climates and to make projections of how it might behave in the future.

Despite these formidable advances, we must remain conscious of the shortcomings of our tools when we interpret their output. The observational network for surface temperature is full of gaps, especially in critical areas where warming proceeds faster than average (Cowtan and Way 2014). In the areas we do observe, there are biases related to location and our methods of measurement (Karl et al. 2015; Williams et al. 2012). Surface temperature can be simulated without these measurement issues by climate models, but models systematically misrepresent observable large-scale features of climate (for example, Li and Xie 2014; Mueller and Seneviratne 2014; Siongco et al. 2014; Wang et al. 2014). Furthermore, these two tools are not as independent of each

*Observations versus
simulations*

other as we sometimes imagine: atmospheric models help fill gaps in observational data (Dee et al. 2014), while many models are ‘tuned’ to match certain aspects of observed climate (Mauritsen et al. 2012).

However, it can be particularly fruitful for science when observations and models conflict. A conflict creates dissonance in trusted assumptions. It creates a critical space in which we are forced to scrutinise the limits of our tools and, perhaps more importantly, our interpretation of them.

In this dissertation I examine two such conflicts. The first conflict occurred when the observed surface temperature increased more slowly over the period 1998–2012 than most models simulated. This event has come to be known as the surface-warming hiatus. The uncertainty created by the hiatus was exploited by those seeking to spread doubt about the science of global warming, and placed climate scientists in an uncomfortable position (Lewandowsky et al. 2015). The hiatus is now attributed largely to internal variability and not to any systematic conflict between models and observations. However, the search for the origin of that internal variability is ongoing.

*The
surface-warming
hiatus*

The second, ongoing conflict is the difference between simulated and observed estimates of Earth’s climate sensitivity. Climate sensitivity describes the long-term surface warming response to increases in atmospheric CO₂. It is therefore of critical importance for negotiating the appropriate response to climate change. Models and proxies of past climate suggest that recent observations could underestimate the climate sensitivity. Unlike the hiatus, where the observations represent the ‘true’ behaviour of the surface temperature, the superiority of observations or model simulations in determining climate sensitivity is more ambiguous. The models and proxies suggest that climate sensitivity is not constant but could change in the future. Observations of the current climate would not be able to predict such behaviour.

*A changing climate
sensitivity*

In spaces of conflict between climate models and observations, our interpretation of the outputs from these tools can be influenced by our perspective. For example, we might choose to adopt a regional or a global perspective. Global behaviour is simply the sum of regional behaviour, and yet the global perspective can provide simplicity and oversight that the regional cannot. On the other hand, the regional perspective can provide physical insights that are difficult to obtain from the global perspective. Each perspective disposes us to favour one particular explanation of the climate over others.

*Regional versus
global perspectives*

A regional perspective has been adopted by those searching for drivers of the internal variability during the hiatus. The consensus explanation is that surface warming was slowed by wind-driven mixing in the Pacific Ocean. In Chapter 2, I will show how a return to the global perspective affords insights into our interpretation of observa-

tions of this period – and into internal variability more generally – that the regional perspective has obscured.

The regional perspective informs recent research into climate sensitivity, which breaks with the traditional global perspective by examining how spatial patterns of warming might influence global behaviour. But studies examining the regional warming patterns come to different conclusions about their global effect. In Chapter 3, I develop a framework to better understand studies that use the regional perspective and their differing findings, and I suggest implications for how we can position simulated and observed climate sensitivity estimates in relation to one another.

In the final Chapter, I summarise my results and integrate my findings into a wider scientific context. I consider how the movement between regional and global perspectives can shape our view of climate phenomena. I also consider the nature of conflicts between observations and climate models, and reflect on what the conflicts in this study can tell us about the ‘epistemic status’ of these tools.

First of all, however, I will explore the background of the two conflicts in more detail and derive the motivating research questions for the work that follows.

1.2 THE SURFACE-WARMING HIATUS

From around 1998 to 2012, the rise in global mean surface temperature appeared to stall (see [Figure 1.1](#)). The surface did not actually stop warming, but the warming measured by global observations of surface temperature slowed in comparison to long-term warming, producing a gap of around -0.07 °C per decade (Flato et al. 2013). The gap between the observed surface-warming trend and the trend simulated by models was even larger. The multi-model ensemble mean of the Coupled Model Intercomparison Project Phase 5 (CMIP5) suggested surface warming 2.5 times faster than the observed warming, a gap of -0.17 °C per decade (Flato et al. 2013).

The climate science community came under fire from their detractors, who used the hiatus to question the science behind global warming (Lewandowsky et al. 2015). Some misplaced claims from climate scientists exacerbated the confusion: in the Fourth Assessment Report of the Intergovernmental Panel on Climate Change (IPCC), a misleading figure intimated that surface warming would not slow down, but instead *accelerate* (see [Figure A.1](#)). The perceived threat to the science of global warming, and the open question of what had caused the slowdown, led to a flood of publications about the hiatus.

Some scientists claimed we needn’t look further than the observations themselves. The recent warming had been underestimated due to the methods by which some data products account for unobserved regions (Cowtan and Way 2014) and by changes in the methods used

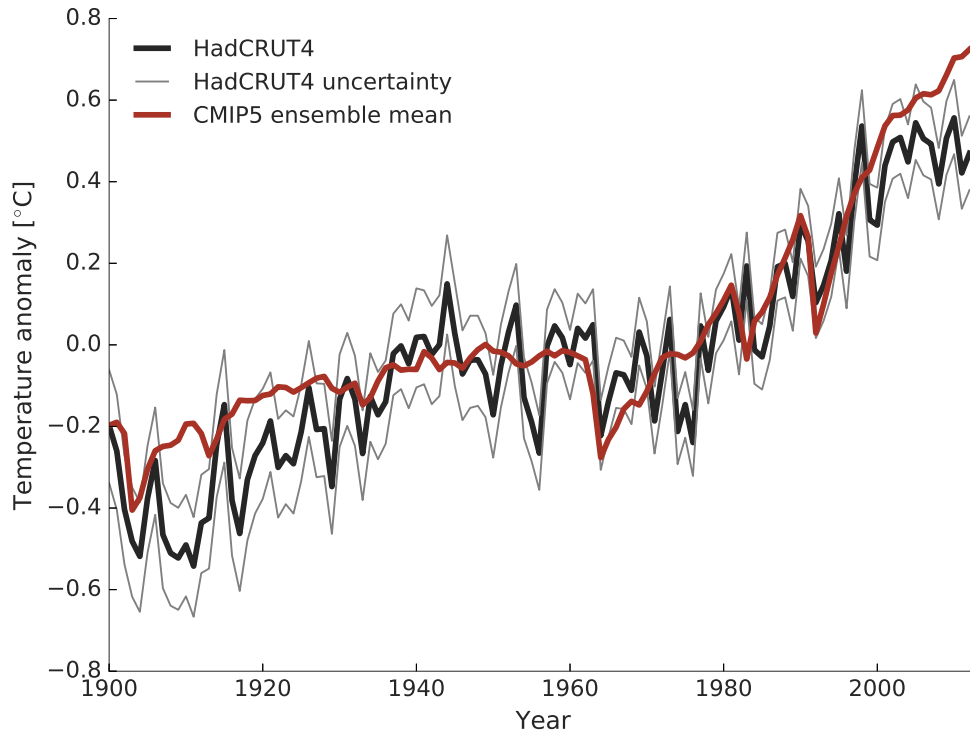


Figure 1.1: THE SURFACE-WARMING HIATUS. Anomalies in global mean surface temperature are shown, relative to the period 1961–1990. The CMIP5 ensemble mean (of 36 models encompassing 114 realisations; Taylor et al. 2012) is shown in red; the observations according to HadCRUT4 (Morice et al. 2012) are shown in black, with thin lines representing the 95% confidence interval for uncertainty in observations. The ‘surface-warming hiatus’ describes the period from 1998–2012 when the warming trend appears to slow and diverge from the model mean, although periods in which warming progresses faster or slower than the model mean occur multiple times over the twentieth century (see Marotzke and Forster 2015).

to observe sea surface temperatures (Karl et al. 2015). Whether these bias corrections explain the gap between the 1998–2012 trend and the long-term trend or not depends on how the long-term trend is defined (Fyfe et al. 2016; cf Karl et al. 2015). However, the corrections certainly cannot explain the larger gap between the models and observations (Fyfe et al. 2016).

Assuming a slowdown had occurred, other scientists suggested that decreases in radiative forcing were the cause. These were forcing decreases that had not been considered in CMIP5 models. A series of small volcanic eruptions over the 2000s may have contributed between -0.1 and -0.2 W m^{-2} (Ridley et al. 2014; Solomon et al. 2011) to forcing, almost enough to counteract the approximately 0.27 W m^{-2} per decade from increasing CO_2 concentrations. The resulting impact on surface temperature was claimed to be between $0.02 \text{ }^\circ\text{C}$ (Haywood et al. 2014) and 0.07°C (Fyfe et al. 2013; Solomon et al. 2011), perhaps enough to account for the deviation from the long-term trend, but not the gap between models and observations. However, if one includes the decreased irradiance from the solar-cycle minimum (Kopp and Lean 2011), possibly around -0.1 W m^{-2} (Trenberth and Fasullo 2013), and other small forcing adjustments, then even the gap between models and observations can be explained (Schmidt et al. 2014), or so it was suggested.

One group tested this hypothesis. They performed 60 simulations with a CMIP5 model, half with updated forcing and half with the old forcing, and found that there was no distinguishable difference in temperature trends over 1998–2012 (Thorne et al. 2015). Forcing differences across CMIP5 models have relatively little influence on the differences in their 15-year GMST trends; it takes longer, perhaps up to 60 years, for forcing to cause systematic differences in GMST trends amongst the models (Marotzke and Forster 2015). In any case, despite their oversight of small volcanoes and the solar minimum, the CMIP5 models actually did not systemically overestimate the forcing in observations (Flato et al. 2013): some models did, but many didn't. So while a forced contribution cannot be excluded, it is not sufficient to explain the hiatus. This suggests that internal variability had a significant role to play (Flato et al. 2013; Guemas et al. 2013; Marotzke and Forster 2015; Thorne et al. 2015).

Internal variability describes quasi-random fluctuations in the climate: unforced variations due to the chaotic nature of the system that may channel into particular modes like the El Niño-Southern Oscillation. In models, decadal internal variability is thought to be responsible for fluctuations in the Earth's energy budget of around 0.1 W m^{-2} and to account for trends in GMST as large as $0.3 \text{ }^\circ\text{C}$ per decade (Palmer and McNeill 2014). Because of internal variability's quasi-random nature, models are not expected to be able to capture its influence during the hiatus, unless they are initialised from a re-

cent climate state (Guemas et al. 2013). This would explain the gap between observations and the CMIP5 ensemble mean. Single ensemble members or the observations represent just one realisation of climate that can deviate on decadal timescales from the forced trend, but taking the mean of many members cancels this variability. It would not be the first time in the historical period that observed decadal trends in GMST had wandered away from the CMIP5 ensemble mean (Marotzke and Forster 2015).

A particular form of internal variability known as the Interdecadal Pacific Oscillation (IPO) has become important to the hiatus narrative. Whenever the IPO turns negative, sea surface temperatures of the tropical Pacific become cooler-than-average for a decade or longer (Power et al. 1999). The pattern associated with the IPO is thought to have had a key role in producing the variability observed during the hiatus (Dai et al. 2015; England et al. 2014; Kosaka and Xie 2013; Meehl et al. 2011, 2013) and events similar to the hiatus in the past (Maher et al. 2014). One study in particular showed how cooling in a relatively small area of the Pacific, accounting for less than 10% of the global surface, could influence the global evolution of GMST, bringing it in line with observations (Kosaka and Xie 2013). A further study suggested a plausible explanation for the Pacific cooling, linking it to mixing caused by the exceptional winds observed over this region during the hiatus (England et al. 2014). Discoveries of large heat uptake in the Pacific (Liu et al. 2016; Nieves et al. 2015) appeared to complete the physical picture, and helped form the consensus among many scientists that the hiatus was caused by heat uptake in the Pacific Ocean.

Whereas the arguments about forcing rely on a global perspective, the internal variability explanation has intuitively suggested a regional perspective, because of the spatial signatures that modes like the IPO imprint on the surface. But the regional perspective has not clinched the internal variability debate at all. The focus on the Pacific has sidelined other explanations, including the fact that cooling over the Eurasian land mass was important (Cohen et al. 2012; Li et al. 2015). And while the Pacific variability argument stresses the role of ocean heat uptake, there has been only minimal and tentative discussion of the role that variability in energy entering the surface from the top-of-atmosphere (TOA) might play (Smith et al. 2015; Zhou et al. 2016). In some cases the TOA variability has been explicitly dismissed as too small to explain the hiatus (Brown et al. 2014; Trenberth and Fasullo 2013). Even amongst those who subscribe to the explanation of ocean heat uptake, the regional perspective has led to the discovery of a bewildering array of ocean basins, each of which could individually have caused the hiatus. The ocean basins that were declared responsible for the heat uptake include: the Pacific (England et al. 2014; Nieves et al. 2015), the Indian Ocean (Lee et al. 2015), the Atlantic (Katsman

et al. 2011), the Atlantic and the Southern Ocean (Chen and Tung 2014), and other different combinations of these basins (Drijfhout et al. 2014; Guemas et al. 2013; Liu et al. 2016; Meehl et al. 2011, 2013).

In Chapter 2, I will show how returning to the global perspective helps explain these divergent results and allows for alternative explanations. I consider the following research questions:

1. a) **Why are there multiple and conflicting accounts that regional ocean heat uptake caused the 1998–2012 hiatus?**
- b) **What can we learn from the hiatus about the origins of decadal internal variability in global mean surface temperature (GMST)?**

Motivating research questions for Chapter 2

Chapter 2 is modelled on work that I have recently published with co-authors (Hedemann et al. 2017), but which has been re-structured and adapted to fit the format of this dissertation.

When the GMST experienced its small deviation off-course, the total energy gained by the Earth due to global warming hardly changed. Some studies therefore considered the Earth's energy imbalance a more robust measurement of global warming (Schuckmann et al. 2016; Yan et al. 2016). While the energy imbalance may be more robust, the surface temperature more tangibly influences our lives, and many important climate variables for life on the surface scale linearly with the GMST (Giorgetta et al. 2013; Huntingford and Cox 2000). In any case, measuring global warming via the energy balance could present difficulties in the future, since the simple relationship between the energy imbalance and surface temperature may eventually change. This phenomenon is the topic I turn to next.

1.3 CLIMATE SENSITIVITY AND THE PATTERN EFFECT

For more than one hundred years, scientists have attempted to use the Earth's energy imbalance to estimate the change in temperature that might result from increased CO₂ concentrations (Arrhenius 1896). In the 1960s, with the development of the first numerical models of radiative convective equilibrium, it was proposed that the outgoing radiation might not develop with the fourth-power of temperature, as expected from the Stefan-Boltzmann Law. Instead, the makeup of the atmosphere produces a relationship between the energy imbalance and surface temperature that is near linear (Manabe and Wetherald 1967).

Using the roughly linear relationship between the global energy imbalance and the global mean surface temperature, Gregory established a regression method to predict the final state of equilibrium warming after an abrupt doubling in atmospheric CO₂ concentration (Gregory et al. 2004). According to the method, one plots the global imbalance in energy at the top of the Earth's atmosphere (R) against

the change in global mean surface temperature (T) after an initial forcing (F), and performs a linear regression to imply T at the horizontal intercept, $R = 0$.

$$R = F + \lambda T, \quad (1.1)$$

In this formulation, λ is less than zero and represents the global feedback parameter. If the initial forcing is equivalent to an abrupt doubling of CO_2 , the implied equilibrium temperature is known as the equilibrium climate sensitivity (ECS), which has become a powerful yardstick for comparing the behaviour of global warming in different models of climate.

Observations of the Earth's imbalance and temperature during the instrumental record suggest that a doubling of CO_2 could lead to an ECS of around 2°C (Otto et al. 2013). However, the uncertainties in the temperature record and estimates of forcing mean that values of ECS spanning 1.2 – 3.9°C are likely (Otto et al. 2013). Recent observational studies continue to tweak the central observed value of 2°C , either by accounting for volcanic activity (1.6°C ; Lewis and Curry 2015) or by adjusting for the efficacy of different types of forcing (2.6°C ; Marvel et al. 2015).

Continuing improvements in the accuracy of observations and their interpretation are surely crucial for narrowing our estimates of ECS, but our expectations must also be directed by evidence from climate models, which can paint a very different picture. The multi-model mean ECS for the CMIP5 models is higher than suggested by observations: 3.2°C with a range of 2.1 – 4.7°C (Flato et al. 2013). More importantly, many of the CMIP5 models display a tendency for the implied ECS to increase over time or with warming, with some attaining an ECS of as much as 5 – 6°C (Andrews et al. 2015). The possibility that the ECS is not constant, but can evolve, places the observational estimates in a different light: narrowing the range of ECS that we can observe currently would not necessarily be a strong constraint on future warming estimates. Bloch-Johnson et al. (2015) considered the effect of a changing ECS on observational estimates by including a T^2 term in Equation 1.1. While the lower range of the observational estimates hardly changed, the probability that the true ECS fell into the higher range increased drastically. Some question whether we can trust this simulated behaviour (Lewis and Curry 2015), since a changing ECS might simply be an artefact of model physics and not relate to the real world.

Reconstructions of the geological past suggest otherwise. During the warm, early period of the Pliocene (5.3 to 2.8 Myr ago) the climate sensitivity could have been higher than 7°C according to one study (Royer 2016), although there are large uncertainties inherent in reconstructions of past climate (Huber and Caballero 2011). Approaches combining proxy data with model reconstructions suggest

a much more modest range for the Pliocene (1.9–3.7°C; Hargreaves and Annan 2016). But, as shown in Figure 1.2, higher values for ECS are thought to have been obtained 55 million years ago during the Paleocene-Eocene Thermal Maximum (3.7–6.5 K; Shaffer et al. 2016). Most proxy or modelling-based studies of the past agree that climate sensitivity appears to increase in warmer climates (Caballero and Huber 2013; Hargreaves and Annan 2016; Royer 2016; Shaffer et al. 2016).

There are good physical reasons why the ECS might change in warmer climates: it could be state-dependent. Radiative feedbacks, which determine λ in Equation 1.1, are thought to change with climate state on different timescales (Rohling et al. 2012). In warmer climates, feedback changes could be related to a combination of water vapour and cloud feedbacks over the tropics (Caballero and Huber 2013; Hansen et al. 2005; Meraner et al. 2013; Popp et al. 2016; Shaffer et al. 2016). Climate sensitivity could be higher in colder climates too, due to changes in high-latitude albedo feedbacks (Kutzbach et al. 2013).

The changes in feedbacks need not only be state-dependent. Many climate models produce noticeable changes in the implied climate sensitivity within several decades of an abrupt increase in forcing (Andrews et al. 2015; Block and Mauritsen 2013; Geoffroy et al. 2013b; Gregory et al. 2004; Held et al. 2010; Rugenstein et al. 2016a; Senior and Mitchell 2000; Williams et al. 2008). These relatively rapid changes have led to the suggestion that the ECS is also time-dependent, depending not necessarily on the GMST change but on the time elapsed since the forcing has been applied (see Figure 1.2). However, the modelling studies do not usually cover timescales longer than several hundred years, or extreme states of climate, such as those expected during the Paleocene-Eocene Thermal Maximum, so the issues of state-dependence or time-dependence may be related to the forcing strength and the timescale.

Whether state-dependent or time-dependent, the changing relationship between energy imbalance and surface warming has posed a problem for the global perspective described by Equation 1.1. There have been several suggestions for how the changing relationship might be accounted for. Williams et al. (2008) suggested an adjustment to the forcing term (F) is required, since fast adjustments in cloud cover and other climate properties occur in response to increased CO₂ that are not related to GMST change. But even after accounting for these rapid changes, there are still apparent changes in feedbacks that occur with warming (Block and Mauritsen 2013).

The idea of an ocean heat uptake efficacy or efficiency factor has also been proposed, which multiplies the imbalance term R in Equation 1.1 and can change with time (Geoffroy et al. 2013b; Held et al. 2010; Watanabe et al. 2013; Winton et al. 2010). The factor is intended to mimic the slow response timescale of deep ocean heat uptake to

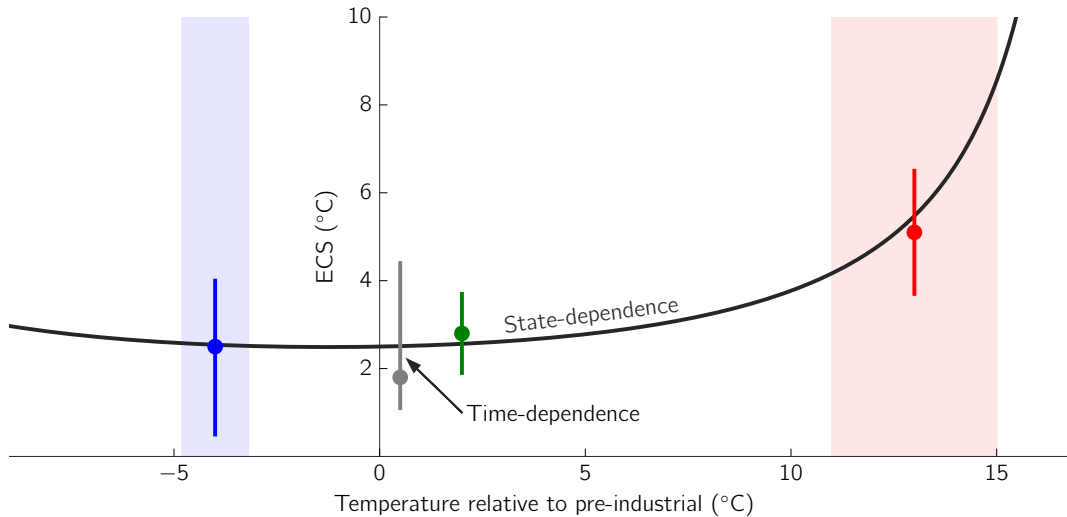


Figure 1.2: ESTIMATES OF EQUILIBRIUM CLIMATE SENSITIVITY (ECS) IN PROXIES AND OBSERVATIONS. Estimates of ECS over Earth’s history are shown with their uncertainties, including: the Paleocene-Eocene Thermal Maximum (red; Shaffer et al. 2016), the Pliocene (green; Hargreaves and Anan 2016), and the last glacial maximum (blue; Hargreaves et al. 2012). The grey dot represents an estimate and uncertainty bars for the observational record (Mauritsen and Pincus 2017). The black line represents a quadratic relationship between ECS and temperature, and is shown for illustrative purposes only. Time-dependence could cause a temporary depression in the value of ECS for a particular state of temperature. Figure provided courtesy of Thorsten Mauritsen.

forcing and its influence on the relationship between the imbalance and surface temperature. Geoffroy et al. (2013b) justified the efficacy concept by explaining that deep ocean heat uptake affects the spatial pattern of warming at the surface, and therefore may eventually excite different local feedbacks than the initial, faster response to forcing. The concept of efficacy, although couched in a global formulation, had already begun the move towards accounting for regional behaviour.

A proper adoption of the regional perspective was suggested by Armour et al. (2013). Their study claimed that the changing non-linear relationship between imbalance and warming can be explained if we incorporate regional warming information. The spatial pattern of warming controls apparent changes to the global feedback by differently weighting regional feedbacks, which can be constant. Several studies have questioned this proposition by demonstrating the regional feedbacks do change (Block and Mauritsen 2013; Rose and Rayborn 2016; Rose et al. 2014; Rugenstein et al. 2016a), although the changes may still be connected to the warming pattern (Andrews et al. 2015). The idea that the surface warming pattern drives changes in the ECS has since been coined ‘the pattern effect’. However, this single term belies the variety of definitions of the pattern effect and how it works at a regional level.

In Chapter 3, I consider the different formulations of the pattern effect in previous studies. By introducing a new framework for understanding the regional perspective, I show how the varying results of previous modelling studies may be attributed to their definition of the pattern effect and not to divergent model behaviour alone. By examining the pattern effect under multiple forcing strengths and on the millennial timescale, I also return to the ideas of time-dependence and state-dependence and suggest implications for how we might position observed estimates of the ECS in relation to estimates from model simulations and proxies. In Chapter 3, I ask:

2. a) **How do differences between existing formulations of the pattern effect influence the interpretation of changes to equilibrium climate sensitivity (ECS)?**
- b) **How does a regional framework help us position simulated estimates of ECS in relation to observed estimates?**

*Motivating research
questions for
Chapter 3*

Before we dive into the murky realms of future surface warming, let us first explore how surface warming proceeds today. In the following chapter, the surface-warming hiatus provides an opportunity to grapple with the contemporary relationship between the Earth's energy budget and its surface warming. The hiatus also helps us to understand the tension between observations and model simulations of climate, even for events that occur right before our eyes.

THE SUBTLE ORIGINS OF SURFACE-WARMING HIATUSES

2.1 SUMMARY

During the first decade of the 21st Century, the Earth's surface warmed more slowly than climate models simulated (Flato et al. 2013). This surface-warming hiatus is attributed by some studies to model errors in external forcing (Kopp and Lean 2011; Santer et al. 2014; Solomon et al. 2011), while others point to heat rearrangements in the ocean caused by internal variability (Balmaseda et al. 2013; Guemas et al. 2013; Katsman et al. 2011; Meehl et al. 2011, 2013; Watanabe et al. 2013), the timing of which cannot be predicted by the models (Flato et al. 2013). However, observational analyses disagree about which ocean region is responsible (Chen and Tung 2014; Drijfhout et al. 2014; England et al. 2014; Lee et al. 2015; Liu et al. 2016; Nieves et al. 2015). I show here that the hiatus could also have been caused by internal variability in the top-of-atmosphere energy imbalance. Energy budgeting for the ocean surface layer over a 100-member historical ensemble reveals that hiatuses are caused by energy-flux deviations as small as 0.08 Wm^{-2} , which can originate at the top of the atmosphere, in the ocean, or both. Budgeting with existing observations cannot constrain the origin of the recent hiatus, because the uncertainty in observations dwarfs the small flux deviations that could cause a hiatus. The sensitivity of these flux deviations to the observational dataset and to energy budget choices helps explain why previous studies conflict, and suggests that the origin of the recent hiatus may never be identified.

2.2 INTRODUCTION

The surface temperature of the Earth warmed more slowly over the period 1998–2012 than could be expected by examining either most model projections or the long-term warming trend (Flato et al. 2013). Even though some studies now attribute the deviation from the long-term trend to observational biases (Cowtan and Way 2014; Karl et al. 2015), the gap between observations and models persists. The observed trend deviated by as much as $-0.17 \text{ }^\circ\text{C}$ per decade from the CMIP5 ensemble mean projection (Flato et al. 2013) – a gap two to four times the observed trend. The hiatus therefore continues to challenge climate science.

Many studies propose that heat was drawn down from the surface into deeper ocean layers by quasi-random decadal fluctuations known as internal variability. The trouble with this proposition is that most major ocean regions – the Pacific (England et al. 2014; Nieves et al. 2015), the Indian Ocean (Lee et al. 2015), the Atlantic (Katsman et al. 2011), the Atlantic and the Southern Ocean (Chen and Tung 2014), and other combinations of basins (Drijfhout et al. 2014; Guemas et al. 2013; Liu et al. 2016; Meehl et al. 2011, 2013) – have been named individually responsible for the heat uptake.

Here I explain these conflicting results and point to alternative interpretations. I develop a surface energy budget, which I apply to hiatuses in a 100-member historical ensemble (‘the large ensemble’), generated with the coupled climate model `MPI-ESM1.1` (Giorgetta et al. 2013). Using the surface energy budget, I quantify how much deviation in energy flux occurs during a hiatus. For each hiatus in the ensemble, I then determine its origin by quantifying energy contributions to the surface from ocean heat exchange and from the TOA radiative imbalance. Finally, I use the energy budget to compare interpretations of the recent hiatus in existing observations (Balmaseda et al. 2013; Levitus et al. 2012; Smith et al. 2015; Trenberth et al. 2014).

2.3 HIATUSES IN THE LARGE ENSEMBLE

The ‘large historical ensemble’ in this study was generated by the Max Planck Institute Earth System Model version 1.1 (`MPI-ESM1.1`), an incremental improvement of the coupled ocean-atmosphere general circulation model submitted to CMIP5 in the LR configuration (Giorgetta et al. 2013). The 100 ensemble members were generated under CMIP5 historical forcing from 1850 until 2005, with extensions to 2015 under the RCP4.5 scenario (Giorgetta et al. 2013).

The ensemble’s internal variability of 15-year global mean surface temperature (`GMST`) trends (5–95% range of 0.30 °C per decade) is slightly larger than an estimate for the CMIP5 ensemble (5–95% range of 0.26 °C per decade; Marotzke and Forster 2015).

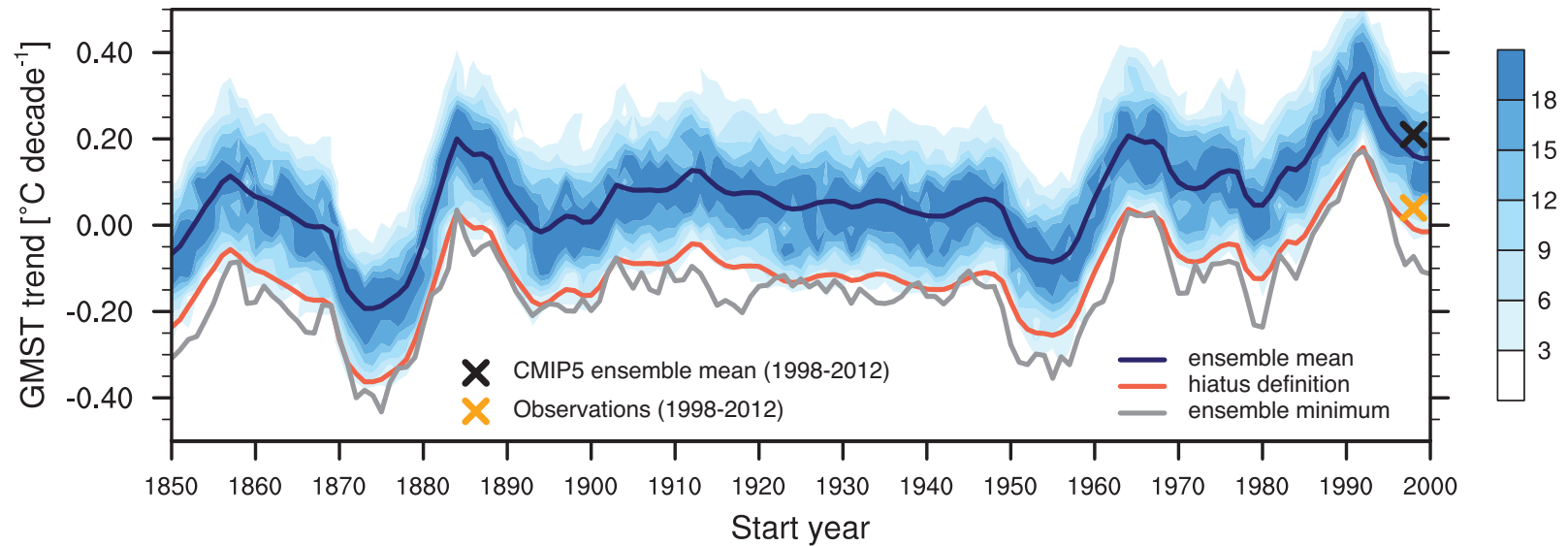


Figure 2.1: DISTRIBUTION OF 15-YEAR TRENDS IN GMST IN THE 100-MEMBER ENSEMBLE. The coupled climate model MPI-ESM1.1 is forced with CMIP5-prescribed historical forcing from 1850 until 2005, and extended until 2015 with the RCP4.5 scenario. When the red line lies above the grey line, at least one ensemble member is experiencing a hiatus, defined as a deviation of more than 0.17 °C per decade below the ensemble mean. This deviation is the same as the gap between the CMIP5 ensemble mean (black cross) and the observed (yellow cross) GMST trends for the period 1998–2012. Contours represent the number of ensemble members in bins of 0.05 °C per decade.

GMST trends are first calculated from the slope of an ordinary least-squares linear regression over a 15-year sliding window, to be consistent with the hiatus as described in Flato et al. (2013). Ensemble anomalies are then calculated at each time step (t) for each ensemble member (n):

$$X'_{t,n} = X_{t,n} - \frac{1}{100} \sum_{n=1}^{100} X_{t,n} \quad (2.1)$$

I define hiatuses in the large ensemble as any 15-year period where the GMST trend deviates by at least -0.17 °C per decade from the ensemble mean. This definition is consistent with the gap between models and observations over the period 1998–2012 (Figure 2.1), as described in the IPCC Assessment Report 5 (Flato et al. 2013). Deviations in each ensemble member from the large-ensemble mean represent internal variability, which can be cleanly separated from the forced component (the ensemble mean) due to the ensemble’s unprecedented size. There are hundreds of such hiatuses (364, or 2.4% of all 15,200 trends) – subject to historical forcing but due entirely to internal variability – distributed across all time periods in the ensemble (Figure 2.1).

2.4 ENERGY BUDGETING FOR THE SURFACE LAYER

The origin of each hiatus can be deduced from energy budgeting for the ocean’s surface layer, which dominates the thermal capacity of the Earth’s surface and therefore mediates the decadal GMST response to flux perturbations. I consider two main flux components acting on the ocean surface layer over decadal timescales: the TOA component from above and the ocean component from below (Figure 2.2). The TOA component is the top-of-atmosphere radiative flux imbalance minus atmospheric heat uptake. The ocean component is the total heat-content change below the ocean surface layer, defined at 100 m depth. Both components are converted to ensemble anomalies (to isolate the internal variability component) from values filtered over a 15-year sliding window and warm the surface layer when positive.

The budget is constructed this way for two reasons. First, the chosen boundary fluxes (Figure 2.2) close the surface energy budget and correlate well with GMST trends. Second, the choice of 100 m for the surface layer depth maximises the flux-divergence necessary for a hiatus, and therefore represents the most conservative choice for our analysis. Energy budgeting in a coupled climate model is less than straightforward, and so the following subsections explain the details of these budget choices.

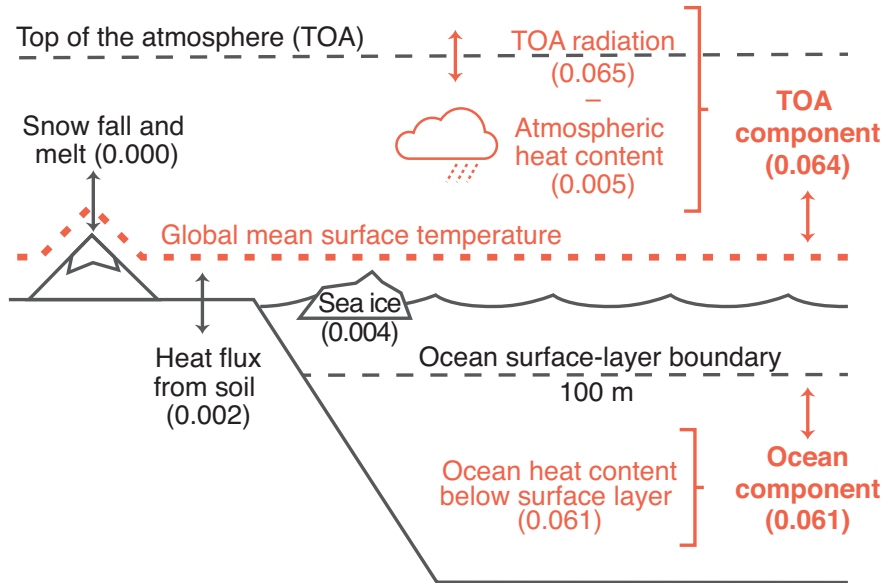


Figure 2.2: THE SURFACE ENERGY BUDGET IN THE LARGE ENSEMBLE. Red colouring indicates the global mean surface temperature (GMST) and the components included in the surface-layer flux-divergence. The smaller flux components in black are excluded because they do not improve budget closure or the relationship with GMST trends. Numbers in brackets represent the variability of each heat flux (Wm^{-2}), given as the root-mean-square of 15-year ensemble anomalies.

2.4.1 The flux-divergence combination

There are two criteria for determining the choice of fluxes that make up the surface-layer energy budget:

1. The simplest closure of the energy budget, implying high correlation and a near one-to-one relationship between the surface-layer flux-divergence and total heat content changes within the surface layer; and
2. A high correlation between the energy budget and GMST trends.

For the first criterion, I compare the surface-layer flux-divergence with changes in surface-layer heat content over 15-year periods. For this purpose, only the start and end states of each 15-year period are relevant. However, the ordinary least-squares method, which is used in this chapter and in the hiatus literature to diagnose temperature trends (Flato et al. 2013; Hartmann et al. 2013) is problematic, because it is influenced by the pathway from start- to end-states. Instead, an alternative trend method is used for the budget closure: a difference filter is calculated from the start- and end-years in the 15-year sliding window, divided by the time difference of 14 years:

$$\Delta X_t = \frac{1}{14} (X_{t+14} - X_t) \quad (2.2)$$

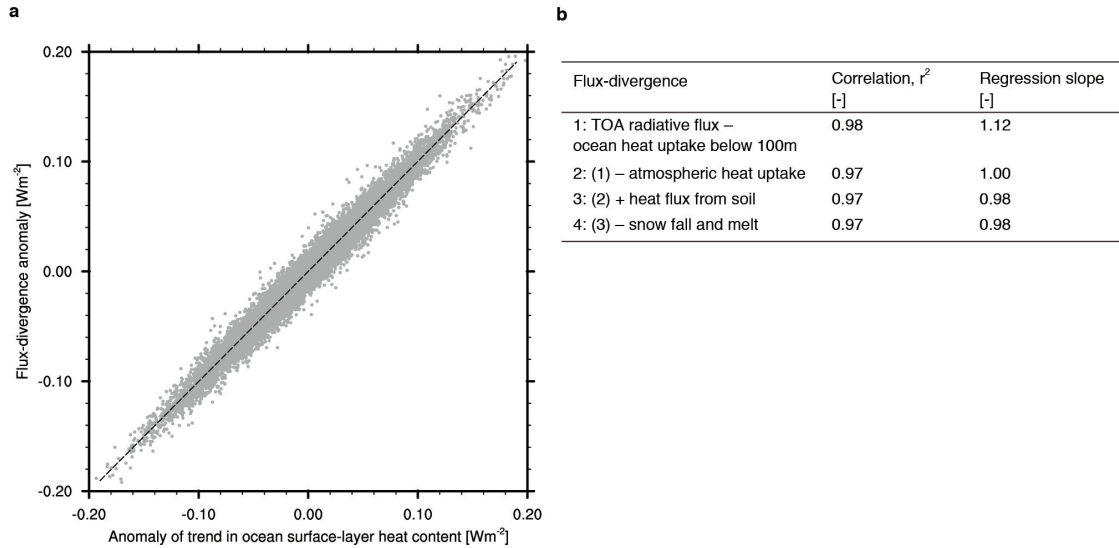


Figure 2.3: REGRESSION OF OCEAN SURFACE-LAYER HEAT CONTENT WITH FLUX-DIVERGENCE. *a*, Regression between ensemble anomalies in ocean surface-layer heat content and the flux-divergence chosen in this study (combination 2 in *b*). *b*, Different energy-flux combinations are regressed against changes in the ocean surface-layer heat content (including sea ice) to find the best closure of the energy budget in the 100-member historical ensemble (MPI-ESM1.1). Combination 2 achieves the expected one-to-one regression slope with ocean surface-layer heat content. All values are first filtered with a 15-year sliding window by taking the heat-content difference between start- and end-years, and then converted to ensemble anomalies.

Ensemble anomalies are then calculated in the usual way, as in [Equation 2.1](#). Using a difference filter instead of the ordinary least-squares method significantly improves the accuracy of the budget terms and the ability to close the model’s energy budget.

Any energy budget in a coupled climate model must also account for energy leakage. Leakage is energy created or destroyed by model error, which includes energy lost in grid cells seen by the atmospheric model component but not by the ocean model component; and, rainfall and river runoff entering the ocean, which both violate energy conservation by adopting the temperature of the ocean without energy exchange (Mauritsen et al. 2012). MPI-ESM1.1 has improved energy conservation compared to its predecessor, MPI-ESM, and both have relatively small leakage compared to models in the CMIP5 ensemble (Mauritsen et al. 2012). Energy leakage of 0.44 Wm^{-2} is first estimated from 2000 years of the control run and then removed as a constant from the surface-layer energy budget.

The selected flux-divergence combination is the sum of two components: the TOA radiative imbalance minus atmospheric heat uptake (trends in vertically integrated moist static energy); and trends in ocean heat content below the ocean surface layer. This is the simplest flux combination that matches the expected one-to-one relationship between flux-divergence and change in surface-layer heat content (combination 2 in [Figure 2.3](#)). The sum of the TOA component and

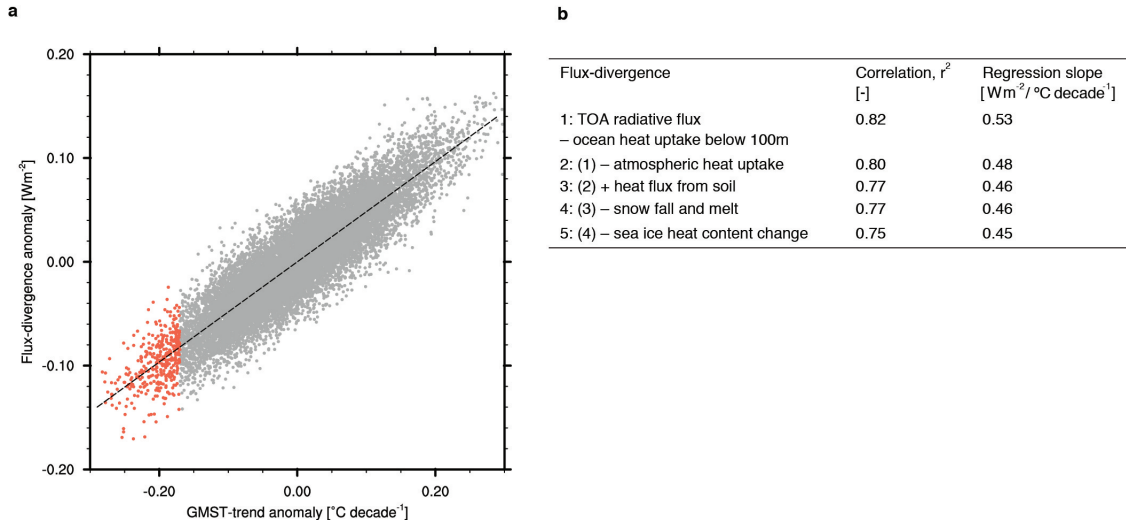


Figure 2.4: REGRESSION OF GLOBAL MEAN SURFACE TEMPERATURE (GMST) TRENDS WITH FLUX-DIVERGENCE. *a*, Regression between ensemble anomalies in GMST trends and the flux-divergence chosen for this study (combination 2 in *b*). Red dots indicate hiatuses. *b*, The regression between GMST trends and ensemble anomalies in flux-divergence is shown for different flux combinations in the 100-member historical ensemble (MPI-ESM1.1). Linear trends in heat content and GMST are calculated over a 15-year sliding window and converted to ensemble anomalies .

ocean component highly correlates with heat-content changes within the ocean surface layer ($r^2 = 0.97$, slope=1.00). Other flux components (Figure 2.2) are excluded because they are small, are connected with known energy leakages, and because they do not improve budget closure (Figure 2.3). The TOA imbalance and ocean heat uptake dominate decadal internal variability in the global energy budget of other CMIP5 models as well (Palmer and McNeall 2014).

Although the difference method provides more exact energy accounting, the ordinary least-squares trending method is used for the comparison between the energy budget and GMST trends. This choice is necessary because the least-squares method corresponds to the definition of the hiatus in the literature (Flato et al. 2013; Hartmann et al. 2013), and using different time-filtering methods for each variable in the correlation would introduce significant errors. Any terms expressed as heat content (Joules) are thus converted to trend anomalies in the same way as GMST, and then converted to units of Wm^{-2} over the total surface area of the Earth. All energy fluxes that are already output from the model as Wm^{-2} are first time-integrated and then treated the same as heat content. This step ensures the same time-filtering for all aspects of the energy budget.

For the selected flux-divergence combination, the correlation with GMST trends is high ($r^2=0.80$; Figure 2.4). Removing the minor budget terms that are related to phase changes (land-ice and sea-ice changes) or including the heat flux from the soil does not improve the relationship with GMST trends (Figure 2.4).

2.4.2 The surface-layer depth

The ocean component represents heat uptake below the ocean surface layer. Because budget closure is not influenced by the choice of ocean surface layer depth, the choice of surface layer should meet the second criterion for the energy budget: the heat content of the surface layer must have a high correlation with changes in GMST. The highest correlation would be achieved by defining the ocean surface layer at the bottom boundary of the sixth model layer (62 m depth; Figure 2.5).

However, I choose to define the ocean surface layer at 100 m (as in Baker and Roe 2009; Brown et al. 2014; Geoffroy et al. 2013a), because around this depth the flux-divergence anomaly for a hiatus reaches a maximum (Figure 2.5) and is therefore the most conservative choice for the following analysis. Choosing a surface depth beyond 100 m further exceeds the globally averaged mixed layer, and so the correlation between the energy budget and GMST trends sharply decays (Figure 2.5).

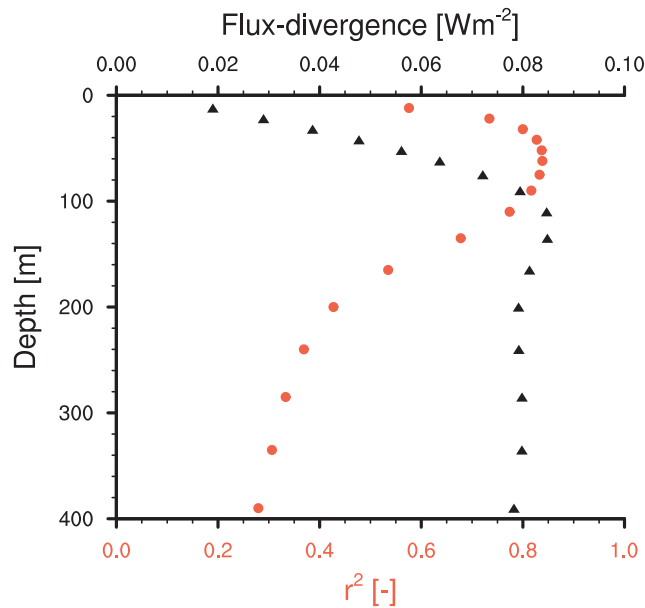


Figure 2.5: RESULTS FROM SURFACE BUDGETS DETERMINED BY INCREASINGLY DEEPER DEFINITIONS OF THE OCEAN SURFACE LAYER. For each depth, a linear regression is performed for GMST trends against the surface-layer flux-divergence (both as 15-year ensemble anomalies). Shown in black (top axis) is the expected deviation in flux-divergence required to cause a hiatus, calculated from the regression slope. Shown in red (bottom axis) is the correlation (r^2) of each regression. The correlation rapidly deteriorates for definitions of the surface layer below 100 m.

2.5 THE ENERGETIC ORIGINS OF HIATUSES IN THE LARGE ENSEMBLE

2.5.1 *How much flux-divergence causes a hiatus?*

Using the energy budget I can determine the magnitude of flux anomalies associated with each hiatus. From the slope of the regression between surface-layer flux-divergence and GMST trends, I find that the expected flux-divergence anomaly for a hiatus (a -0.17 °C per decade anomaly) is merely -0.082 Wm^{-2} . If all of this flux-divergence were concentrated in the the ocean's top 100 m, it would correspond to an average cooling of only -0.10 °C per decade, and indeed this is what occurs in the model: the ocean surface layer cools on average by only -0.10 °C per decade during hiatuses. However, the effects of that cooling are amplified at the land surface (Byrne and O’Gorman 2013). Hiatuses caused only by ocean heat uptake tend to cool the land surface more effectively, which means they generally require a lower flux-divergence anomaly than other hiatuses to achieve the same cooling. Variation in the ratio of land to ocean surface-cooling leads to variation around the expected flux-divergence anomaly: an interval of -0.082 ± 0.038 Wm^{-2} covers the 5–95% range for all hiatuses.

These results suggest that the total combined anomaly in TOA fluxes and ocean heat uptake that caused the gap between observations and models during the hiatus could be on the order of 0.1 Wm^{-2} . Defining hiatuses as equal to the observed 1998–2012 anomaly from the long-term observed trend (an anomaly of 0.04 – 0.07 C per decade) would reduce the threshold to just 0.02 – 0.03 Wm^{-2} .

2.5.2 *Which ocean regions can provide the flux-divergence?*

Across the large ensemble, the 0.082 Wm^{-2} threshold in energy flux is frequently exceeded by anomalous heat-content changes in all major ocean basins¹, especially in the Atlantic, Pacific and Southern Oceans (Figure 2.6).

However, these heat-content changes are dominated by interbasin heat exchange, which does not contribute to the surface-layer flux-divergence. In each major basin, the variations in heat content below the surface layer cannot predict trends in GMST (Figure 2.6), and indeed would falsely predict many more hiatuses than actually occur.

Even the global ocean heat uptake below 100 m correlates poorly with GMST trends (Figure 2.6), because the TOA component tends to oppose the ocean component’s contribution to the energy budget (see below, Figure 2.8). The flux-divergence anomaly, which has less

¹ Ocean boundaries are identical to those used in CMIP5. See Jungclaus et al. (2013b).

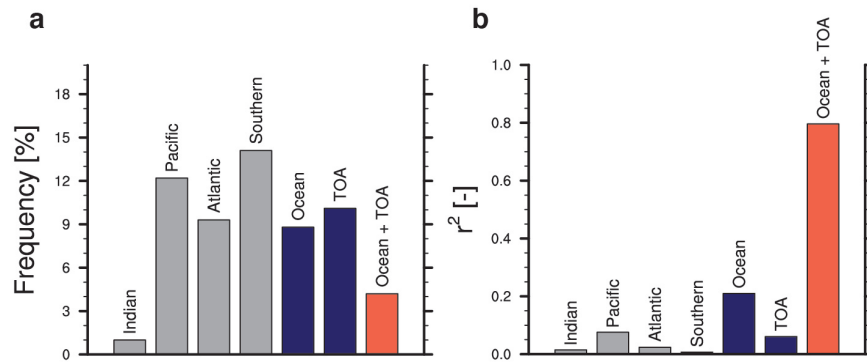


Figure 2.6: HEAT FLUXES AND THEIR PREDICTIVE POWER FOR GMST TRENDS. *a*, Frequency with which each component exceeds the expected threshold for a hiatus (-0.082 Wm^{-2}). *b*, Correlation between global mean surface temperature (GMST) trends and heat fluxes in the large ensemble (as 15-year ensemble anomalies). In *a* and *b*, grey bars represent changes in ocean heat content below the ocean surface layer (100 m) by basin, blue bars represent the ocean and TOA components, and the red bar is the surface-layer flux-divergence (TOA + ocean components).

than half the variability of either the TOA or ocean component alone, is the only reliable predictor of GMST trends.

The role of the TOA and the ocean in each hiatus can be determined by comparing their relative contributions to the flux-divergence anomaly, as in Figure 2.7. For hiatuses in the large historical ensemble, the negative (cooling) anomaly is caused entirely by the TOA in 12% of cases and entirely by the ocean in 24%. In the remainder (64%), the negative anomaly is caused by the TOA and ocean acting together (bottom left quadrant of Figure 2.8). TOA variability is therefore involved in 76% of all hiatuses².

2.6 THE ORIGIN OF THE HIATUS IN OBSERVATIONS

Applying a similar analysis to observations should reveal the energetic origin of the gap between models and observations during the recent hiatus. I convert two observation-based estimates of fluxes over 2000–2010 to anomalies by subtracting the mean energy budget of the large ensemble for the same period (see Table 2.1 and Table 2.2). These anomalies include both the effect of internal variability and any potential effects of forcing differences between model and observations. Choosing 2000–2010 means that we do not cover the full hiatus period (1998–2012) and that the corresponding gap in GMST trend between models and observations is reduced, because the warming rate increased after 2000 (Karl et al. 2015). However, this choice allows us to construct temporally consistent energy budgets from multiple

² There is no significant relationship between the origin of hiatuses and different periods in time. See Table B.1.

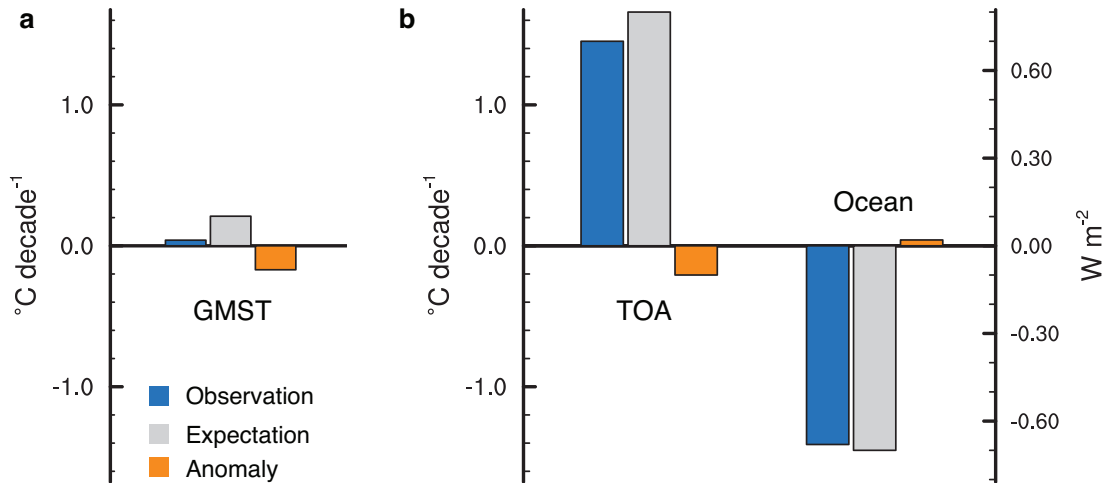


Figure 2.7: EXAMPLE ILLUSTRATING THE ENERGETIC ORIGIN OF A HIATUS. *a*, A hiatus is an observed negative deviation from the expected global mean surface temperature trend, where the expectation could be the long-term warming trend, or the warming simulated by climate models. The deviation, or anomaly, is the observation minus the expectation. *b*, The trend in GMST is determined by the surface-layer energy budget, which is dominated over decadal timescales by energy fluxes from the top-of-atmosphere (TOA) radiation imbalance and ocean heat uptake below the ocean surface layer. In a standard global warming scenario, the TOA contributes a positive absolute (warming) flux to the surface, and ocean heat uptake contributes a negative absolute (cooling) flux to the surface, which is the case for both the observation and expectation in the example shown. The anomalies, which are much smaller than the absolute TOA and ocean fluxes, reveal the energetic source of this hiatus: the Ocean anomaly is small and positive (warming), whereas the TOA anomaly is larger and negative (cooling). Therefore, the shown hiatus is caused only by variation in the TOA. The example fluxes are displayed in W m^{-2} (right axis) and as contributions to the GMST trend in $^{\circ}\text{C per decade}$ (left axis). To determine the values in $^{\circ}\text{C per decade}$, the fluxes in W m^{-2} are divided by the constant $0.48 \text{ W m}^{-2} / (^{\circ}\text{C decade}^{-1})$, which represents the relationship between internal variability in surface-layer flux-divergence and GMST trends in the large ensemble.

sources and to take advantage of the improved quality of observations after 2000.

A third budget is based on the results of England et al. (2014), in which the authors present a plausible mechanism for the hiatus. Although their results are model-derived, the model is forced with extreme winds that were observed during the hiatus.

2.6.1 *Constructing observation-based budgets*

The first observation-based budget uses a recent estimate of TOA fluxes, which is based on the CERES satellite data-product, Argo floats and AMIP simulations (Smith et al. 2015). The ocean component uses the WOA dataset (Levitus et al. 2012): pentadal heat-content values for 700–2000 m and yearly heat content values for the upper 700 m. A separate estimate for deep-ocean warming below 2000 m is used (Purkey and Johnson 2010). From the total heat uptake, I subtract the heat-content trend for the first 100 m in the WOA objective analysis data (Levitus et al. 2012), calculated from in-situ temperature with a constant density and specific heat of 4×10^6 Joules $\text{m}^{-3} \text{ } ^\circ\text{C}^{-1}$.

For this first budget, the 1-sigma error bars for the TOA estimate are taken from the same source as the estimate itself (Smith et al. 2015). The error bars for the WOA ocean heat-content trend are calculated as plus or minus the standard error of the slope parameter, assuming that the errors in heat content are auto-correlated and behave like an AR(1) process (Hartmann et al. 2013; Santer et al. 2008). The auto-correlation coefficient for the errors is estimated from residuals in heat-content data preceding the 2000s (1957–1999). A reduced degrees-of-freedom is calculated from the auto-correlation coefficient and scales the estimate of the standard error in heat content, which is calculated directly from the error estimates provided with the WOA data (not from the regression residuals).

The second observation-based budget uses ORAS4 ocean reanalysis data. The total-depth heat uptake in the 2000s is taken from Balmaseda et al. (2013). The trend for the top 100 m is calculated from the available ORAS4 potential temperature values with a constant density and specific heat of 4×10^6 Joules $\text{m}^{-3} \text{ } ^\circ\text{C}^{-1}$. The 1-sigma error bars are taken directly from Balmaseda et al. (2013). For this second budget, the corresponding TOA flux estimate and its error bars are taken from Trenberth et al. (2014).

Both observation-based budgets are converted to anomalies by subtracting the large ensemble mean energy budget for 2000–2010. The large ensemble budget is first adjusted to account for ocean drift. Although the ocean model component conserves energy internally, ‘drift’ occurs when the ocean is not at equilibrium, and absorbs or releases heat due to adjustment processes that occur on multi-millennial timescales. MPI-ESM1.1 has limited drift, because pre-industrial sim-

BUDGET	TOTAL	TOP 2000M	BELOW 2000M	TOP 100M	ENS. MEAN	ANOMALY
ORAS ₄	-0.84 ± 0.08	—	—	-0.02	-0.66	-0.16 ± 0.08
WOA	-0.56 ± 0.15	-0.49 ± 0.09	-0.07 ± 0.06	-0.07	-0.66	$+0.17 \pm 0.15$

Table 2.1: OBSERVATIONAL ESTIMATES FOR THE OCEAN COMPONENT OVER 2000–2010 IN Wm^{-2} . The anomaly for the ocean component is calculated by subtracting the top 100 m from the total, and then subtracting the corresponding ensemble mean (over the period 2000–2010 in the large ensemble). The estimate for below 2000 m in the WOA estimate is taken from Purkey and Johnson (2010) for the period 1990–2010. Uncertainties are shown as \pm one standard error.

BUDGET	TOTAL	ENSEMBLE MEAN	ANOMALY
ORAS ₄	$+0.91 \pm 0.1$	+0.77	$+0.14 \pm 0.1$
WOA	$+0.62 \pm 0.28$	+0.77	-0.15 ± 0.28

Table 2.2: OBSERVATIONAL ESTIMATES FOR THE TOA COMPONENT OVER 2000–2010 IN Wm^{-2} . The anomaly for the TOA component is calculated from the total observational estimate minus the corresponding ensemble mean (over the period 2000–2010 in the large ensemble). Uncertainties are shown as \pm one standard error.

ulations are spun-up not from a climatology or an ocean-state estimate, but from the control simulations of previous model versions (Jungclaus et al. 2013a); the spin-up period therefore extends over multiple millenia. Drift poses no issue for energy budgeting within the large ensemble itself, because the process of taking ensemble anomalies removes any such effects. But for the observation-based budgets, drift could artificially weight the interpretation of the hiatus origin toward the ocean or the TOA. To calculate the drift, a quadratic function is first fitted to ocean heat content over the 2000-year control run (as in Sen Gupta et al. 2013). Since each ensemble member starts from a different point in the control run, the drift is estimated from the rate-of-change in the quadratic that corresponds to each ensemble member’s midpoint. The resulting ensemble-mean drift of 0.01 Wm^{-2} is removed from both the ocean component and the TOA component in the two observation-based budgets.

For third budget, the values are taken from England et al. (2014), where they are expressed as anomalies from their control experiment for the heat-content change in the top 125m of ocean and the remaining ocean depth. I convert these values to 15-year fluxes over the total Earth surface to compare their values with the flux-divergence in the large ensemble. I assume that the anomaly they cite for the ocean below 125m represents the ocean component, and that the sum of surface and deep-ocean components is equivalent to the TOA component.

2.6.2 *What the budgets imply*

Although the two observation-based budgets do not cover the full hiatus period, they do illustrate how observational uncertainty affects interpretations of the hiatus. The CERES/WOA budget suggests that the hiatus was caused purely by the reduced influx of energy at the TOA (orange dot, [Figure 2.8](#)). The second budget, based on ocean reanalysis data from ORAS4, suggests the hiatus was caused purely by increased heat uptake in the ocean (green dot, [Figure 2.8](#)).

The anomalies diagnosed from England et al. (2014) likewise suggest an ocean origin (purple dot, [Figure 2.8](#)), but their result lies well outside the large ensemble. Since the authors force an ocean-only model with reanalysis-based winds, there may be effects in coupled models that the authors' set-up does not reproduce, such as the amplification of hiatus cooling at the land surface. The lack of coupled effects might necessitate a greater surface-layer flux-divergence during hiatuses than in the large ensemble.

From this analysis of observational estimates, I am unable to exclude the TOA anomaly as a possible cause of the recent hiatus. Referencing the observations to an alternative energy budget (rather than that of the large ensemble) could shift the absolute position of the green and orange crosses in [Figure 2.8](#). However, their relative distance from one another and the size of their error bars would not change.

2.7 RESOLVING CONFLICTS IN PREVIOUS STUDIES

Interpretations of the hiatus are not only sensitive to the observational dataset, but also to the method of energy budgeting. The methods used in previous studies may reveal why their results conflict. For example, the hiatus has been explained as the result of heat being transferred from the surface ocean to the layers immediately below it, in the upper 300–350 m (Liu et al. 2016; Nieves et al. 2015). However, an energy budget that only accounts for heat exchange between the top 100 m and depths up to 300–350 m correlates poorly with GMST trends in the large ensemble ($r^2=0.08$, [Figure 2.9](#)). A poor correlation also results when we exclude heat-content changes below the upper 700 m ($r^2=0.14$, [Figure 2.9](#); see Lee et al. 2015) and the upper 2000 m of ocean ($r^2=0.36$, [Figure 2.9](#); see Chen and Tung 2014). Heat-content changes up to as much as 4000 m may be important for decadal internal variability, despite claims to the contrary (Liu et al. 2016). Furthermore, the pattern of surface-layer cooling overlying a warming trend may be common during ocean hiatuses, but it also occurs in around half of hiatuses caused purely by the TOA ([Figure B.2](#)). During these TOA hiatuses, the subsurface warming is caused by heat transfer from deeper layers. Energy budgets that do not consider up-

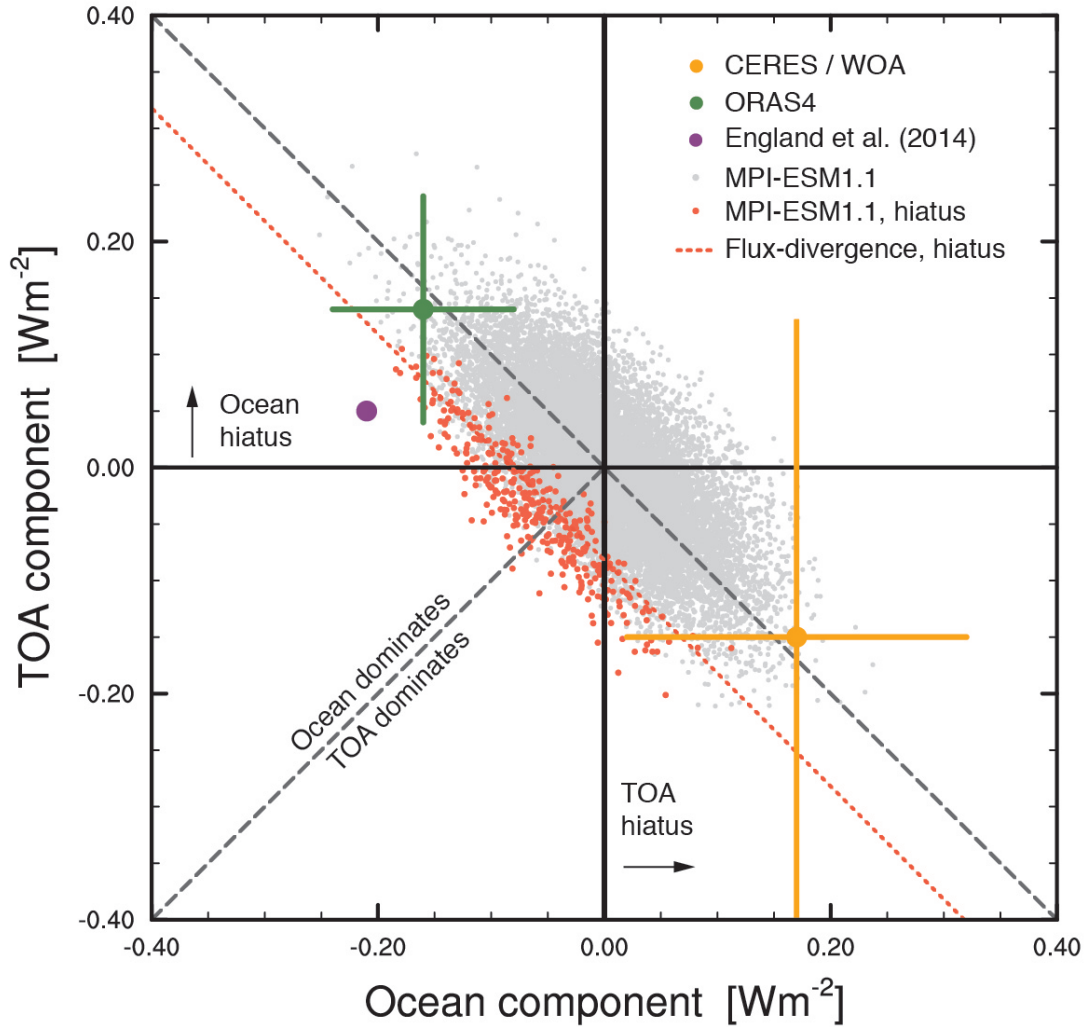


Figure 2.8: HIATUSES AND THEIR ORIGINS IN MODELS AND OBSERVATIONS. Contributions to hiatuses from TOA and ocean components. Positive values indicate fluxes that warm the surface. Small red dots represent hiatuses in the large ensemble and small grey dots represent all other trends; the red dotted line is a flux-divergence of -0.082 Wm^{-2} . Observational estimates and their 1-sigma error bars are compiled from multiple sources that rely either on CERES and WOA data (large orange dot) or ORAS4 data, shown as anomalies from the large-ensemble mean budget over the 2000s. The large purple dot represents results from an ocean model forced with reanalysis-based winds as reported in England et al. (2014), converted to mean fluxes over 15 years.

take across the whole ocean depth may therefore misrepresent crucial energy fluxes and misdiagnose the hiatus.

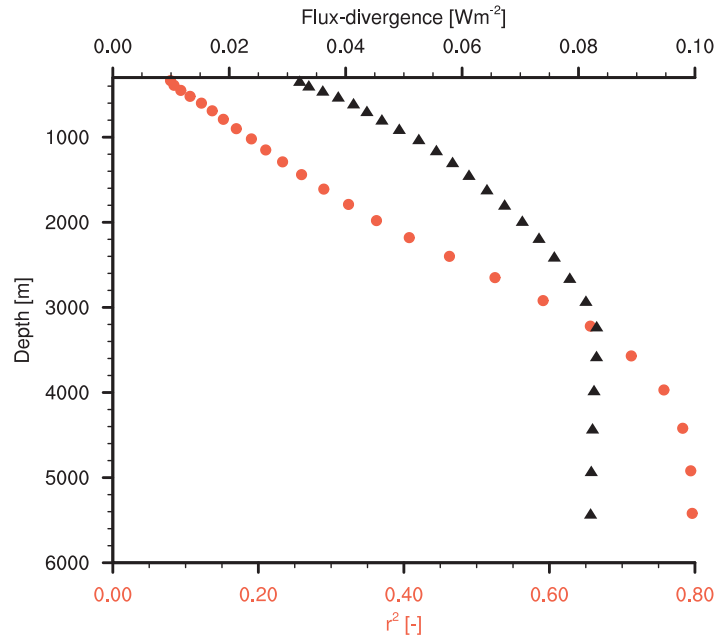


Figure 2.9: ENERGY BUDGETS THAT ONLY CONSIDER UPPER-LEVEL OCEAN HEAT CONTENT FAIL TO PREDICT GMST VARIABILITY. Each data point represents the results of a regression between global mean surface temperature (GMST) trends and the surface-layer energy budget – consisting of the TOA component and ocean heat uptake below 100 m – in the 100-member historical ensemble (MPI-ESM1.1). Heat-content changes below the indicated depth are excluded from the budget. For example, the data points for 700 m show the regression for a budget comprising TOA fluxes and ocean heat uptake between 100–700 m ($r^2 = 0.14$). Red dots (bottom axis) represent the correlation (r^2) of each regression. Black dots (top axis) represent the expected flux-divergence for a 0.17°C per decade hiatus, as determined from the slope of each regression.

The hiatus may also be misdiagnosed by misrepresenting the surface layer in energy budgeting. For example, the surface layer has been defined at 300 m ocean depth or more (Balmaseda et al. 2013; Chen and Tung 2014; Katsman et al. 2011; Meehl et al. 2011, 2013; Watanabe et al. 2013). I perform energy budgeting in the large ensemble with a surface layer that extends to 300 m instead of 100 m and find that the flux-divergence correlates comparatively poorly with GMST trends ($r^2=0.33$ for 300 m, Figure 2.5).

2.8 THE TRUE HIATUS DILEMMA

I conclude that the TOA may have been a source of significant internal variability during the hiatus. This conclusion is not an artefact of model-generated TOA variability (Stephens et al. 2015) – the large ensemble produces TOA variability that is similar to that in the ob-

servational record (Figure 2.10). Rather, this conclusion is based on a simple yet robust principle, namely that the Earth's surface layer has a small heat capacity. The surface temperature can therefore be influenced by small variations in the large yet mutually compensating fluxes that make up this layer's energy budget. Comparing the small variability in the TOA imbalance with the total TOA imbalance under global warming, as other studies have done (Brown et al. 2014; Trenberth and Fasullo 2013), obscures the significance of these small variations for the hiatus.

Other observational studies associate the hiatus with heat-flux anomalies that range from 0.21 Wm^{-2} (Trenberth and Fasullo 2013) to 0.50 Wm^{-2} (Drijfhout et al. 2014). But when I perform energy budgeting for the surface layer in the large ensemble, I find that anomalies closer to 0.08 Wm^{-2} can account for hiatuses as large as $0.17 \text{ }^\circ\text{C}$ per decade, and $0.02\text{--}0.03 \text{ Wm}^{-2}$ for a hiatus equal to the 1998–2012 anomaly from the observed long-term trend. Because the flux-divergence anomaly is so small, ascribing the origin of the recent hiatus to the TOA or ocean requires that each of their contributions to the anomaly are known with considerable accuracy. However, the uncertainty in TOA imbalance from satellite measurements is two orders of magnitude larger ($\sim 8 \text{ Wm}^{-2}$; Loeb et al. 2009) than the anomaly I calculate. Satellite data are commonly anchored with ocean heat-content measurements, but the uncertainty range in TOA imbalance during the 2000s still remains around 0.56 Wm^{-2} (Smith et al. 2015), and even for the most recent estimate based on improved ocean observations over 2005–2015, the range is 0.2 Wm^{-2} (Johnson et al. 2016).

This is the true dilemma at the heart of the hiatus debate: the variability in ocean heat content alone has no power to explain the hiatus, and the measure that can – the surface-layer flux-divergence – is dwarfed by observational uncertainty. While there are attempts to fill the gaps in observations with ocean reanalyses like ORAS4, the resulting data are of questionable integrity during the hiatus (Nieves et al. 2015; Smith et al. 2015) and, as I show, disagree with the budget based on CERES and WOA. Even if these disagreements could be reconciled, the process of anchoring satellite observations with ocean heat uptake makes the contributions from TOA and ocean difficult to disentangle, because their absolute difference is unknown. Therefore, unless the uncertainty of observational estimates can be considerably reduced, the true origin of the recent hiatus may never be determined.

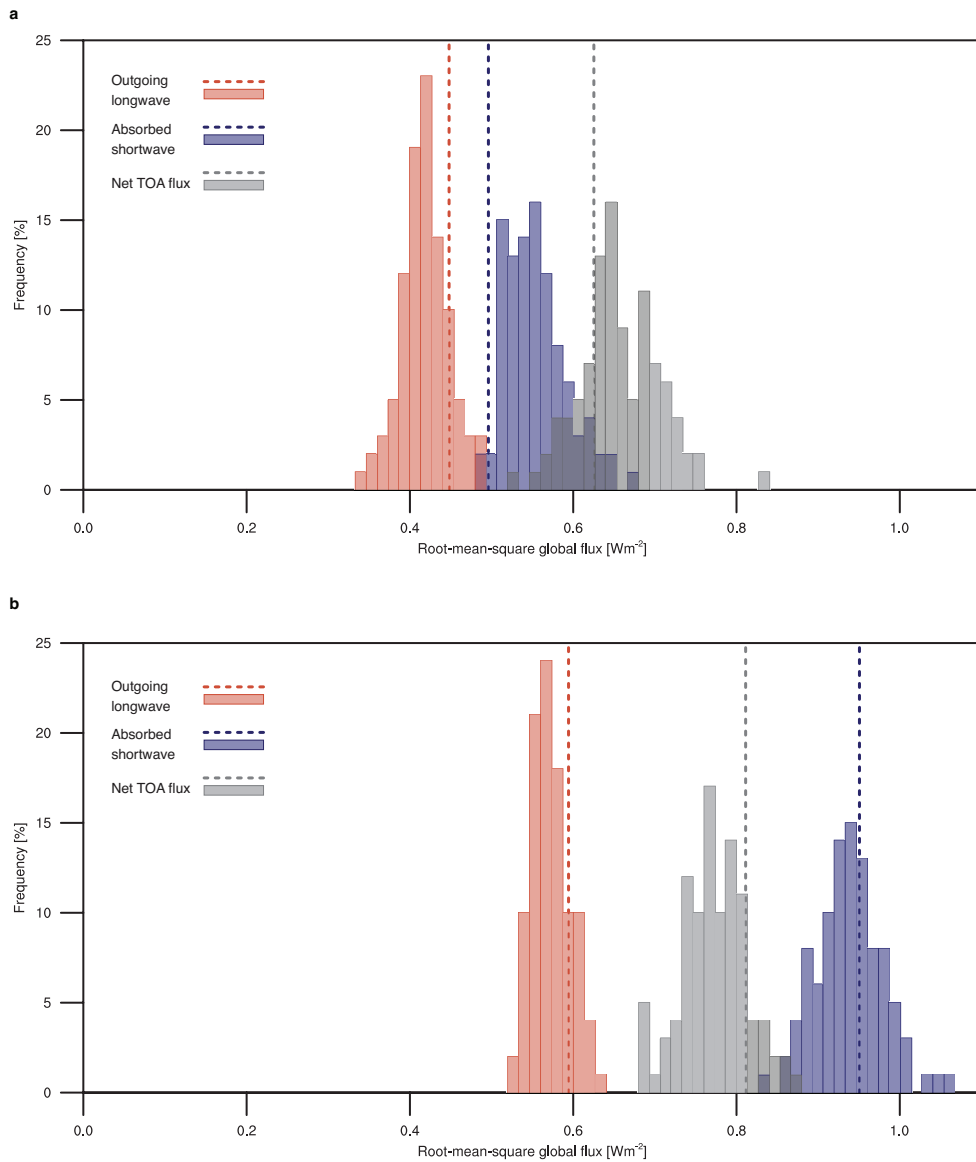


Figure 2.10: VARIABILITY IN TOP-OF-ATMOSPHERE (TOA) FLUXES IN OBSERVATIONS, RECONSTRUCTIONS AND MPI-ESM1.1. *a*, Variability in observations and the model for the period March 2000 – May 2015. Dotted lines are single values calculated from observations (CERES EBAF-TOA Ed2.8; Loeb et al. 2009). *b*, Variability in reconstructions and the model for the longer period January 1985 – February 2013. Dotted lines are single values calculated from flux reconstructions (Allan et al. 2014). In *a* and *b*, bars represent the frequency distribution (in bins of 0.0133 Wm^{-2}) of values calculated for each of the 100 historical ensemble members over the relevant period. Variability is calculated from all sources as the root-mean-square in monthly means, after the mean annual cycle for the period is removed.

HOW THE PATTERN EFFECT CHANGES CLIMATE SENSITIVITY

3.1 SUMMARY

The climate sensitivity in model simulations has been shown to increase over time due to the changing spatial pattern of warming (Andrews et al. 2015; Armour et al. 2013; Rose et al. 2014; Rugenstein et al. 2016a). However, many studies reach different conclusions about which processes and which regions are the most critical for increasing climate sensitivity. Here, I present a framework that can account for different definitions of the ‘pattern effect’. The framework is applied to four 1000-year simulations with a coupled climate model, subjected to abrupt CO₂ increases up to sixteen-times the pre-industrial concentrations. I show that the differing results in previous studies might be a result of their assumptions, not divergent model behaviour. The assumptions made in some studies further lead to a misdiagnosis of the radiative forcing in the four simulations. The fact that the pattern effect depends partially on the time since the forcing increase, and not on the surface temperature alone, supports the view that current observational estimates might underestimate climate sensitivity.

3.2 INTRODUCTION

In many climate models exposed to abrupt increases in CO₂ concentrations, the relationship between surface warming and the global energy imbalance changes over time (Andrews et al. 2015; Armour et al. 2013; Bloch-Johnson et al. 2015; Block and Mauritsen 2013; Geoffroy et al. 2013b; Gregory et al. 2004; Jonko et al. 2012; Li et al. 2013; Meraner et al. 2013; Rose et al. 2014; Rugenstein et al. 2016a; Senior and Mitchell 2000; Winton et al. 2010). This behaviour in models could mean that the Earth’s equilibrium climate sensitivity (ECS) – the long-term warming resulting from a CO₂ doubling – will change, so that future warming will overshoot estimates based on current observations (Armour 2017).

Some studies explain that changing climate sensitivity in models is caused by changing spatial patterns of warming (Andrews et al. 2015; Armour et al. 2013; Rose et al. 2014; Rugenstein et al. 2016a). This concept has been called the ‘pattern effect’ (Stevens et al. 2016), although exactly how the pattern effect works is a matter of debate. In this Chapter, I address the differing explanations of the pattern effect. I propose a framework for assessing regional contributions to

a changing climate sensitivity and attempt to reconcile the findings in previous studies.

Previous studies differ not only in their explanation of how the pattern effect works, but also the critical regions in which it is most active. Senior and Mitchell (2000) point to changes in regional radiative feedbacks caused by changing cloud properties, particularly over the Southern Ocean. These changes in regional feedback are suspected to be connected to spatial warming patterns induced by extra-tropical ocean heat uptake (Rose et al. 2014; Rugenstein et al. 2016a; Senior and Mitchell 2000). Armour et al. (2013) find that the extra-tropics in general are critical for the pattern effect, but their explanation favours the role of changing temperature patterns, not regional feedbacks. Yet another explanation is offered by Block and Mauritsen (2013), who find, contrary to Senior and Mitchell (2000), that Southern Ocean feedbacks actually work against increasing climate sensitivity. The global increase in climate sensitivity is instead driven by changes in multiple feedbacks, with strong contributions from the tropics (Block and Mauritsen 2013). A review of CMIP5 models (Andrews et al. 2015) also argues that the tropics dominate the increase in climate sensitivity, but the authors implicate changes in cloud feedbacks. We might expect different model set-ups to favour different mechanisms for a changing climate sensitivity, but this diversity of explanations is less than satisfying.

However, these studies do not always mean the same thing when they diagnose regional influences. What if part of the differences between studies arise because of how they define the pattern effect? Armour et al. (2013) focussed only on the changing warming pattern when replicating the changing climate sensitivity in their coupled model: they assumed that regional feedbacks were constant. In this formulation of the pattern effect, the warming pattern changes over time, and weights the regional feedbacks to different extents. Even though regional feedbacks are constant, their changing weighting leads to time-dependence in the global feedback parameter.

However, other studies provide evidence that regional feedbacks do change (Andrews et al. 2015; Block and Mauritsen 2013; Meraner et al. 2013; Rose and Rayborn 2016; Rose et al. 2014; Rugenstein et al. 2016a; Senior and Mitchell 2000). In this case, the changing global feedback parameter arises not only from weighting by the warming pattern, but also from the regional changes that the pattern excites in the radiative properties of the atmospheric column. This second explanation does not necessarily exclude the theory of Armour et al. (2013), but provides for the additional effect of changing regional feedbacks.

There is a third possible explanation, in which changes to the global feedback parameter are exclusively the result of changing regional feedbacks, and the warming pattern is assumed to be constant in time.

No study I am aware of has explicitly considered this view, but Senior and Mitchell (2000) use a similar approach because they point to regional changes in cloud properties with respect to the regional warming (see their Figure 2), but neglect how regional warming weights these changes at the global level.

Here I propose a framework that can encompass all the formulations of the pattern effect. I isolate the effect of a changing warming pattern by assuming constant regional feedbacks, as in Armour et al. (2013), and call this the ‘temperature component’. I also isolate the effect of changing regional feedbacks by assuming a constant warming pattern and call this the ‘feedback component’. By allowing both the warming pattern and the feedbacks to change, I consider the full ‘combined effect’. For each formulation of the pattern effect, I attempt to reconstruct the relationship between the energy imbalance and surface warming simulated by MPI-ESM1.2, subjected to abrupt increases in atmospheric CO₂ concentrations. In doing so, I ask which formulation best represents the pattern effect in MPI-ESM1.2, and whether the different assumptions in previous studies can lead to different results with the same set of model output.

As in previous studies, I dissect the regional contributions to the pattern effect from clouds, water vapour, temperature and albedo. But instead of the commonly-used radiative kernel method, I use diagnostics based on the partial radiative perturbation (PRP) method (Colman and McAvaney 1997; Meraner et al. 2013; Wetherald and Manabe 1988), which allow me to cleanly separate fast adjustments (Williams et al. 2008) from true changes to radiative feedbacks in each region. The PRP method is also more accurate than radiative kernels when analysing a large perturbation in climate state (Block and Mauritsen 2013; Jonko et al. 2012) caused by strong radiative forcing.

The pattern effect has thus far been investigated under forcing strengths of two times and four times CO₂, and mostly out to time periods of several hundred years. Some studies have reviewed the millennial timescale under a single forcing strength (Andrews et al. 2015; Rugenstein et al. 2016b). Here I consider a larger range of forcing strengths – two, four, eight and sixteen times the pre-industrial CO₂ levels – and integrate each simulation out to 1000 years. This allows me to examine the pattern effect over multiple timescales and how its evolution might depend on the forcing strength. Better understanding the pattern effect’s time- or state-dependent evolution will influence how we interpret observations of climate sensitivity in decades to come, and how we position the observed estimates in relation to simulated estimates of climate sensitivity.

3.3 MODEL INTEGRATIONS AND DIAGNOSTICS

Four model runs using the Max Planck Institute Earth System Model version 1.2 (MPI-ESM1.2) were integrated out to 1000 years. Each run was started from a pre-industrial control state, but atmospheric CO₂ concentrations were abruptly increased, to either 2x, 4x, 8x or 16x the pre-industrial concentration of 284.7 ppm.

The effective radiative forcing is determined from four experiments with the atmospheric component of MPI-ESM1.2, ECHAM6.3, where the sea surface temperature (SST) is held fixed but the CO₂ concentrations are increased to match each of the coupled runs (Myhre et al. 2013). The small amount of land warming in these runs is corrected for in the forcing estimate, as suggested in Hansen et al. (2005).

The contributions of individual feedback types are separated using PRP diagnostics (Colman and McAvaney 1997; Meraner et al. 2013; Wetherald and Manabe 1988), into contributions from temperature (lapse-rate plus Planck), water vapour, clouds and albedo feedbacks. Instantaneous snapshots of model variables are read out every 10 hours over the 1000 year run to complete the PRP calculations, and compared with a pre-industrial control run, integrated over 300-years with the diagnostics switched on. The PRP method allows separation of the initial adjustment (Williams et al. 2008) from the true radiative feedbacks, and provides more accurate estimates of feedbacks than the commonly used radiative kernel technique, which has inaccuracies associated with the need to linearise otherwise state-dependent kernels (Block and Mauritsen 2013). This is particularly important for runs with strong forcing examined in this chapter.

The error of the PRP method can be estimated by summing up all the radiative contributions, include those from atmospheric CO₂, and comparing this with the actual change in the TOA imbalance. The error in the PRP diagnostic reaches a maximum at the end of the 16xCO₂ integration of 0.29 Wm⁻² in longwave and -0.05 Wm⁻² in shortwave radiation. This represents 1.6% and 0.3% of the total forcing respectively. In contrast, similar estimates for the kernel method suggest almost 50% error for forcings, under forcing of only 8xCO₂ (Jonko et al. 2012).

3.4 ESTIMATING THE GLOBAL FEEDBACK PARAMETER

A temperature increase at the Earth's surface implies an increase in the energy radiated to space. This allows the Earth to return to a new state of radiative balance after an increase in external forcing (F). The total warming required to reach the new equilibrium can be determined from the initial warming response if the relationship between

the top-of-atmosphere (TOA) energy imbalance (R) and warming (T) is linear:

$$R = F + \lambda T, \quad (3.1)$$

This sign convention implies that $\lambda < 0$ if the global feedbacks stabilise the surface temperature. To obtain the ECS, we can set $F = F_{2 \times \text{CO}_2}$ and $R = 0$:

$$\text{ECS} = \frac{F_{2 \times \text{CO}_2}}{-\lambda_{\text{eff}}} \quad (3.2)$$

The effective climate feedback parameter, λ_{eff} , is a constant that describes the relationship between initial forcing and final equilibrium warming (T_{eq}),

$$\lambda_{\text{eff}} = \frac{-F}{T_{\text{eq}}}, \quad (3.3)$$

and [Equation 3.2](#) is a special case where the forcing is equivalent to a single doubling of CO_2 .

Since the pattern effect causes a break-down in the assumption of a constant λ , we can write the feedback parameter not as a constant but as a function of surface warming, which is analogous to the differential climate feedback parameter suggested by Gregory et al. (2004).

$$\bar{R} = \bar{F} + \int \lambda(\bar{T}) d\bar{T} \quad (3.4)$$

$$\lambda(\bar{T}) = \frac{d\bar{R}}{d\bar{T}} \quad (3.5)$$

I include overbars to represent the global spatial mean, since we need to distinguish it from the regional level in the sections that follow. $\lambda(\bar{T})$ represents the instantaneous gradient of the line in a Gregory analysis (Gregory et al. 2004; see [Figure 3.1](#) for an example). Now the global feedback parameter and thus climate sensitivity can change with the state of warming, but what if the changes are, in fact, time-dependent?

One method for diagnosing a changing λ uses two linear fits: one in the initial two decades of warming, and one for the remainder of the response to forcing (Andrews et al. 2015; Block and Mauritsen 2013). This allows for changes to λ that may be connected to a ‘fast’ and ‘slow’ response to forcing (Geoffroy et al. 2013a; Held et al. 2010). The disadvantage of this method is that only a step-change in λ can be inferred. Bloch-Johnson et al. (2015) introduce a quadratic term proportional to T^2 into [Equation 3.1](#), which allows a continuous evolution of λ but restricts this evolution to temperature-dependence.

I want to allow for the possibility of both types of changes in λ : those related to fast and slow timescales, and those related to temperature. I use a hybrid of both methods: I estimate $\lambda(\bar{T})$ by fitting a quadratic spline with a single node at 25 years to $\bar{R}(\bar{T})$. This allows two quadratic functions to be fit to the data, one before 25 years and one after. At the node, the quadratic functions and their first derivative are continuous.

$$\bar{R} = \begin{cases} a_1 \bar{T}^2 + b_1 \bar{T} + c_1 & \bar{T} \leq \bar{T}_{t=25} \\ a_2 \bar{T}^2 + b_2 \bar{T} + c_2 & \bar{T} \geq \bar{T}_{t=25} \end{cases} \quad (3.6)$$

The fit over each run is shown in [Figure 3.1](#). For the first doubling of CO_2 , the equilibrium climate sensitivity is estimated to be 2.8 °C. However, the climate sensitivity implied by each subsequent doubling increases, until a total of almost 10 °C difference between $8\times\text{CO}_2$ and $16\times\text{CO}_2$ is reached. The slope of the line in [Figure 3.1](#), $\lambda(\bar{T})$, increases as the surface warms, and this is particularly apparent for higher forcings. We will return to the evolution of $\lambda(\bar{T})$ for each forcing strength in [Section 3.8](#). But first of all, let us develop a framework for what causes changes in $\lambda(\bar{T})$ at the regional level.

3.5 ISOLATING THE COMPONENTS OF THE PATTERN EFFECT

Changes in $\lambda(\bar{T})$ might occur due to the influence of changing warming patterns or changing regional feedbacks, or a combination of both. To isolate each effect, we first write the global TOA imbalance as the spatial average of the imbalance in each region. The regional imbalance is assumed to be a function of regional temperature change, $R_i(T_i)$, and the regional temperature change is assumed to evolve as a function of the global mean surface temperature change, $T_i(\bar{T})$. Expanding [Equation 3.5](#) to include these assumptions gives:

$$\lambda(\bar{T}) = \frac{d}{d\bar{T}} \left(\overline{R_i(T_i(\bar{T}))} \right) = \frac{dR_i}{dT_i} \frac{dT_i}{d\bar{T}}. \quad (3.7)$$

Each region is represented by the subscript i . To allow for state-dependence of the warming pattern and regional feedbacks, I assume a quadratic relationship for $R_i(T_i)$ and $T_i(\bar{T})$:

$$R_i(T_i) = \beta_{2i} T_i^2 + \beta_{1i} T_i + \beta_{0i} \quad (3.8)$$

$$T_i(\bar{T}) = \rho_{2i} \bar{T}^2 + \rho_{1i} \bar{T} + \rho_{0i} \quad (3.9)$$

Each β and ρ is a constant. Since quadratic splines are fitted to the data, the constants change at the node point ($t = 25$ years), but this does not affect the analysis.

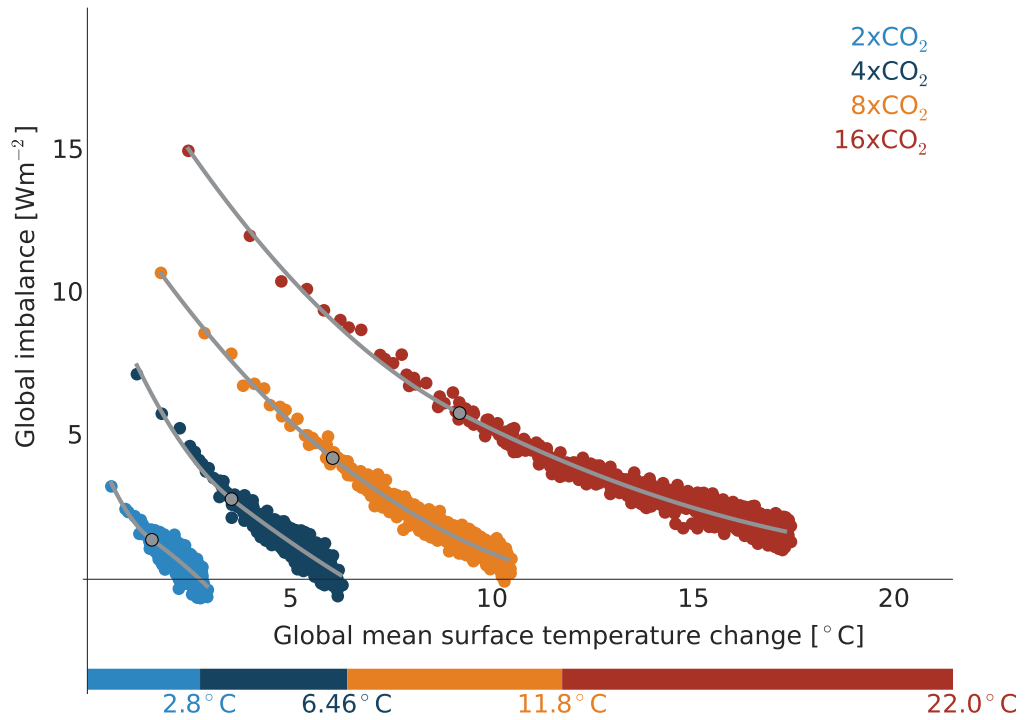


Figure 3.1: THE NON-LINEAR RELATIONSHIP BETWEEN ENERGY IMBALANCE AND SURFACE WARMING IN ABRUPT FORCING EXPERIMENTS. Top-of-atmosphere radiation imbalance plotted against global mean surface temperature change, for abrupt forcing simulations of one or multiple CO₂ concentration doublings integrated out to 1000 years. Grey lines represent quadratic spline fits with a single node at 25 years (grey dots). Coloured bars indicate the equilibrium warming estimated by extending the slope of the line out to the horizontal axis, using the slope diagnosed at year 1000. In a linear forcing-feedback framework with constant climate sensitivity, all coloured bars should be equal in length.

The parameter β_{2i} determines the changes in regional feedbacks. The parameter ρ_{2i} determines the changes in the warming pattern. By setting $\beta_{2i} = \rho_{2i} = 0$ everywhere, we assume constant regional feedbacks and a constant spatial warming pattern, which returns to the linearity assumption, denoted here with the asterisk:

$$R_i^*(T_i) \equiv R_{i,\beta_2=0} = \beta_{1i} T_i + \beta_{0i} \quad (3.10)$$

$$T_i^*(\bar{T}) \equiv T_{i,\rho_2=0} = \rho_{1i} \bar{T} + \rho_{0i} \quad (3.11)$$

Linear approximations for both R_i and T_i give $\bar{R}^* \equiv \overline{R_i^*(T_i^*)}$ and the following expression for λ^* , from [Equation 3.7](#):

$$\lambda^* \equiv \lambda_{\beta_2,\rho_2=0} = \overline{\beta_{1i} \rho_{1i}} \quad (3.12)$$

The linear approximation λ^* is therefore a constant equal to the spatial mean of constant regional feedbacks weighted by the warming pattern. I now derive expressions for the temperature and feedback components, by allowing either the warming pattern or the regional feedbacks to evolve as a function of \bar{T} .

3.5.1 The temperature component

If the spatial warming pattern evolves with \bar{T} but regional feedbacks are static, we can set $\beta_{2i} = 0$ everywhere, and estimate the regional feedbacks (β_{1i}) from a linear regression between regional TOA and regional temperature in each region. This represents the pattern effect as described in Armour et al. (2013), which I call the ‘temperature component’. The imbalance becomes $\bar{R}_T \equiv \overline{R_i^*(\bar{T}_i)}$, and from [Equation 3.7](#) the expression for λ_T is:

$$\lambda_T \equiv \lambda_{\beta_2=0} = 2\overline{\beta_{1i} \rho_{2i}} \bar{T} + \lambda^* \quad (3.13)$$

Note that λ_T is the combination of the linear component, λ^* , and a temperature-dependent term, which is determined by the warming pattern’s change with temperature (ρ_{2i}) weighted by the regional feedback strength (β_{1i}).

3.5.2 The feedback component

Assume that the pattern effect is caused only by changes to regional feedbacks. For this case the warming pattern is constant, which sets $\rho_{2i} = 0$ everywhere. The regional warming rates with respect to the global mean (ρ_{1i}) are estimated by linear regression over the entire run. This formulation, the ‘feedback component’, gives $\bar{R}_F \equiv \overline{R_i(T_i^*)}$ and the expression for λ_F is:

$$\lambda_F \equiv \lambda_{\rho_2=0} = 2\overline{\beta_{2i} \rho_{1i}^2} \bar{T} + 2\overline{\beta_{2i} \rho_{1i} \rho_{0i}} + \lambda^* \quad (3.14)$$

λ_F contains the linear approximation λ^* as well. The temperature-dependent term is determined by how regional feedbacks change with temperature (β_{2i}), weighted by the regional warming rate squared (ρ_{1i}^2).

3.5.3 The combined pattern effect

The combined pattern effect takes into account the temperature-dependent changes in both regional feedbacks and the spatial warming pattern ($\bar{R}_C \equiv \bar{R}_i(\bar{T}_i)$). The global feedback parameter for the combined pattern effect, λ_C , becomes:

$$\lambda_C = \frac{\overline{4\beta_{2i} \rho_{2i}^2} \bar{T}^3 + 6\overline{\beta_{2i} \rho_{2i} \rho_{1i}} \bar{T}^2 + \overline{4\beta_{2i} \rho_{2i} \rho_{0i}} + 2\overline{\beta_{2i} \rho_{1i}^2} + 2\overline{\beta_{1i} \rho_{2i}} \bar{T} + 2\overline{\beta_{2i} \rho_{1i} \rho_{0i}} + \lambda^*}{\overline{4\beta_{2i} \rho_{2i} \rho_{0i}} + 2\overline{\beta_{2i} \rho_{1i}^2} + 2\overline{\beta_{1i} \rho_{2i}} \bar{T} + 2\overline{\beta_{2i} \rho_{1i} \rho_{0i}} + \lambda^*} \quad (3.15)$$

λ_C includes the linear approximation λ^* , the temperature-dependent terms in λ_T and λ_F , as well as higher-order terms in \bar{T} . Errors in the regression model become amplified through these higher-order terms, but if we are willing to neglect them, we can estimate λ_C more parsimoniously by expressing the regional top-of-atmosphere imbalance as a function of global mean surface temperature, $R_i(\bar{T})$. Assuming a quadratic relationship:

$$R_i(\bar{T}) = \gamma_{2i} \bar{T}^2 + \gamma_{1i} \bar{T} + \gamma_{0i}, \quad (3.16)$$

the expression for λ_C becomes

$$\lambda_C = \frac{d}{d\bar{T}} \left(\overline{R_i(\bar{T})} \right) = 2\overline{\gamma_{2i}} \bar{T} + \overline{\gamma_{1i}}. \quad (3.17)$$

The constant $\overline{\gamma_2}$ approximates the combined effects of a changing warming pattern and changing regional feedbacks.

To diagnose regional feedbacks, some studies regress the regional TOA imbalance against regional temperature (Rose and Rayborn 2016; Rose et al. 2014), as per the formulation in Equation 3.8 whereas others regress the regional TOA imbalance against the global mean surface temperature (Andrews et al. 2015; Block and Mauritsen 2013; Rugenstein et al. 2016a), as per Equation 3.16. This leads to a nomenclature problem of which the reader should be aware (Feldl and Roe 2013). Although the result of both methods is called the ‘regional feedback’, the first method returns regional feedbacks as we define them in this study (β_2, β_1), whereas the second method diagnoses the regional contribution to the combined pattern effect (γ_2, γ_1), which implicitly includes the effects of both regional feedbacks and the warming pattern.

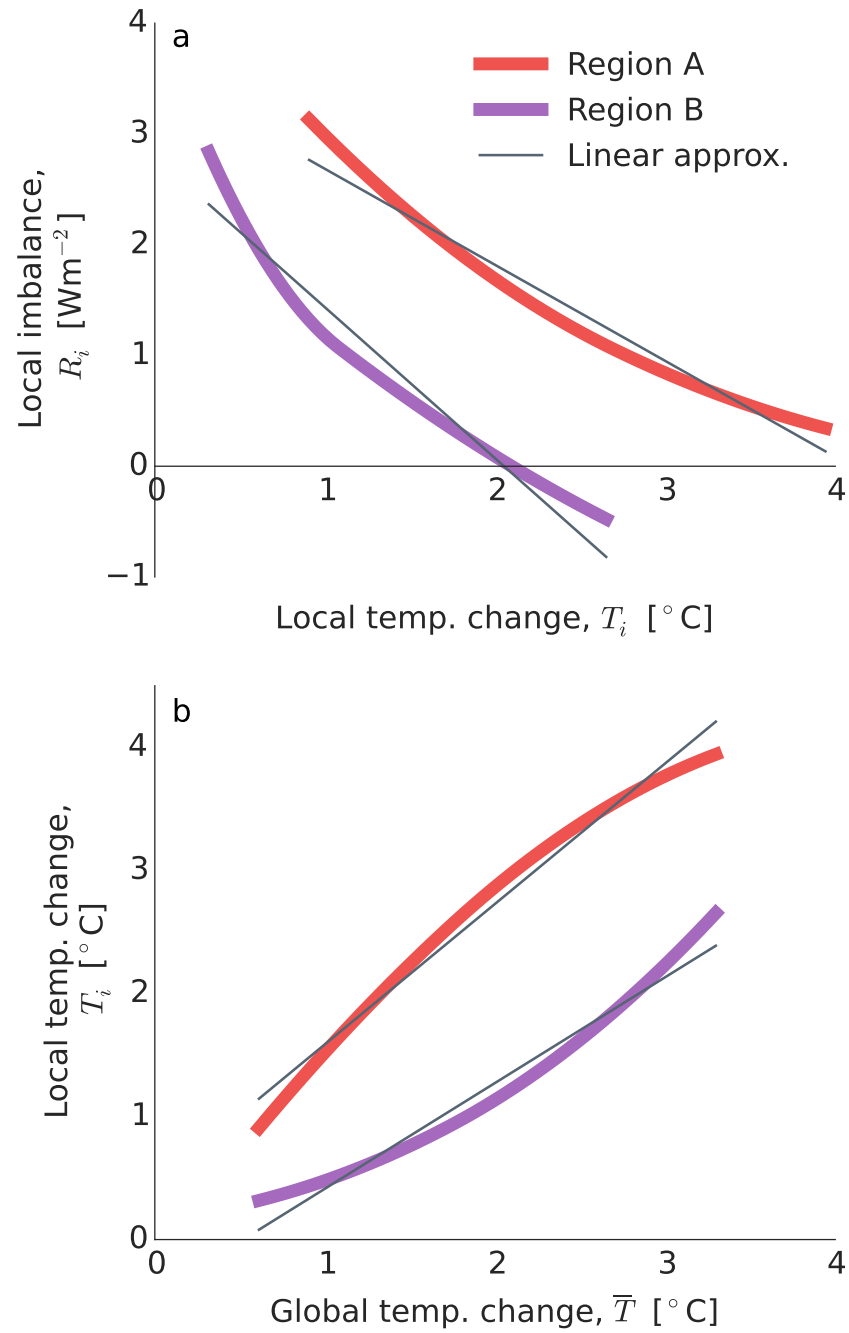


Figure 3.2: A TWO-REGION EXAMPLE OF THE PATTERN EFFECT. *a*, The relationship between the regional top-of-atmosphere radiation imbalance and regional surface warming. *b*, The relationship between regional surface warming and the global mean surface warming. Grey lines represent linear approximations of the true relationships, which are based on splines selected for illustrative purposes only.

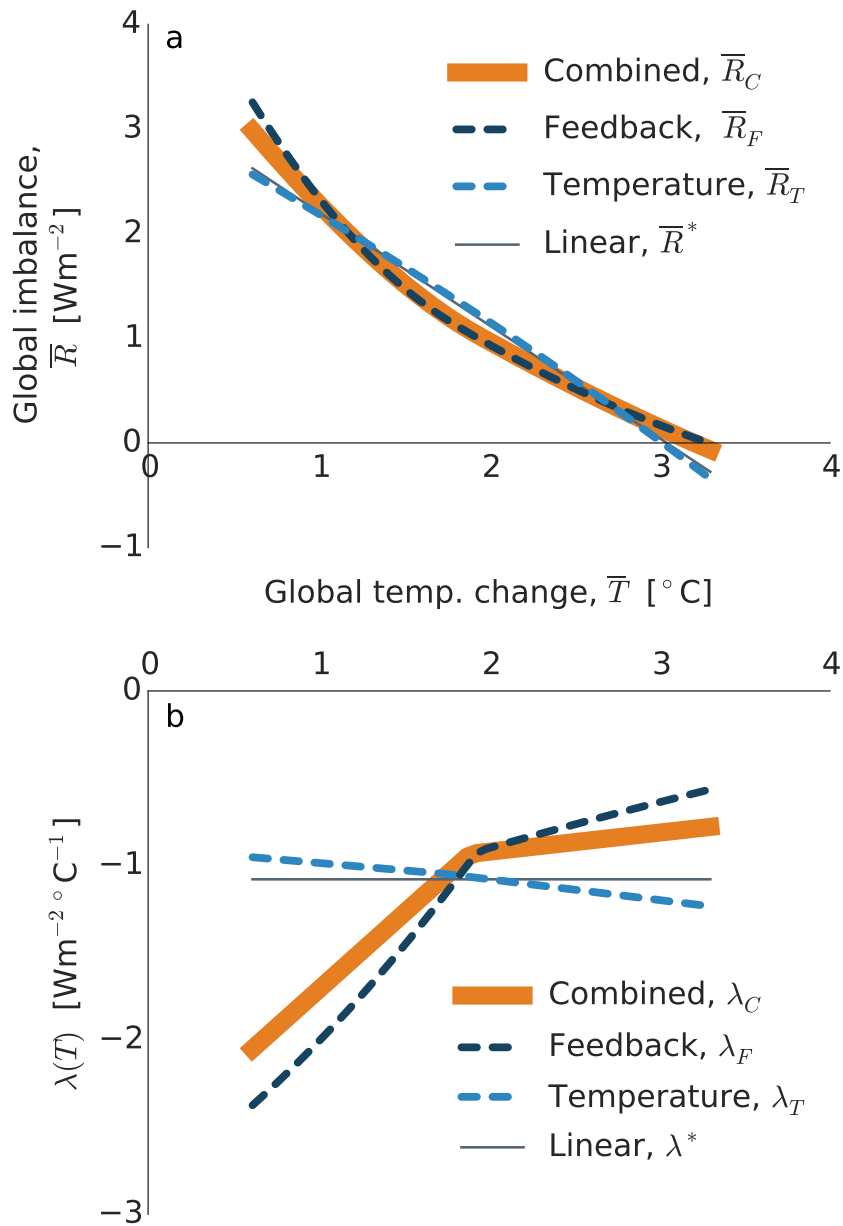


Figure 3.3: COMPONENTS OF THE PATTERN EFFECT IN THE TWO-REGION EXAMPLE. *a*, The global top-of-atmosphere imbalance against surface warming. *b*, The evolution of $\lambda(\bar{T})$ with surface warming. Shown are the true values ('combined'); reconstructions for the 'feedback' and 'temperature' components of the pattern effect; and a linear approximation, based on the assumption of a constant warming pattern and constant regional feedbacks.

3.6 A SIMPLE TWO-REGION EXAMPLE

Before applying the framework developed in the preceding section to the full model output, it is helpful to consider a simple two-region example.

Figure 3.2 shows $R_i(T_i)$ and $T_i(\bar{T})$ for each of two regions with equal area. The regions are based on a quadratic spline fit to data defined by 30°N–90°N (Region A) and 30°S–90°S (Region B) in the 2xCO₂ run; the global mean is defined as the average of the two regions. Exclusion of the tropics makes the example non-physical, but it is useful for illustrative purposes, because it helps highlight the non-linear warming rates in the extra-tropics (Armour et al. 2013).

For each region the grey lines represent the linear approximations, R_i^* or T_i^* , which assume no change in the warming pattern or the regional feedbacks. Using only these linear approximations to reconstruct the global imbalance and the global feedback parameter, we get the constant λ^* and a corresponding linear estimate of the change in imbalance, \bar{R}^* , as shown in Figure 3.3. The temperature component is the combination of the linear approximation in Figure 3.2a and coloured splines in Figure 3.2b. Conversely, the feedback component is the combination of coloured splines in Figure 3.2a and the linear approximation in Figure 3.2b.

In this simple two-region example, the temperature component has little explanatory power for the combined pattern effect. In Figure 3.3, the temperature component is almost identical to the linear approximation, despite the visible non-linearity in regional warming rates (see Figure 3.2b). Changing regional feedbacks, which are indicated by the non-linear relationship between regional TOA imbalance and regional temperature (Figure 3.2a), largely determine the changes to $\lambda(\bar{T})$: compare the dark blue dashed line and the yellow line in Figure 3.3b.

Examining the different expressions for $\lambda(\bar{T})$ can help us understand why. Both temperature and feedback components share the linear part, λ^* , which defines the first-order response to forcing. This is why the estimates of \bar{R} in Figure 3.3a are relatively similar. What sets the temperature and feedback components apart are the temperature-dependent terms in $\lambda(\bar{T})$. For the temperature component this term is $\frac{d\lambda_T}{d\bar{T}} = 2\beta_{1i} \rho_{2i}$. In the two-region example the expression becomes:

$$\begin{aligned} \frac{d\lambda_T}{d\bar{T}} &= \beta_{1A} \rho_{2A} + \beta_{1B} \rho_{2B} = (\beta_{1A} - \beta_{1B}) \rho_{2A} \\ &= 2\beta'_1 \rho_2, \end{aligned} \quad (3.18)$$

where the anomaly of Region A's regional feedback from the mean regional feedback is $\beta'_1 \equiv \beta_{1A} - \bar{\beta}_{1i}$, and we write $\rho_2 = \rho_{2A} = -\rho_{2B}$ since the spatial mean of all regional temperature change must be equal to the global temperature change, implying $\bar{\rho}_{2i} = 0$.

For the feedback component, the temperature-dependent term is $\frac{d\lambda_F}{d\bar{T}} = 2\beta_{2i} \rho_{1i}^2$, which in the two-region example becomes

$$\begin{aligned} \frac{d\lambda_F}{d\bar{T}} &= \rho_{1A}^2 \beta_{2A} + \rho_{1B}^2 \beta_{2B} \\ &= (1 + \rho_1')(\beta_{2A} + \beta_{2B}) + 2\rho_1'(\beta_{2A} - \beta_{2B}) \end{aligned} \quad (3.19)$$

The deviation of Region A's regional warming rate from unity is defined by:

$$\rho_1' \equiv \rho_{1A} - \bar{\rho}_{1i} = \rho_{1A} - 1.$$

In each of [Equation 3.18](#) and [Equation 3.19](#) there are two groups of terms. The first group, β_1' or ρ_1' , represents the difference in slope between the linear approximations in each region. This group multiplies a second group of terms, ρ_2 or β_2 , which represents the non-linear behaviour in each relationship respectively – a changing warming pattern or changing regional feedbacks.

These formulations help explain why the temperature component is less effective at influencing changes $\lambda(\bar{T})$ at the global level than the feedback component. For either component, the role of the second group of constants is clear: if these are zero, there can be no changes to $\lambda(\bar{T})$ and the linear approximation λ^* holds. The behaviour of the first group of constants is, however, different for each component.

For the temperature component, a non-zero $\frac{d\lambda}{d\bar{T}}$ requires that the regional feedbacks are different in magnitude so that β_1' is not zero. In this particular two-region example, the temperature component is small because there is only a small difference in slope between the grey lines in [Figure 3.2a](#), and so β_1' is small.

For the feedback component, there are fewer constraints: when the difference between regional warming rates is zero ($\rho_1' = 0$), changes to $\lambda(\bar{T})$ occur:

$$\frac{d\lambda_F}{d\bar{T}} = \beta_{2A} + \beta_{2B}.$$

On the other hand, when the difference between regional warming rates ρ_1' is large, $\frac{d\lambda_F}{d\bar{T}}$ is still non-zero. For example, if $\rho_{1A} = 0$ then $\rho_1' = 2$ and

$$\frac{d\lambda_F}{d\bar{T}} = 4\beta_{2B}.$$

The only cases in which $\frac{d\lambda_F}{d\bar{T}}$ can be zero are if the β_2 terms are all zero or when the feedback changes cancel each other: $\beta_{2A} = -\beta_{2B}$ and $\rho_1' = 0$. Since there are fewer constraints on the feedback component, we can expect more cases in which it influences changes in $\lambda(\bar{T})$ than does the temperature component.

The disadvantage of using the two-region model is that non-linearities in $T_i(\bar{T})$ *within* each region are disguised by area-averaging and interpreted as non-linearities in $R_i(T_i)$. In other words, the feedback component is favoured if large regions are chosen that can support changing warming patterns internally. I now turn to the full model output, and increase the spatial resolution of the framework.

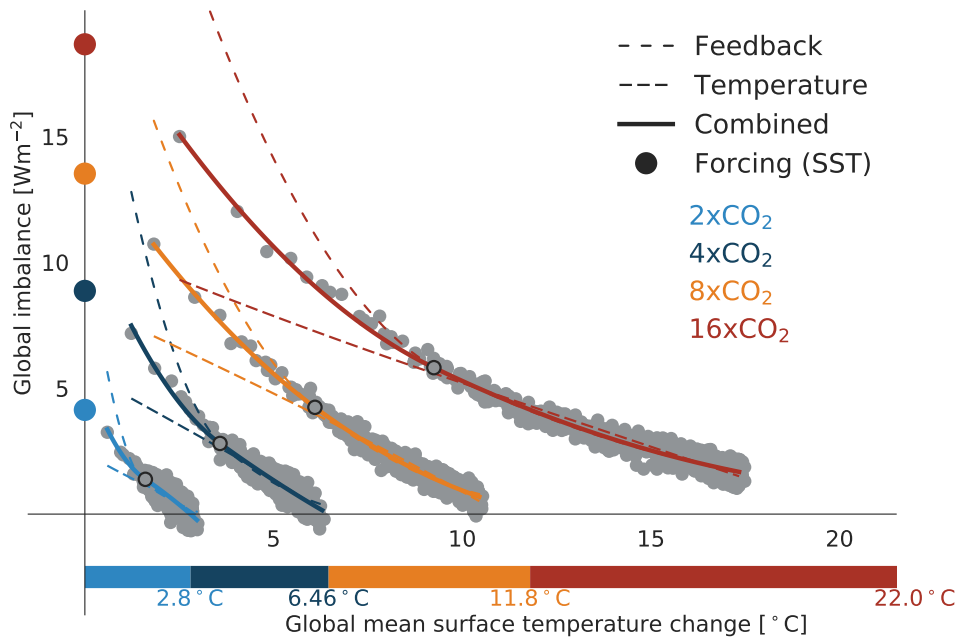


Figure 3.4: COMPONENTS OF THE PATTERN EFFECT MISREPRESENT THE INITIAL RESPONSE TO FORCING. Coloured lines reconstruct the global relationship between top-of-atmosphere radiation and surface warming from zonal values, according to: the feedback component, which estimates feedbacks with a spline fit but assumes a constant warming pattern; the temperature component, which estimates warming rates with a spline fit but assumes constant feedbacks; and, the combined effect, which estimates both feedbacks and warming patterns with spline fits. Large coloured dots on the vertical axis represent effective radiative forcing estimated from fixed-SST experiments. Grey dots represent coupled model output, as in Figure 3.1.

3.7 RECONSTRUCTING THE ENERGY IMBALANCE

In this section I reconstruct the global TOA imbalance shown in Figure 3.1 by using the assumptions for the temperature and feedback components of the pattern effect. For the combined effect, I use Equation 3.16. I use zonal means of TOA imbalance and surface warming at each model latitude to perform the necessary spline or linear fits for the relationships $R_i(T_i)$ and $T_i(\bar{T})$. I choose zonal means because further reducing the area of each region increases the noise due to internal variability and introduces error into the results. And, since regional feedbacks and differences in warming rate are by far most varied in the meridional direction (Armour et al. 2013), further increasing the resolution beyond the zonal regions adds only limited descriptive information. The results are shown in Figure 3.4.

Both temperature and feedback components of the pattern effect approximate the long-term response well. The good fit in this period is achieved for two reasons. Firstly, since the temperature component,

the feedback component, and the combined pattern effect all contain the linear approximation λ^* , their first-order approximations of $R(\bar{T})$ are similar. This was also the case in the two-region example.

Secondly, the regressions are weighted toward the long-term response. Each regression implies a relationship in temperature space but is constrained by the degrees of freedom related to time-based model output. The regressions are weighted toward the long-term response, because the model spends considerably more time there (Stevens et al. 2013). This is the case in most studies that analyse climate sensitivity with regression methods, and some weight the long-term response even more strongly by averaging the data in time (see, for example Armour et al. 2013).

Despite representing the long-term response well, both temperature and feedback components misrepresent the initial decades. If we were to extend either component back to the vertical axis in Figure 3.4, using the gradient diagnosed for the first year ($\lambda(\bar{T}_{t=1})$), we would severely misdiagnose the external forcing that we estimated from fixed-SST experiments (large coloured dots in Figure 3.4). The temperature component underestimates the forcing, and the feedback component overestimates it. The combined pattern effect, however, can capture the initial non-linear behaviour and can better estimate the external forcing diagnosed from fixed-SST experiments.

The varying estimates of forcing imply different interpretations of climate feedbacks diagnosed from the Gregory method – the effective climate feedback parameter, λ_{eff} . In Figure 3.5 I calculate λ_{eff} for the temperature and feedback components, and for the combined pattern effect, by extrapolating each curve in Figure 3.4 out to the intersection with the horizontal and vertical axes. To make the extrapolation, I use the initial and final diagnosed gradients ($\lambda(\bar{T}_{t=1})$ and $\lambda(\bar{T}_{t=1000})$). The extrapolation provides estimates of the initial forcing (F) and equilibrium warming (T_{eq}) in Equation 3.3. I compare the results with a best-estimate based on external forcing, diagnosed from fixed-SST experiments, and equilibrium warming estimated from the combined effect, as shown by the coloured bars in Figure 3.1 and Figure 3.4.

Misrepresenting the initial period has serious implications for λ_{eff} . The feedback component overestimates the forcing, and so also overestimates the magnitude of λ_{eff} . The temperature component underestimates the forcing, and so underestimates the magnitude of λ_{eff} . The combined effect shows similar results to the best estimate ('SST' in Figure 3.5), at least for 8xCO₂ and 16xCO₂. In 2xCO₂ and 4xCO₂, there are larger differences in λ_{eff} between the fixed-SST and the combined method, because of small discrepancies in the forcing estimate. For small initial forcings, λ_{eff} is very sensitive to errors in the forcing because the errors are concentrated over a smaller total range of warming.

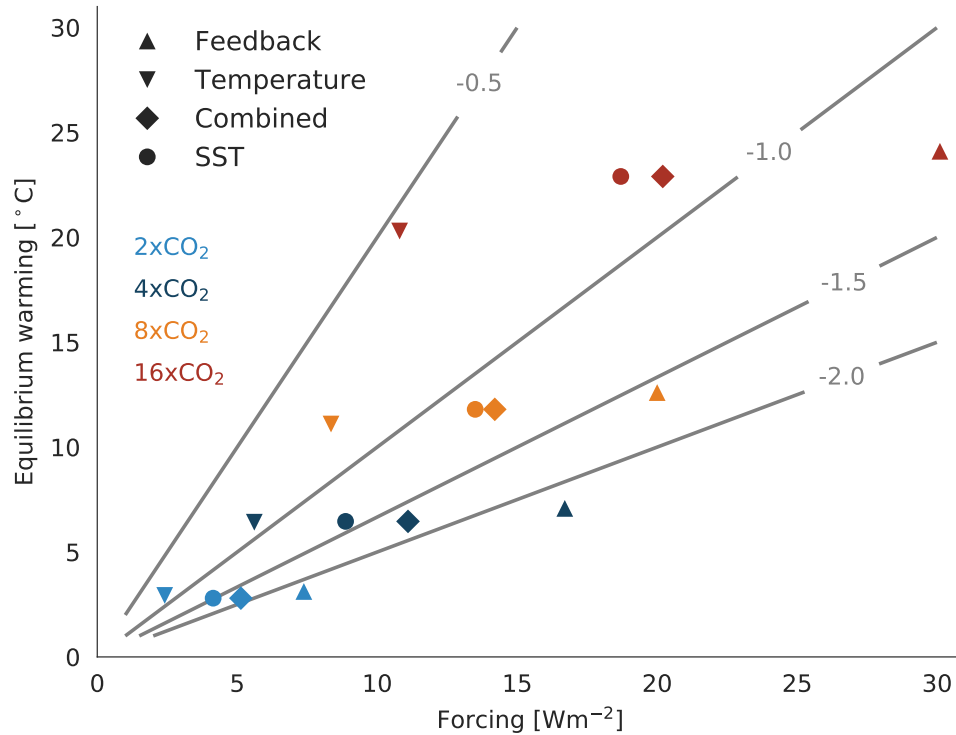


Figure 3.5: COMPONENTS OF THE PATTERN EFFECT MISDIAGNOSE THE EFFECTIVE CLIMATE FEEDBACK PARAMETER. The relationship between the forcing estimate and equilibrium warming for each component of the pattern effect are shown. Forcing and equilibrium warming are first estimated by extrapolating each curve in Figure 3.4 out to its intercept with the vertical and horizontal axes. Contours show the estimated effective climate feedback parameter λ_{eff} . 'SST' denotes forcing estimated from fixed-SST experiments and equilibrium warming as estimated in Figure 3.1. All the methods calculate similar equilibrium warming, but the temperature and feedback components misrepresent the forcing and therefore the climate feedback parameter.

The differential global feedback parameter $\lambda(\bar{T})$ avoids carrying these forcing errors across all timescales, because the differential form is not effected by the definition of forcing, only the relationship between TOA imbalance and warming. $\lambda(\bar{T})$ further allows us to understand how the pattern effect evolves over different timescales and surface temperatures, which is what I turn to next.

3.8 THE CHANGING GLOBAL FEEDBACK PARAMETER

The evolution of $\lambda = \lambda(\bar{T})$ for each forcing strength is shown in [Figure 3.6](#), with corresponding estimates from the temperature and feedback components. Across all temperatures and forcings, the temperature component predicts almost no change to the global feedback parameter. As in the two-region example, the non-linear feedbacks provide the changes. The combined interaction between temperature and feedback components is needed to reconstruct $\lambda(\bar{T})$ in the initial period.

The reason why the temperature and feedback components individually fail to represent the initial behaviour of $\lambda(\bar{T})$ can be appreciated at the regional level. From the perspective of the temperature component, rapid changes in the warming pattern suggest that the extra-tropics dominate the pattern effect in all runs (compare [Figure 3.7g](#) and [Figure 3.7h](#)). However, the temperature component estimates constant feedbacks by a linear regression that favours the long-term response. The assumed feedbacks therefore approximately match the values shown in [Figure 3.7f](#), in which the Northern and Southern extra-tropics have similar feedbacks. This is equivalent to a small β'_1 in the two region model ([Equation 3.18](#)), and accordingly a negligible $\frac{d\lambda}{d\bar{T}}$ for the temperature component.

From the perspective of the feedback component, the most drastic changes in the initial response occur over the Southern Ocean. The regional feedbacks there rapidly change from strongly negative values (as much as $-18 \text{ Wm}^{-2} \text{ }^\circ\text{C}^{-1}$ for the $2\times\text{CO}_2$ scenario) to more moderate negative values (compare [Figure 3.7d](#) and [Figure 3.7e](#)). The feedback component assumes a constant warming pattern biased toward the long-term response, and neglects that warming rates near the beginning of the run are near zero over the Southern Ocean ([Figure 3.7g](#)). Therefore, the feedback component inflates the value of ρ_{1i} for a region in which β_{2i} is very large. According to the two-region example and [Equation 3.19](#), this overestimates $\frac{d\lambda}{d\bar{T}}$. The Southern Ocean's true contribution to changes in $\lambda(\bar{T})$ is more modest, as can be seen by comparing the change between [Figure 3.7a](#) and [Figure 3.7b](#) and between [Figure 3.7d](#) and [Figure 3.7e](#) for this region.

The initial changes over the Southern Ocean are indicative of an intimate link between warming patterns and feedback changes. The PRP diagnostics show that the increasing regional feedbacks are a re-

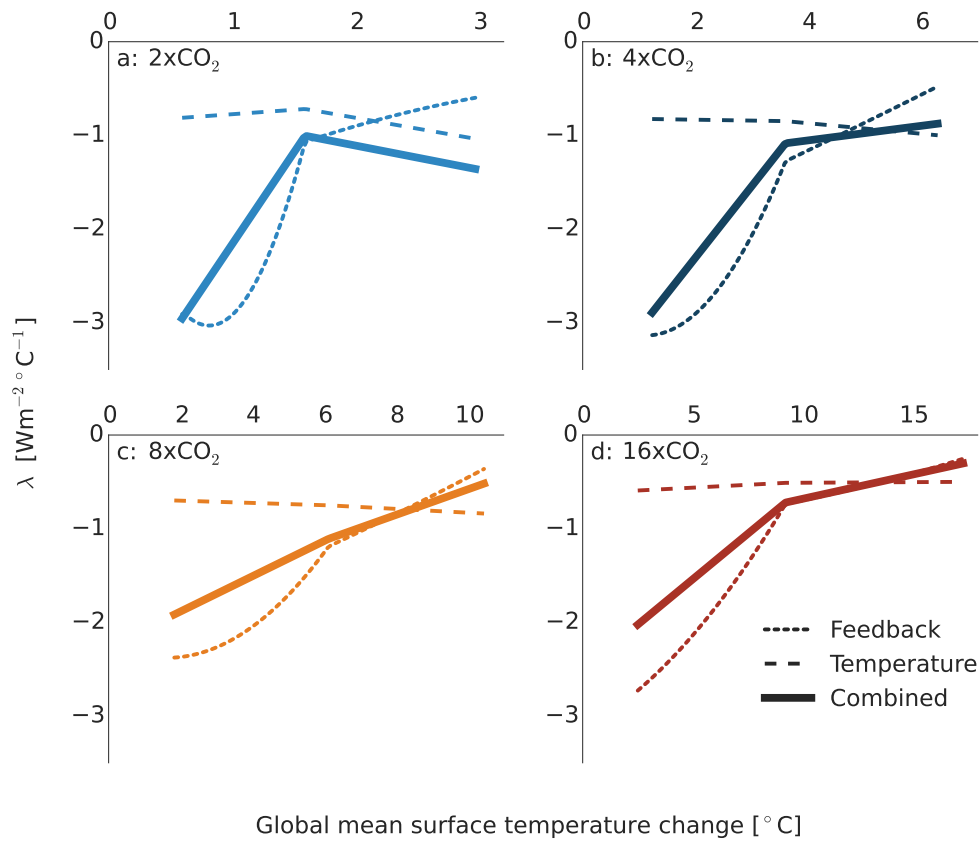


Figure 3.6: TEMPERATURE COMPONENT DIAGNOSES NEAR-CONSTANT GLOBAL FEEDBACK PARAMETER. For each forcing strength, the changes in the global feedback parameter are reconstructed from the temperature and feedback components, and for the combined effect (coloured solid lines). For the initial response, neither the temperature nor the feedback component represent the combined effect, but the changes in λ are almost exclusively a result of the feedback component. Under strong forcings and after the first 25 years, the feedback component alone closely matches the combined effect.

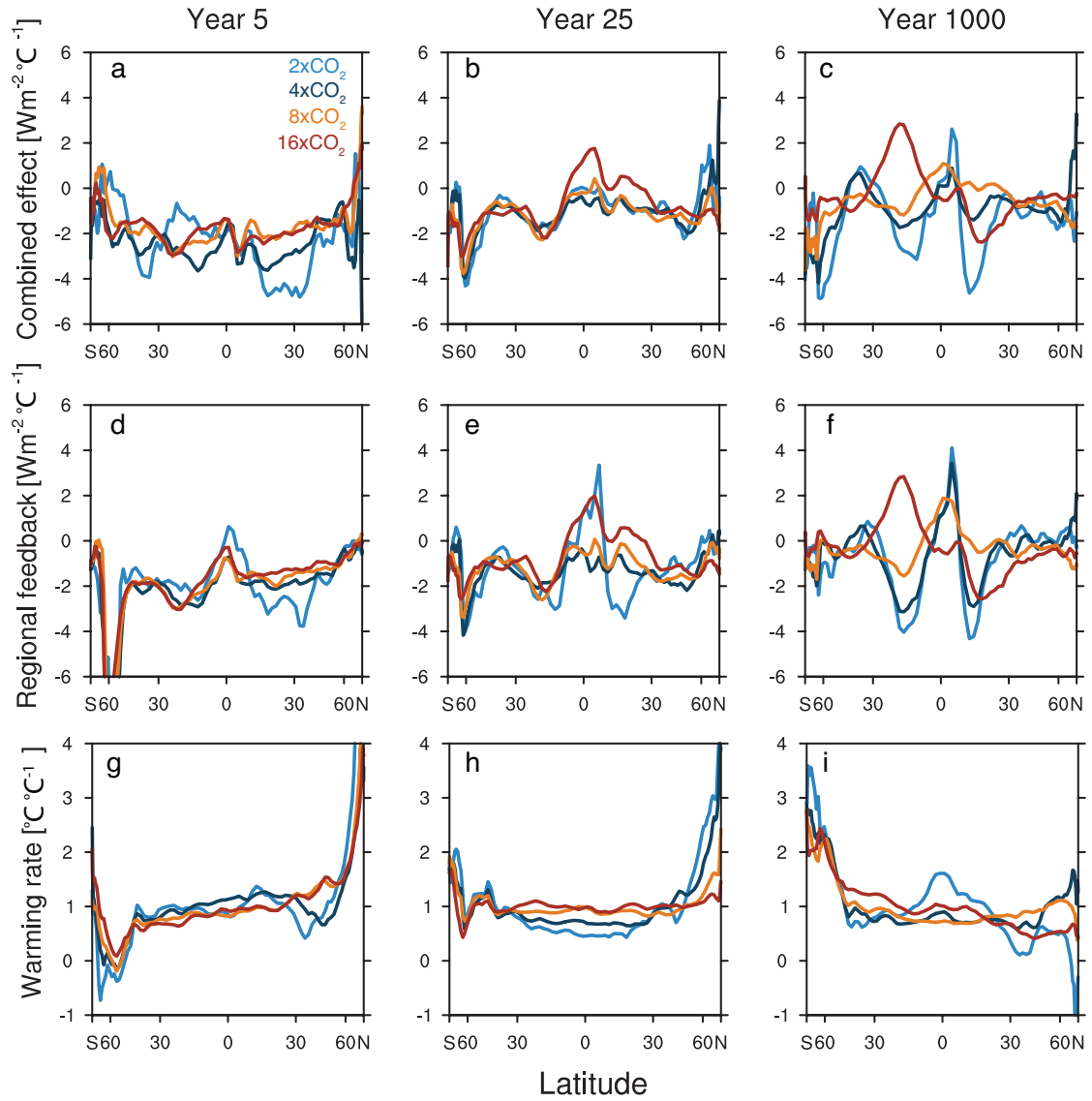


Figure 3.7: REGIONAL CONTRIBUTIONS TO THE PATTERN EFFECT. The estimates for the regional contributions to the combined pattern effect are shown in *a-c*. The area-weighted integral under each curve in *a-c* returns the combined effect (solid line) in Figure 3.4. The combined effect is a result of changing regional feedbacks (*d-f*) and changing regional warming rates with respect to the global mean (*h-j*). Values are shown for each latitude at three timesteps representing the initial response (years 5 to 25) and the long-term response (years 25 to 1000).

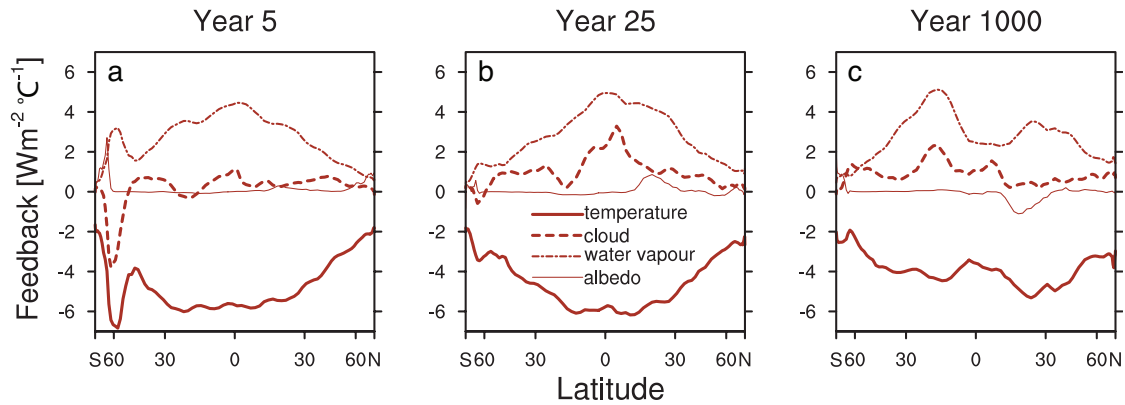


Figure 3.8: INDIVIDUAL RADIATIVE FEEDBACKS IN $16\times\text{CO}_2$. The regional influence of individual radiative feedbacks is calculated using partial-radiative-feedback diagnostics (Methods), only for the $16\times\text{CO}_2$ scenario. Feedbacks are then calculated in the same way as the total feedbacks: the regression between the regional contribution to the radiative imbalance at the top of the atmosphere against regional surface temperature. Local feedbacks are shown for year 5 (a), 25 (b) and 1000 (c).

sult of temperature and cloud feedbacks (compare Figure 3.8a and Figure 3.8b). The regional delay in warming, caused by ocean heat uptake, allows the surface warming to temporarily decouple from warming in the troposphere (Figure 3.9), resulting in a strong lapse rate feedback. The tropospheric warming might also induce a shift from ice to liquid clouds (Ceppi et al. 2016; Choi et al. 2014; McCoy et al. 2015; Tan et al. 2016) or changes to atmospheric stability that influence cloud cover (Kay et al. 2014), which would both lead to more positive feedbacks. These feedback changes are therefore inseparable from the changes to regional warming patterns over the Southern Ocean.

When we consider the combined pattern effect, we see contributions to an increasing $\lambda(\bar{T})$ from almost all latitudes, but especially in the tropics (compare Figure 3.7d and Figure 3.7e). Partial radiative perturbation diagnostics for the $16\times\text{CO}_2$ scenario show that the changes over the tropics are mostly due to increases in cloud, with some water vapour contribution (compare Figure 3.8a and Figure 3.8b). A rising tropopause is perhaps responsible (Meraner et al. 2013).

In the long-term response, the changes in $\lambda(\bar{T})$ respective to warming are less pronounced than in the initial response (Figure 3.6). In $2\times\text{CO}_2$ and $4\times\text{CO}_2$, the modest changes in λ are not particularly well represented by either component. But for $8\times\text{CO}_2$ and $16\times\text{CO}_2$, where the signal is stronger, the regional feedback component represents the total combined pattern effect well (Figure 3.6).

At the regional level, we see that changes in regional feedback during the long-term response are strongly dependent on forcing strength. The meridional structure of the pattern effect is strikingly similar across all forcing strengths by year 25 (Figure 3.7b), but in the long-term response the structures diverge. In $2\times\text{CO}_2$ and $4\times\text{CO}_2$, the

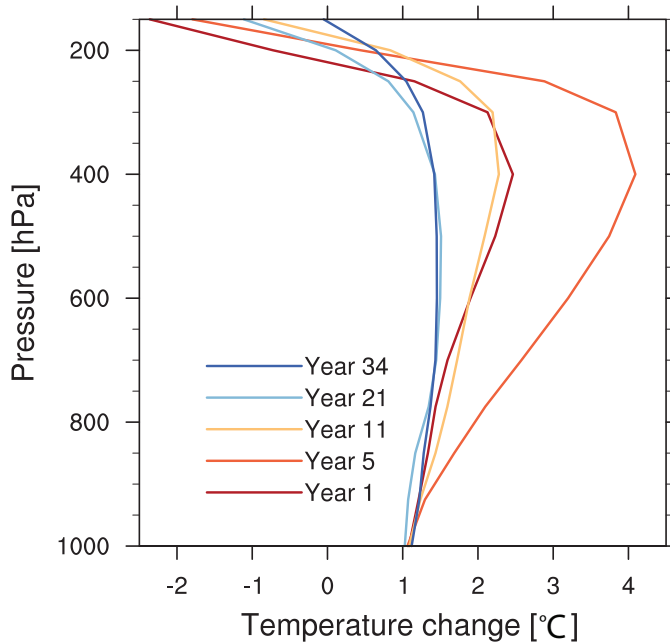


Figure 3.9: INITIAL RAPID WARMING IN THE UPPER TROPOSPHERE CAUSES NEGATIVE FEEDBACKS OVER THE SOUTHERN OCEAN. The spatial average of atmospheric temperature change is shown for 50-65°S during the initial response to 16xCO₂ forcing. Each year is chosen so that the increase between years at the surface is approximately 1°C. During the first decade, the tropospheric temperature warms up to four times as fast as the surface. By the second decade warming is almost uniform throughout the troposphere.

structure is symmetrical about the equator (Figure 3.7c). In 16xCO₂ the structure is anti-symmetrical, with strong positive feedbacks in the Southern Hemisphere tropics (Figure 3.7c), due to temperature and water vapour feedbacks (Figure 3.8c).

Furthermore, the warming pattern does not significantly alter the projection of these feedbacks changes onto the pattern effect (in Figure 3.7, compare panels c, f, and i). The warming pattern plays no notable role in the long-term response, since the different forcings present widely different feedback structures despite similar warming patterns. The concept of the pattern effect therefore appears to lose importance for the global feedback parameter over time, especially for higher forcing strengths.

Instead, total warming drives the changes to feedbacks in the long-term response. Figure 3.10 shows the evolution of global $\lambda(\bar{T})$, as a function of time (note the logarithmic axis), and as a function of surface warming from year 25 onwards. Similarly sharp increases in $\lambda(\bar{T})$ occur in the initial two decades or so, despite the fact that the surface warming is different in each run at this point and spans a difference of around 7 °C from 2xCO₂ to 16xCO₂. In the long-term response, however, the changes to λ appear to follow a relationship that increases according to surface warming and not time.

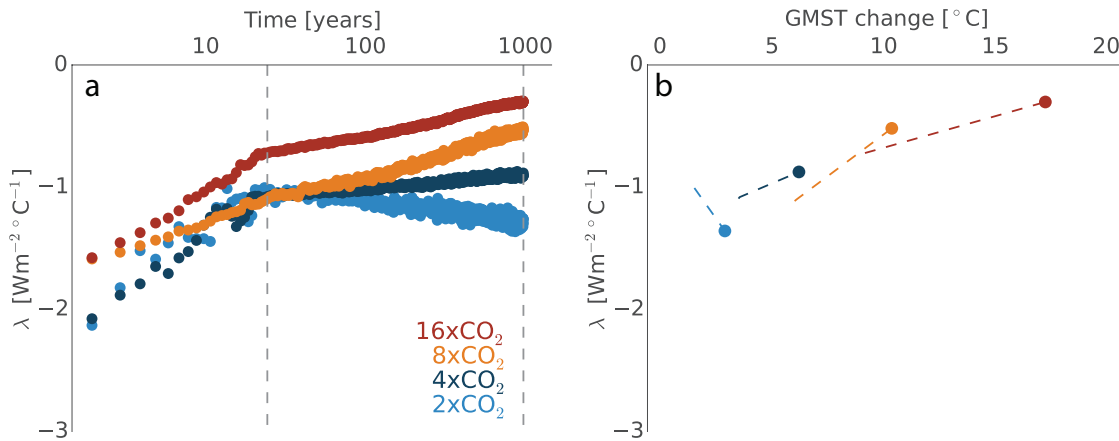


Figure 3.10: THE CHANGING GLOBAL FEEDBACK PARAMETER WITH TIME AND WITH SURFACE WARMING. The global feedback parameter, $\lambda(\bar{T})$, is estimated from the derivative with respect to surface warming of the spline fits in Figure 3.1. $\lambda(\bar{T})$ is shown against time on a logarithmic axis (a), where the axis starts at year 1.5, and against surface warming for years 25–1000 (b). Dotted vertical lines in a mark years 25 and 1000. Values at year 1000 are marked with coloured dots in b.

3.9 DISCUSSION

3.9.1 Reconciling interpretations of the pattern effect

My approach allows me to compare different interpretations of the pattern effect, by isolating its regional temperature and feedback components. I make use of only one climate model and so cannot provide definitive explanations for processes occurring in others. However, my approach does allow me to compare different methodological assumptions made in other studies and how these assumptions influence the interpretation of the pattern effect. Depending on the version of the pattern effect I choose, I can reproduce different results with the same set of model output.

By isolating the temperature component, I make similar assumptions to Armour et al. (2013) and achieve similar results. The temperature component suggests that the warming pattern more heavily weights feedbacks in the extra-tropics over time (Armour et al. 2013).

By isolating the feedback component I find, as do Senior and Mitchell (2000), significantly increasing regional feedbacks over the Southern Ocean. The PRP diagnostics reveal strong increases over the Southern Ocean in cloud and temperature feedbacks in MPI-ESM1.2, whereas Senior and Mitchell’s model and method reveal only cloud influences. Nevertheless, both their study and the feedback component in this study omit the regional combination of non-linear feedbacks and warming rates, and both reach similar conclusions about the Southern Ocean’s contribution to the global change in feedback.

The combined effect suggests that tropical cloud feedbacks dominate the change in climate feedback parameter in the initial response,

a conclusion which a review of CMIP5 models also reaches using a formulation that is equivalent to my combined effect (Andrews et al. 2015).

Not all of these interpretations are equally valid. The approach of Armour et al. (2013) produces a near-constant global feedback parameter across all times and across all forcing strengths in MPI-ESM1.2. Clearly, this version of the pattern effect cannot explain a time- or state-dependent climate sensitivity in the simulations presented here. In their study, Armour et al. (2013) show an excellent match between the simulated global radiative balance and their reconstruction. But because they use multi-decadal averaging, they mask discrepancies in the critical initial response and favour the long-term response. As I have shown here, I can reproduce the long-term response even if I assume that the warming pattern does not change. In fact, all formulations of the pattern effect can reproduce the long-term response because they share the linear feedback assumption and are weighted toward this period by the time-based nature of model output.

Furthermore, the framework that Armour et al. (2013) use shifts the critical initial behaviour in MPI-ESM1.2 into the forcing term, and therefore underestimates the global radiative feedback. Handling the initial period in this way is not trivial because it implies a different definition of forcing and prevents straightforward comparisons of climate sensitivity between models and observations.

Finally, misrepresenting the initial behaviour can also lead to spurious changes in regional feedbacks. The strong Southern Ocean feedbacks suggested by Senior and Mitchell (2000) appear in MPI-ESM1.2 if I neglect the slow warming rate in the initial period. But by considering the combined pattern effect I find, as do Block and Mauritsen (2013), a very different explanation for the initial response over the Southern Ocean: this region actually inhibits the increase in the global feedback parameter.

3.9.2 *Time- and state-dependence of climate feedbacks*

Changing feedbacks are often described as “time-dependent” (Andrews et al. 2015; Li et al. 2013; Senior and Mitchell 2000) or “state-dependent” (Bloch-Johnson et al. 2015; Stevens et al. 2016). There is no clear distinction between these two terms, since a change in feedbacks with the climate state must also necessarily be a change over time. The distinction, however, is not purely academic. Evidence from past climate states suggests that the equilibrium climate sensitivity was slightly higher than today during the last glacial maximum and the Pliocene (Hargreaves and Annan 2016; Hargreaves et al. 2012), and reached extreme values during the Eocene (Shaffer et al. 2016; Zachos et al. 2003). If climate feedbacks are systematically time-dependent, then the current observational estimates of climate sensitivity could

be temporarily suppressed and yield in the future to higher values. However, if feedbacks are state-dependent, then the state of the current climate may explain why we observe a lower sensitivity today compared to past climates.

The framework I propose here attempts to account for both time-dependent and state-dependent changes to climate feedbacks, by allowing for state-dependence and two timescales of response: an initial period of 25 years followed by a long-term response out to 1000 years after the forcing increase. The assumptions I make about the separation of timescales (Andrews et al. 2015; Geoffroy et al. 2013b; Held et al. 2010) and the addition of a quadratic temperature-dependence term (Bloch-Johnson et al. 2015), are simply a hybrid of previous approaches used to study changing climate sensitivity. However, these assumptions can influence the interpretation of climate sensitivity, especially at lower forcings where internal variability introduces uncertainty into the regression method. For the 2xCO₂ simulation, the weaker signal-to-noise ratio makes a determination of the slope in Figure 3.4 difficult.

However, the framework diagnoses similar initial behaviour of the global feedback parameter in the first 100 years or so, even in runs with stronger forcing and a higher signal-to-noise ratio. The overlap is especially strong between 2xCO₂, 4xCO₂ and 8xCO₂ (Figure 3.10). If climate sensitivity were exclusively state-dependent, we would not expect this behaviour, since the warming in the 8xCO₂ simulation is three times greater than that of 2xCO₂ after 25 years. And considering that the warming in 16xCO₂ is six times that of 2xCO₂ at that time, the differences in the global feedback parameter are remarkably small between the two runs. Rugenstein et al. (2016b) also find time-dependent behaviour in their model simulations, but ascribe the behaviour to changes in forcing. Since the surface warms considerably in the initial response – more than half the total warming that is reached after 1000 years occurs in the first 25 years – I find the concept of time-dependent feedbacks more helpful than time-dependent forcing. Whatever the interpretation, it appears that time-dependence does play a role in this initial period, and state-dependence alone cannot adequately describe the simulated behaviour.

In contrast, I find that the long-term response to warming depends on the climate state. The development of the global feedback parameter in the long-term response is clearly dependent on forcing strength and the extent of surface warming (Figure 3.10). In the 2xCO₂ simulation, $\lambda(\bar{T})$ appears to slightly decrease again with warming, as in Li et al. (2013), but this could be an artefact of the low-frequency noise in that run. The meridional structure of regional feedbacks in the tropics also seems strongly dependent on forcing strength, but the warming patterns do not appear to drastically alter the projection of these feedback structures onto the global level (Figure 3.7). This indicates that

the pattern effect is perhaps a misnomer for the long-term response to forcing, particularly under very strong forcing. Here the magnitude of surface warming becomes more important for regional feedbacks than the spatial pattern of that warming.

The fact that the pattern effect is strongest in the first two decades and depends, at least partly, on time could have considerable implications for how we interpret historical observations of climate sensitivity. Time-dependent forcing in the historical period can be reconstructed from multiple smaller step-changes based on abrupt forcing experiments (Good et al. 2011, 2013). If the behaviour in MPI-ESM1.2 is comparable to Earth, then time-dependence could have at least some influence on climate feedbacks not for two decades, as in the simulations presented here, but for as long as forcing is changing. This would imply that the equilibrium climate sensitivity we infer from observations today will continue to grow over time (Armour 2017). In that case, palaeoclimate proxies and model simulations would provide critical evidence for estimating the Earth's climate sensitivity, evidence that current observations could not necessarily provide. A warmer future might await us than that which observations of Earth currently lead us to expect.

CONCLUSIONS

I began this dissertation by asking four questions about the connection between regional and global perspectives of surface temperature change. I wish to summarise the answers to these questions directly, before proceeding to the final section, in which I integrate my results – and the methods I have used to obtain them – into the wider scientific context.

4.1 THE SURFACE-WARMING HIATUS

In Chapter 2, I used 100 simulations of the historical period with a single, coupled climate model to investigate events similar to the 1998–2012 hiatus. That is, I considered 15-year periods in which internal variability was strong enough to allow the GMST trend to deviate by at least -0.17 °C per decade from the 100-member ensemble mean. I compared different choices for the surface layer energy budget, and explored how these choices could influence interpretation of the hiatus. Using insights gained from the large model ensemble, I attempted to diagnose the origin of the hiatus in two energy budgets formed from observational products over the 2000s. In doing so, I found the following answers to my research questions.

1. a) **Why are there multiple and conflicting accounts that regional ocean heat uptake caused the 1998–2012 hiatus?**
 - The methodologies in previous studies will produce false positives: they use energy budget formulations that are inconsistent with changes in GMST and therefore misdiagnose the hiatus.
 - Energy budgeting for decadal variability in GMST must derive from a defensible concept of the global surface ocean. In `MPI-ESM1.1`, defining the surface layer of the ocean as deeper than 100 m leads to a sharp decline in correlation between the energy budget and GMST changes.
 - By separating the global ocean heat uptake into regions, previous studies introduce spurious effects from horizontal heat transports, which do not directly influence the surface layer or GMST variability.
 - By failing to account for internal variability in the TOA, previous accounts overlook an important source of energy fluctuation for the surface layer.

1. b) **What can we learn from the hiatus about the origins of decadal internal variability in global mean surface temperature (GMST)?**

- Deviations like the hiatus can be caused by variability in the TOA imbalance, the subsurface ocean heat uptake, or both, even when the absolute TOA imbalance is positive.
- An event like the hiatus requires an energy flux deviation so small that current observations are unable to detect its origin. Depending on the definition of the hiatus, the expected flux deviation in the large ensemble varies between 0.02 and 0.08 Wm^{-2} , whereas observational uncertainty in the absolute TOA imbalance is closer to 8 Wm^{-2} .
- As observational networks improve and data amass, we may be able to detect the origins of these flux deviations. But the origin of the 1998–2012 hiatus may never be discovered.

4.2 CLIMATE SENSITIVITY AND THE PATTERN EFFECT

In Chapter 3, I investigated changing global climate feedbacks in four simulations over 1000 years, each with a different forcing strength associated with abrupt increases in CO_2 concentrations. I introduced a new framework for understanding regional contributions to global feedback changes, and used this framework to reconcile different theories about the pattern effect. I found the following answers to my research questions.

2. a) **How do differences between existing formulations of the pattern effect influence the interpretation of changes to equilibrium climate sensitivity (ECS)?**

- For several decades after an abrupt forcing increase, both changing warming patterns and changing regional feedbacks are important for correctly simulating global feedback changes in MPI-ESM1.2. Considering the warming pattern changes alone, such as in the formulation of Armour et al. (2013), produces a near-constant estimate of the global feedback parameter, although this parameter is clearly not constant in the simulations.
- Formulations of the pattern effect that fail to account for initial changes to both warming patterns and regional feedbacks misdiagnose the forcing and prevent direct comparison with other estimates of ECS.

2. b) **How does a regional framework help us position simulated estimates of ECS in relation to observed estimates?**

- On longer timescales, the patterns of warming lose significance. The changes to the ECS and global feedback parameter are rather associated with the increase in GMST and not its spatial pattern.
- Both time-dependence and state-dependence of ECS are useful concepts. The pattern effect in `MPI-ESM1.2` cannot be explained by state-dependence alone, but depends additionally on the time since the forcing increase. On the other hand, the long-term response to forcing is more clearly state-dependent.
- My results imply that the time-dependence of the pattern effect could influence observed estimates of ECS for decades to come, since forcing is currently increasing over time. If the results from `MPI-ESM1.2` are indicative of the Earth's true behaviour, a more reliable estimate of the current ECS could be better obtained from proxies of past climate than recent observations, since the latter are likely to be biased toward estimates that are too low.

4.3 KNOWLEDGE CONFLICTS AND KNOWLEDGE PRODUCTION

In the two subsections that follow, I integrate my main findings into the broader scientific context. In the first subsection I examine how the movement between regional and global perspectives can influence the production of knowledge. Depending on the object of investigation, a regional perspective can sharpen our vision, but it can also cause us to lose sight of the bigger picture.

In the second and final subsection, I return to the idea that I introduced in the first chapter, that conflicts between observations and climate models create critical spaces for knowledge production. Sometimes observations are interpreted as having a higher 'epistemic status' than models because they directly access reality, whereas models are abstract constructs. I make the case that climate modelling has allowed me to advance knowledge in ways that observations could not, and that observations and models are of equal epistemic value.

4.3.1 *The forest or the trees?*

When we move from the global to the regional perspective we are usually searching for greater detail. We may assume that by discovering where a phenomenon is located geographically, we are at least closer to explaining its cause. Indeed, sometimes the regional perspective gives us the power we need to see details that are opaque at the global level. But this is not always the case. The regional perspective can also cause us to lose focus on processes that are best explained at the global level. Sometimes, with a regional focus, we cannot see the forest for the trees.

The regional perspective has been used effectively in some hiatus studies, such as in the Pacific cooling experiment by Kosaka and Xie (2013). The authors were able to show how variability in the Pacific might have teleconnections to variability over a much larger area of the global. However, amongst studies that sought to establish the hiatus's true energetic origin, the regional perspective has led to a wild goose chase.

I showed in Chapter 2 how heat content changes in specific ocean regions can account for decadal changes in GMST neither during the hiatus nor more generally for surface temperature variability. The subsurface heat content in a particular region is not only altered by the exchange with the surface ocean, it is also altered by stronger heat fluxes in the horizontal direction. By only considering changes in regional ocean heat content, we lose sight of what we are truly looking for: the vertical heat exchange from surface to subsurface ocean.

Calculating the vertical heat exchange between surface and subsurface for any particular region may not even be feasible. Advective heat transfer in any direction can only be reliably calculated when the mass flux-divergence associated with the heat transfer is zero. Otherwise, the residual mass can be attributed any arbitrary heat content, depending on the temperature used to define zero. If we separate the ocean both vertically *and* horizontally, we create surfaces with a residual mass flux and therefore an arbitrary heat flux. The vertical heat flux can be inferred qualitatively using probabilistic methods (Zika et al. 2013), or calculated directly at the global level, where the residual mass fluxes cancel. In other words, for a definitive value of vertical heat exchange between surface and subsurface ocean, we *must* take the global perspective.

In Chapter 2, I returned to a simplified global perspective. This allowed me to find answers to fundamental questions about GMST variability that others had overlooked, such as how we should define the surface energy budget. My results show that the hiatus studies focussing on particular ocean regions have made budgeting choices – such as their definition of the surface layer and the deep ocean – that prevent them from correctly diagnosing the origins of hiatuses.

In the third chapter, the regional perspective is used very differently. In attempting to understand a changing climate sensitivity in models, taking up the regional perspective has not hindered knowledge gain but has instead contributed to it. Armour et al. (2013) showed that state-dependent feedbacks at the global level could in fact be the product of a regional weighting of spatially-varying local feedbacks according to the spatial warming pattern. Other work uses the regional perspective to expand upon Armour's theory (Rose et al. 2014; Rugenstein et al. 2016a).

However, in adopting the regional perspective, different studies have taken different approaches to determine what 'regional' means

for feedbacks: some regress the TOA imbalance against regional surface warming, and some against the GMST change. My results suggest that at least some of the conflicts in previous findings might simply be due to this variation in nomenclature. The framework I introduce in Chapter 3 clarifies the differences in these regional approaches, so that we can use the same nomenclature for studying the pattern effect.

Finally, I showed that the regional perspective might only be of limited usefulness for describing changes to the global feedback and climate sensitivity. In `MPI-ESM1.2` the long-term changes to climate sensitivity were *not* primarily related to the pattern of warming, but instead to the GMST change. There are some changes in feedback, such a rise in troposphere height, which spatial patterns in temperature cannot account for.

One might assume that switching from a global perspective to a regional perspective, or *vice versa*, is simply a re-ordering of information that should have no effect on the scientific outcome. This is not the case in practice. As I have shown here, the regional perspective can either sharpen our view, or lead us astray, depending on the object of investigation. When we progress from the global to the regional, we must do the scientific housekeeping necessary to make these two perspectives consistent with one another.

4.3.2 *Fairy-tale or fact?*

‘A model is a work of fiction’, wrote Nancy Cartwright in her philosophical treatise on the limits of science, *How the Laws of Physics Lie* (Cartwright 1983). Whereas Cartwright raised important questions about all kinds of models, including statistical models or physical laws, Oreskes et al. (1994) direct their critique specifically toward numerical simulations and the ability of simulations to access reality or produce recommendations for policy. Whether we choose to define ‘models’ in broader terms, or specifically as numerical simulations, the critiques from philosophers of science share commonalities. Models use assumptions and calibration data that can only account for behaviour of systems in special circumstances. Models therefore cannot be used to predict or explain complex systems that may evolve in ways that violate the assumptions or that deviate from past behaviour used to calibrate the model. Models may therefore be useful in a heuristic sense, but not for getting at ‘truth’ (Oreskes et al. 1994).

These claims are not merely theoretical exchanges between philosophers of science. Lewandowsky et al. (2015) have suggested that political discourses aiming to discredit climate science have even served to erode climate scientists’ trust in their very own modelling techniques.

It is therefore important to confront the arguments of Cartwright and Oreskes et al., since the problems I have addressed in this disser-

tation represent areas of conflict between models and observations. I argue here that models and observations are of equal epistemic value; both are crucial tools which assist in our pursuit of knowledge. In this dissertation, I have shown that the relationship between the two tools is not as straightforward as normative notions of models and observations might suggest.

In a strict sense, Cartwright and Oreskes et al. are correct: a climate model is just an imagined world. After all, the results of Chapter 2 are informed by simulating 100 alternate realities of how the Earth might have behaved in the past, but did not; and the results of Chapter 3 rely on four simulations of extreme climate change scenarios up to 1000 years into the future, of which we have no experience yet. We could interpret these uncharitably as mere fictions. On such a view, other forms of knowledge acquisition, such as observations, are superior because they are more ‘in contact with the system’ (Morrison 2009). They have a greater ability to access the truth – a higher ‘epistemic status’ – because they provide us with knowledge taken directly from reality and not mediated by theories, assumptions and reasoning that may be flawed.

Yet observations are also just flawed attempts to access truth. Observations of surface temperature have only recently begun to fill the gaps in key warming regions, such as at the poles and over Africa (Cowtan and Way 2014). Where temperature is measured, it is done inconsistently: over land using air temperature, but over the oceans using the water temperature. Water temperature is sometimes measured with ship buoys, and sometimes with ship engine intake thermometers, which both have different biases (Karl et al. 2015). We also learned in Chapter 2 that some observational instruments have large measurement uncertainties. The calibration error of the TOA imbalance is around 8 Wm^{-2} , an order of magnitude larger than the actual imbalance.

If we want to get at the truth by perfect means then we will have to throw out our imperfect observations along with our models and reduce our problems to simple, closed systems, finding answers of no particular use to anybody. If we discard perfection and the pursuit of idealised and unreachable truth, then we can generate knowledge through a process Hasok Chang calls ‘epistemic iteration’. Chang theorises that science progresses in a ‘spiral of self-improvement’: we respect prior standards, but do not expect those standards to explain everything, which leaves space for progress (Chang 2008).

Once we accept science as an imperfect, iterative progression, we can find infinitely more helpful ways of understanding our models than as mere works of fiction. Clarke and Primo (2012) conceive of models as similar to maps, asking not ‘is the map true or false?’, but rather ‘how can it be useful to us?’. Morrison (2009) suggests that computational simulations can attain the same epistemic status as

laboratory experiments, and that the latter only appear to be superior because of received notions of materiality.

I believe we can go one step further. In the course of researching this dissertation, I have come to appreciate the power of models precisely because they allow us to imagine. I am not talking about fiction, but rather an ‘informed imagining’, which I have repeatedly referred to as ‘simulation’ in this dissertation. When we ‘simulate’ with climate models we ‘imagine’ states of the climate, but we restrict our imagining with hard-won rules determined by the laws of motion, thermodynamics, fluid dynamics, conservation of mass, how to discretise those laws, and so forth. The resulting work is therefore not mere fiction but an informed and rule-bound (re)construction of how things could have been, or could be.

Albert Einstein said: ‘Knowledge is limited. Imagination encircles the world.’ (Viereck 1929). I object to this simplification, since knowledge informs imagination and the two can overlap. But Einstein’s words are an important reminder to value imagination or so-called ‘fictions’ in scientific practice for what they can *achieve* (Godfrey-Smith 2009). This applies to both models and observations, since there is know-how and imagination in the use of each.

My small contribution to this epistemological debate lies in recognising the way in which new knowledge has been generated by using simulations and observations in this dissertation. For example, in Chapter 2, I was able to simulate how the surface temperature could have behaved over 1998–2012 on 100 Earths, all under identical conditions, except for internal variability created by the proverbial flap of a butterfly’s wings. The simulations cannot reproduce precisely how 100 similar Earths would have behaved, but they don’t need to. The knowledge won from imagining this internal variability helped me gain insights about the surface energy balance that shed new light on empirical observations. These insights even allowed me to question claims made by observational studies, and to re-interpret the observational evidence as it stands.

In Chapter 3, I grappled with the pattern effect, which the current observations can describe only in limited ways (Gregory and Andrews 2016). I was able to simulate the ECS and explore its regional dimension over 1000 years into the future and at much higher temperatures than today, and compare behaviour across different potential pathways of warming. All these simulations cannot tell us how the Earth will actually behave in 1000 years’ time. But analysing the simulations did help me to question the superiority of observations over other evidence, such as palaeoclimate proxies, in estimating ECS. Treating simulated evidence as questionable because it fails to represent the observed reality (Lewis and Curry 2015) hinders our ability to imagine how warm our future might actually be.

It might be typical to assume that Chang's epistemic iteration goes in one direction – observations reveal facts about the true system that models misrepresent, so we improve the models. However, in this dissertation the process of creating knowledge has not been so linear. Simulations helped me to gain insights that either support a reinterpretation of the observations, or at least place them in a context of broader possibilities. We should always recognise the limits of our tools and our interpretations of them; they will never give us certainty in understanding surface warming. But the limitations of our scientific tools are emphasised repeatedly by climate change denialists, who have a disproportionate ability to shape public opinion on climate science. Let us therefore appreciate the contribution as well as the limitations of our work. Neither observations nor models are works of fiction, and nor are they perfect conduits of truth. They are simply the most powerful tools we possess at present for navigating and understanding the future of our changing climate.

APPENDICES

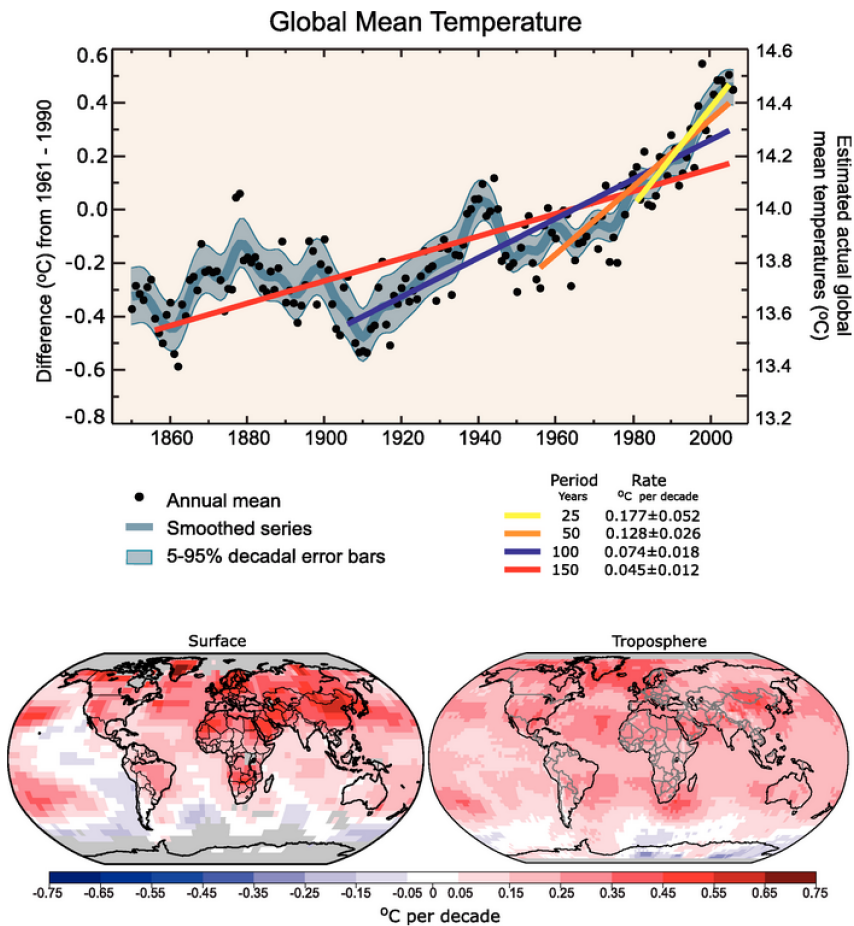


Figure A.1: FAQ3.1, IPCC ASSESSMENT REPORT 4. Figure reproduced completely and without alteration from Trenberth et al. (2007). The figure's original caption refers to the top panel and states: 'Note that for shorter recent periods, the slope is greater, indicating accelerated warming'. In 2007, when Assessment Report 4 was published, surface warming had in fact entered the surface-warming hiatus.

APPENDIX TO CHAPTER 2

B.1 DATA AVAILABILITY

The MPI-ESM1.1 model version was used to generate the large ensemble and is available at

<http://www.mpimet.mpg.de/en/science/models/mpi-esm.html>.

Computer code used in post-processing of raw data has been deposited with the Max Planck Society:

<http://pubman.mpg.de/pubman/faces/viewItemFullPage.jspx?itemId=escidoc:2353695>.

Raw data from the large ensemble were generated at the Swiss National Computing Centre (CSCS) and Deutsches Klimarechenzentrum (DKRZ) facilities. Derived data have been deposited with the Max Planck Society:

<http://pubman.mpg.de/pubman/faces/viewItemFullPage.jspx?itemId=escidoc:2353695>.

Figure 2.10 uses TOA flux reconstructions provided by R Allan (Allan et al. 2014; <http://www.met.reading.ac.uk/~sgs01c11/flux/>) and satellite observations provided by the NASA CERES project (Loeb et al. 2009; <http://ceres.larc.nasa.gov>). For observational estimates in Figure 2.8, I make use of data provided by the NOAA World Ocean Atlas (Levitus et al. 2012; https://www.nodc.noaa.gov/OC5/3M_HEAT_CONTENT/) and by the ECMWF Ocean Reanalysis System 4 (Balmaseda et al. 2013; <http://icdc.zmaw.de/projekte/easy-init/easy-init-ocean.html>).

B.2 EXTENDED FIGURES

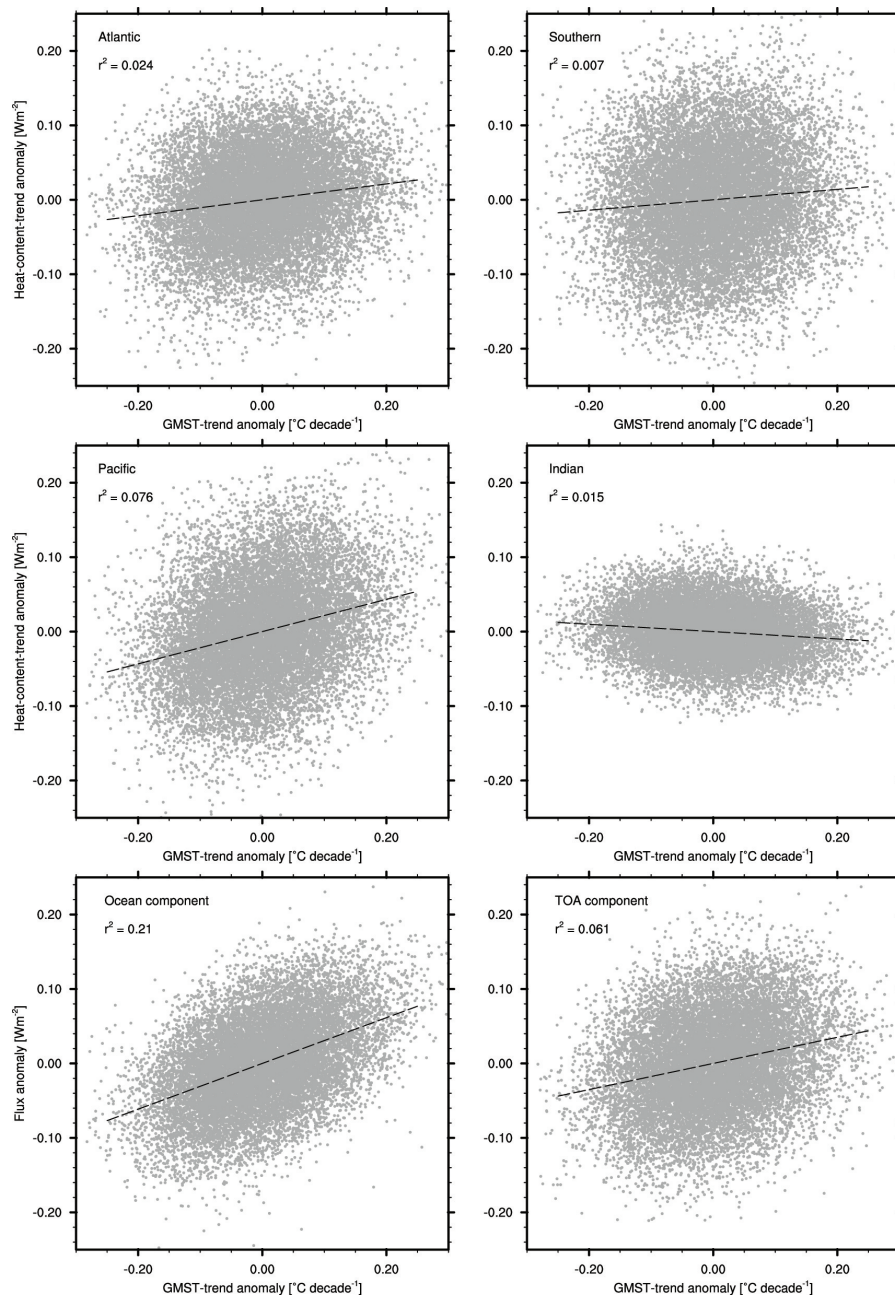


Figure B.1: POOR CORRELATION BETWEEN ENSEMBLE ANOMALIES IN GMST TRENDS AND HEAT-CONTENT TRENDS. Global mean surface temperature (GMST) trends in the 100-member historical ensemble are regressed against heat content trends below 100m in the Atlantic, Southern, Pacific and Indian Oceans, and the ocean and TOA components. The ocean component is the global ocean heat release to the layer above 100m. The TOA component is the top-of-atmosphere net radiative fluxes minus changes in total moist static energy in the atmosphere. Linear trends in heat content and GMST are calculated over a 15-year sliding window and converted to ensemble anomalies

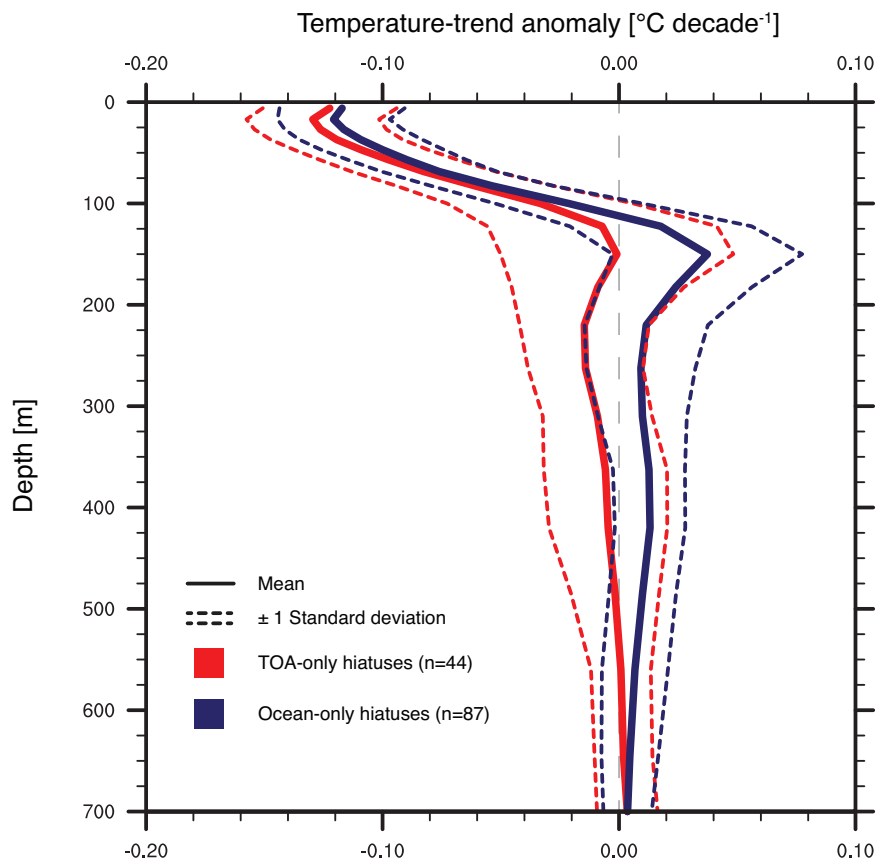


Figure B.2: BOTH TOA-ONLY HIATUSES AND OCEAN-ONLY HIATUSES CAN PRESENT SUB-SURFACE WARMING. Horizontally averaged ocean potential temperature during two types of hiatus in the large ensemble. TOA-only hiatuses (red) are hiatuses in which only the TOA provides a cooling contribution to the surface layer; ocean-only hiatuses (blue) are hiatuses in which only the ocean provides the cooling. The bold line shows the mean of each hiatus type, the dotted lines are ± 1 standard deviation. Linear trends in potential temperature are calculated over a 15-year sliding window and converted to ensemble anomalies.

START-YEAR	TOA-ONLY	OCEAN-ONLY	TOA-AND-OCEAN	TOTAL
1850–1887	10	25	65	100
1888–1925	13	18	57	88
1926–1963	13	19	57	89
1964–2001	8	25	54	87
Total	44	87	233	364

Table B.1: NUMBER OF HIATUSES SORTED BY ORIGIN AND START-YEAR IN THE 100-MEMBER HISTORICAL ENSEMBLE. Hiatuses are labelled ocean-only or TOA-only when only the ocean or the TOA component is responsible for the negative anomaly in the 15-year surface-layer flux-divergence. A TOA-and-ocean hiatus is where both components contribute to the negative anomaly. A Chi-square test of the contingency table yields no significant relationship between periods in time (rows) and origin type (columns), with a p-value of 0.73.

APPENDIX TO CHAPTER 3

C.1 DATA AVAILABILITY

The MPI-ESM1.2 model version was used to generate the four 1000-year integrations on the Deutsches Klimarechenzentrum (DKRZ) facilities. The model version is available at:

<http://www.mpimet.mpg.de/en/science/models/mpi-esm.html>.

BIBLIOGRAPHY

- Allan, R. P. et al. (2014). "Changes in global net radiative imbalance 1985-2012." *Geophysical Research Letters* 41.15, pp. 5588–5597. DOI: [10.1002/2014GL060962](https://doi.org/10.1002/2014GL060962).
- Andrews, T., J. M. Gregory, and M. J. Webb (2015). "The dependence of radiative forcing and feedback on evolving patterns of surface temperature change in climate models." *Journal of Climate* 28.4, pp. 1630–1648. DOI: [10.1175/JCLI-D-14-00545.1](https://doi.org/10.1175/JCLI-D-14-00545.1).
- Armour, K. C. (2017). "Energy budget constraints on climate sensitivity in light of inconstant climate feedbacks." *Nature Climate Change* 7.5, pp. 331–335. DOI: [10.1038/nclimate3278](https://doi.org/10.1038/nclimate3278).
- Armour, K. C., C. M. Bitz, and G. H. Roe (2013). "Time-Varying Climate Sensitivity from Regional Feedbacks." *Journal of Climate* 26.13, pp. 4518–4534. DOI: [10.1175/JCLI-D-12-00544.1](https://doi.org/10.1175/JCLI-D-12-00544.1).
- Arrhenius, S. (1896). "On the Influence of Carbonic Acid in the Air upon the Temperature of the Ground." *Philosophical Magazine and Journal of Science* 41.251, pp. 237–276.
- Baker, M. B. and G. H. Roe (2009). "The shape of things to come: Why is climate change so predictable?" *Journal of Climate* 22.17, pp. 4574–4589. DOI: [10.1175/2009JCLI2647.1](https://doi.org/10.1175/2009JCLI2647.1).
- Balmaseda, M. A., K. E. Trenberth, and E. Källén (2013). "Distinctive climate signals in reanalysis of global ocean heat content." *Geophysical Research Letters* 40.9, pp. 1754–1759. DOI: [10.1002/grl.50382](https://doi.org/10.1002/grl.50382).
- Bloch-Johnson, J., R. T. Pierrehumbert, and D. S. Abbot (2015). "Feedback temperature dependence determines the risk of high warming." *Geophysical Research Letters* 42.12, pp. 4973–4980. DOI: [10.1002/2015GL064240](https://doi.org/10.1002/2015GL064240).
- Block, K. and T. Mauritsen (2013). "Forcing and feedback in the MPI-ESM-LR coupled model under abruptly quadrupled CO₂." *Journal of Advances in Modeling Earth Systems* 5.4, pp. 676–691. DOI: [10.1002/jame.20041](https://doi.org/10.1002/jame.20041).
- Brown, P. T., W. Li, L. Li, and Y. Ming (2014). "Top-of-atmosphere radiative contribution to unforced decadal global temperature variability in climate models." *Geophysical Research Letters* 41, pp. 5175–5183. DOI: [10.1002/2014GL060625](https://doi.org/10.1002/2014GL060625).
- Byrne, M. P. and P. O’Gorman (2013). "Land-ocean warming contrast over a wide range of climates: Convective quasi-equilibrium theory and idealized simulations." *Journal of Climate* 26.12, pp. 4000–4016. DOI: [10.1175/JCLI-D-12-00262.1](https://doi.org/10.1175/JCLI-D-12-00262.1).
- Caballero, R. and M. Huber (2013). "State-dependent climate sensitivity in past warm climates and its implications for future climate

- projections." *Proceedings of the National Academy of Sciences of the United States of America* 110.35, pp. 14162–7. DOI: [10.1073/pnas.1303365110](https://doi.org/10.1073/pnas.1303365110).
- Cartwright, N. (1983). *How the Laws of Physics Lie*. Oxford: Clarendon Press.
- Ceppi, P., D. L. Hartmann, and M. J. Webb (2016). "Mechanisms of the Negative Shortwave Cloud Feedback in Middle to High Latitudes." *Journal of Climate* 29.1, pp. 139–157. DOI: [10.1175/JCLI-D-15-0327.1](https://doi.org/10.1175/JCLI-D-15-0327.1).
- Chang, H. (2008). *Inventing Temperature: Measurement and Scientific Progress*. New York: Oxford University Press.
- Chen, X. and K.-K. Tung (2014). "Varying planetary heat sink led to global-warming slowdown and acceleration." *Science* 345.6199, pp. 897–903. DOI: [10.1126/science.1254937](https://doi.org/10.1126/science.1254937).
- Choi, Y.-S., C.-H. Ho, C.-E. Park, T. Storelvmo, and I. Tan (2014). "Influence of cloud phase composition on climate feedbacks." *Journal of Geophysical Research: Atmospheres* 119.7, pp. 3687–3700. DOI: [10.1002/2013JD020582](https://doi.org/10.1002/2013JD020582).
- Clarke, K. A. and D. M. Primo (2012). *A Model Discipline: Political Science and the Logic of Representations*. New York: Oxford University Press.
- Cohen, J. L., J. C. Furtado, M. Barlow, V. A. Alexeev, and J. E. Cherry (2012). "Asymmetric seasonal temperature trends." *Geophysical Research Letters* 39.4, pp. 1–7. DOI: [10.1029/2011GL050582](https://doi.org/10.1029/2011GL050582).
- Colman, R and B. J. McAvaney (1997). "A study of general circulation model climate feedbacks determined from perturbed sea surface temperature experiments." *Journal of Geophysical Research: Atmospheres* 102.D16, pp. 19383–19402. DOI: [10.1029/97JD00206](https://doi.org/10.1029/97JD00206).
- Cowtan, K. and R. G. Way (2014). "Coverage bias in the HadCRUT4 temperature series and its impact on recent temperature trends." *Quarterly Journal of the Royal Meteorological Society* 140.683, pp. 1935–1944. DOI: [10.1002/qj.2297](https://doi.org/10.1002/qj.2297).
- Dai, A., J. C. Fyfe, S.-P. Xie, and X. Dai (2015). "Decadal modulation of global surface temperature by internal climate variability." *Nature Climate Change* 5.6, pp. 555–559. DOI: [10.1038/nclimate2605](https://doi.org/10.1038/nclimate2605).
- Dee, D. P. et al. (2014). "Toward a consistent reanalysis of the climate system." *Bulletin of the American Meteorological Society* 95.8, pp. 1235–1248. DOI: [10.1175/BAMS-D-13-00043.1](https://doi.org/10.1175/BAMS-D-13-00043.1).
- Drijfhout, S. S. et al. (2014). "Surface warming hiatus caused by increased heat uptake across multiple ocean basins." *Geophysical Research Letters* 41.22, pp. 7868–7874. DOI: [10.1002/2014GL061456](https://doi.org/10.1002/2014GL061456).
- England, M. H. et al. (2014). "Recent intensification of wind-driven circulation in the Pacific and the ongoing warming hiatus." *Nature Climate Change* 4.3, pp. 222–227. DOI: [10.1038/nclimate2106](https://doi.org/10.1038/nclimate2106).

- Feldl, N. and G. H. Roe (2013). "Four perspectives on climate feedbacks." *Geophysical Research Letters* 40.15, pp. 4007–4011. DOI: [10.1002/grl.50711](https://doi.org/10.1002/grl.50711).
- Flato, G. et al. (2013). "Evaluation of Climate Models." *Climate Change 2013: The Physical Science Basis*. Ed. by T. Stocker et al. Cambridge, United Kingdom: Cambridge University Press. Chap. 9, pp. 741–866.
- Fyfe, J. C., K. Von Salzen, J. N. S. Cole, N. P. Gillett, and J. P. Vernier (2013). "Surface response to stratospheric aerosol changes in a coupled atmosphere-ocean model." *Geophysical Research Letters* 40.3, pp. 584–588. DOI: [10.1002/grl.50156](https://doi.org/10.1002/grl.50156).
- Fyfe, J. C. et al. (2016). "Making sense of the early-2000s warming slowdown." *Nature Clim. Change* 6.3, pp. 224–228. DOI: [10.1038/nclimate2938](https://doi.org/10.1038/nclimate2938).
- Geoffroy, O. et al. (2013a). "Transient climate response in a two-layer energy-balance model. Part I: Analytical solution and parameter calibration using CMIP5 AOGCM experiments." *Journal of Climate* 26.6, pp. 1841–1857. DOI: [10.1175/JCLI-D-12-00195.1](https://doi.org/10.1175/JCLI-D-12-00195.1). arXiv: [0402594v3](https://arxiv.org/abs/0402594v3) [arXiv:cond-mat].
- Geoffroy, O. et al. (2013b). "Transient climate response in a two-layer energy-balance model. Part II: Representation of the efficacy of deep-ocean heat uptake and validation for CMIP5 AOGCMs." *Journal of Climate* 26.6, pp. 1859–1876. DOI: [10.1175/JCLI-D-12-00196.1](https://doi.org/10.1175/JCLI-D-12-00196.1).
- Giorgetta, M. A. et al. (2013). "Climate and carbon cycle changes from 1850 to 2100 in MPI-ESM simulations for the Coupled Model Intercomparison Project phase 5." *Journal of Advances in Modeling Earth Systems* 5.3, pp. 572–597. DOI: [10.1002/jame.20038](https://doi.org/10.1002/jame.20038).
- Godfrey-Smith, P. (2009). "Models and fictions in science." *Philosophical Studies* 143.1, pp. 101–116. DOI: [10.1007/s11098-008-9313-2](https://doi.org/10.1007/s11098-008-9313-2).
- Good, P., J. M. Gregory, and J. A. Lowe (2011). "A step-response simple climate model to reconstruct and interpret AOGCM projections." *Geophysical Research Letters* 38.1, n/a–n/a. DOI: [10.1029/2010GL045208](https://doi.org/10.1029/2010GL045208).
- Good, P., J. M. Gregory, J. A. Lowe, and T. Andrews (2013). "Abrupt CO₂ experiments as tools for predicting and understanding CMIP5 representative concentration pathway projections." *Climate Dynamics* 40.3-4, pp. 1041–1053. DOI: [10.1007/s00382-012-1410-4](https://doi.org/10.1007/s00382-012-1410-4).
- Gregory, J. M. and T Andrews (2016). "Variation in climate sensitivity and feedback parameters during the historical period." *Geophysical Research Letters* 43.8, pp. 3911–3920. DOI: [10.1002/2016GL068406](https://doi.org/10.1002/2016GL068406).
- Gregory, J. M. et al. (2004). "A new method for diagnosing radiative forcing and climate sensitivity." *Geophysical Research Letters* 31.3, p. L03205. DOI: [10.1029/2003GL018747](https://doi.org/10.1029/2003GL018747).

- Guemas, V., F. J. Doblas-Reyes, I. Andreu-Burillo, and M. Asif (2013). "Retrospective prediction of the global warming slowdown in the past decade." *Nature Climate Change* 3.4, pp. 1–5. DOI: [10.1038/nclimate1863](https://doi.org/10.1038/nclimate1863).
- Hansen, J. et al. (2005). "Efficacy of climate forcings." *Journal of Geophysical Research D: Atmospheres* 110.18, pp. 1–45. DOI: [10.1029/2005JD005776](https://doi.org/10.1029/2005JD005776).
- Hargreaves, J. C. and J. D. Annan (2016). "Could the Pliocene constrain the equilibrium climate sensitivity?" *Climate of the Past* 12.8, pp. 1591–1599. DOI: [10.5194/cp-12-1591-2016](https://doi.org/10.5194/cp-12-1591-2016).
- Hargreaves, J. C., J. D. Annan, M. Yoshimori, and A. Abe-Ouchi (2012). "Can the Last Glacial Maximum constrain climate sensitivity?" *Geophysical Research Letters* 39.24, pp. 1–5. DOI: [10.1029/2012GL053872](https://doi.org/10.1029/2012GL053872).
- Hartmann, D. J. et al. (2013). "Observations: Atmosphere and Surface Supplementary Material." *Climate Change 2013: The Physical Science Basis. Contribution of Working Group I to the Fifth Assessment Report of the Intergovernmental Panel on Climate Change*. Ed. by T. F. Stocker et al., pp. 159–254. DOI: [10.1017/CB09781107415324.008](https://doi.org/10.1017/CB09781107415324.008).
- Haywood, J. M., A. Jones, and G. S. Jones (2014). "The impact of volcanic eruptions in the period 2000–2013 on global mean temperature trends evaluated in the HadGEM2-ES climate model." *Atmospheric Science Letters* 15.2, pp. 92–96. DOI: [10.1002/asl2.471](https://doi.org/10.1002/asl2.471).
- Hedemann, C., T. Mauritsen, J. Jungclaus, and J. Marotzke (2017). "The subtle origins of surface-warming hiatuses." *Nature Climate Change* 7.5, pp. 336–339. DOI: [10.1038/nclimate3274](https://doi.org/10.1038/nclimate3274).
- Held, I. M. et al. (2010). "Probing the Fast and Slow Components of Global Warming by Returning Abruptly to Preindustrial Forcing." *Journal of Climate* 23.9, pp. 2418–2427. DOI: [10.1175/2009JCLI3466.1](https://doi.org/10.1175/2009JCLI3466.1).
- Huber, M. and R. Caballero (2011). "The early Eocene equable climate problem revisited." *Climate of the Past* 7.2, pp. 603–633. DOI: [10.5194/cp-7-603-2011](https://doi.org/10.5194/cp-7-603-2011).
- Huntingford, C. and P. M. Cox (2000). "An analogue model to derive additional climate change scenarios from existing GCM simulations." *Climate Dynamics* 16.8, pp. 575–586. DOI: [10.1007/s003820000067](https://doi.org/10.1007/s003820000067).
- Johnson, G. C., J. M. Lyman, and N. G. Loeb (2016). "Improving estimates of Earth's energy imbalance." *Nature Climate Change* 6.7, pp. 639–640. DOI: [10.1038/nclimate3043](https://doi.org/10.1038/nclimate3043).
- Jonko, A. K., K. M. Shell, B. M. Sanderson, and G. Danabasoglu (2012). "Climate Feedbacks in CCSM3 under Changing CO₂ Forcing. Part I: Adapting the Linear Radiative Kernel Technique to Feedback Calculations for a Broad Range of Forcings." *Journal of Climate* 25.15, pp. 5260–5272. DOI: [10.1175/JCLI-D-11-00524.1](https://doi.org/10.1175/JCLI-D-11-00524.1).
- Jungclaus, J. H. et al. (2013a). "Characteristics of the ocean simulations in the Max Planck Institute Ocean Model (MPIOM) the ocean component of the MPI-Earth system model." *Journal of Ad-*

- vances in Modeling Earth Systems* 5.2, pp. 422–446. DOI: [10.1002/jame.20023](https://doi.org/10.1002/jame.20023).
- Jungclaus, J. et al. (2013b). *CMIP5 simulations of the Max Planck Institute for Meteorology (MPI-M) based on the MPI-ESM-LR model: The decadal2000 experiment, served by ESGF*. DOI: [10.1594/WDC/CMIP5.MXEL00](https://doi.org/10.1594/WDC/CMIP5.MXEL00).
- Karl, T. R. et al. (2015). “Possible artifacts of data biases in the recent global surface warming hiatus.” *Science* 348.6242, pp. 1469–72. DOI: [10.1126/science.aaa5632](https://doi.org/10.1126/science.aaa5632).
- Katsman, C. A. C., G. van Oldenborgh, and G. J. van Oldenborgh (2011). “Tracing the upper ocean’s “missing heat”.” *Geophysical Research Letters* 38.14, n/a–n/a. DOI: [10.1029/2011GL048417](https://doi.org/10.1029/2011GL048417).
- Kay, J. E. et al. (2014). “Processes controlling Southern Ocean short-wave climate feedbacks in CESM.” *Geophysical Research Letters* 41.2, pp. 616–622. DOI: [10.1002/2013GL058315](https://doi.org/10.1002/2013GL058315).
- Kopp, G. and J. L. Lean (2011). “A new, lower value of total solar irradiance: Evidence and climate significance.” *Geophysical Research Letters* 38.1, pp. 1–7. DOI: [10.1029/2010GL045777](https://doi.org/10.1029/2010GL045777).
- Kosaka, Y. and S.-P. Xie (2013). “Recent global-warming hiatus tied to equatorial Pacific surface cooling.” *Nature* 501.7467, pp. 403–7. DOI: [10.1038/nature12534](https://doi.org/10.1038/nature12534).
- Kutzbach, J. E., F. He, S. J. Vavrus, and W. F. Ruddiman (2013). “The dependence of equilibrium climate sensitivity on climate state: Applications to studies of climates colder than present.” *Geophysical Research Letters* 40.14, pp. 3721–3726. DOI: [10.1002/grl.50724](https://doi.org/10.1002/grl.50724).
- Lee, S.-K. et al. (2015). “Pacific origin of the abrupt increase in Indian Ocean heat content during the warming hiatus.” *Nature Geoscience* 8.6, pp. 445–449. DOI: [10.1038/ngeo2438](https://doi.org/10.1038/ngeo2438).
- Levitus, S. et al. (2012). “World ocean heat content and thermosteric sea level change (0–2000 m), 1955–2010.” *Geophysical Research Letters* 39.10. DOI: [10.1029/2012GL051106](https://doi.org/10.1029/2012GL051106).
- Lewandowsky, S., N. Oreskes, J. S. Risbey, B. R. Newell, and M. Smithson (2015). “Seepage: Climate change denial and its effect on the scientific community.” *Global Environmental Change* 33, pp. 1–13. DOI: [10.1016/j.gloenvcha.2015.02.013](https://doi.org/10.1016/j.gloenvcha.2015.02.013).
- Lewis, N. and J. A. Curry (2015). “The implications for climate sensitivity of AR5 forcing and heat uptake estimates.” *Climate Dynamics* 45.3–4, pp. 1009–1023. DOI: [10.1007/s00382-014-2342-y](https://doi.org/10.1007/s00382-014-2342-y).
- Li, C., J.-S. Storch, and J. Marotzke (2013). “Deep-ocean heat uptake and equilibrium climate response.” *Climate Dynamics* 40.5–6, pp. 1071–1086. DOI: [10.1007/s00382-012-1350-z](https://doi.org/10.1007/s00382-012-1350-z).
- Li, C., B. Stevens, and J. Marotzke (2015). “Eurasian winter cooling in the warming hiatus of 1998–2012.” *Geophysical Research Letters* 42.19, pp. 8131–8139. DOI: [10.1002/2015GL065327](https://doi.org/10.1002/2015GL065327).
- Li, G. and S. P. Xie (2014). “Tropical biases in CMIP5 multimodel ensemble: The excessive equatorial Pacific cold tongue and dou-

- ble ITCZ problems." *Journal of Climate* 27.4, pp. 1765–1780. DOI: [10.1175/JCLI-D-13-00337.1](https://doi.org/10.1175/JCLI-D-13-00337.1).
- Liu, W., S.-P. Xie, and J. Lu (2016). "Tracking ocean heat uptake during the surface warming hiatus." *Nature Communications* 7, p. 10926. DOI: [10.1038/ncomms10926](https://doi.org/10.1038/ncomms10926).
- Loeb, N. G. et al. (2009). "Toward optimal closure of the Earth's top-of-atmosphere radiation budget." *Journal of Climate* 22.3, pp. 748–766. DOI: [10.1175/2008JCLI2637.1](https://doi.org/10.1175/2008JCLI2637.1).
- Maher, N., A. S. Gupta, and M. H. England (2014). "Drivers of decadal hiatus periods in the 20th and 21st centuries." *Geophysical Research Letters* 41.16, pp. 5978–5986. DOI: [10.1002/2014GL060527](https://doi.org/10.1002/2014GL060527).
- Manabe, S. and R. T. Wetherald (1967). *Thermal Equilibrium of the Atmosphere with a Given Distribution of Relative Humidity*. DOI: [10.1175/1520-0469\(1967\)024<0241:TEOTAW>2.0.CO;2](https://doi.org/10.1175/1520-0469(1967)024<0241:TEOTAW>2.0.CO;2).
- Marotzke, J. and P. M. Forster (2015). "Forcing, feedback and internal variability in global temperature trends." *Nature* 517.7536, pp. 565–570. DOI: [10.1038/nature14117](https://doi.org/10.1038/nature14117).
- Marvel, K., G. A. Schmidt, R. L. Miller, and L. S. Nazarenko (2015). "Implications for climate sensitivity from the response to individual forcings." *Nature Climate Change* 6.4, pp. 386–389. DOI: [10.1038/nclimate2888](https://doi.org/10.1038/nclimate2888).
- Mauritsen, T. and R. Pincus (2017). "Committed warming inferred from observations." *Submitted*.
- Mauritsen, T. et al. (2012). "Tuning the climate of a global model." *Journal of Advances in Modeling Earth Systems* 4.M00A01. DOI: [10.1029/2012MS000154](https://doi.org/10.1029/2012MS000154).
- McCoy, D. T., D. L. Hartmann, M. D. Zelinka, P. Ceppi, and D. P. Grosvenor (2015). "Mixed-phase cloud physics and Southern Ocean cloud feedback in climate models." *Journal of Geophysical Research: Atmospheres* 120.18, pp. 9539–9554. DOI: [10.1002/2015JD023603](https://doi.org/10.1002/2015JD023603).
- Meehl, G. A., J. M. Arblaster, J. T. Fasullo, A. Hu, and K. E. Trenberth (2011). "Model-based evidence of deep-ocean heat uptake during surface-temperature hiatus periods." *Nature Climate Change* 1.7, pp. 360–364. DOI: [10.1038/nclimate1229](https://doi.org/10.1038/nclimate1229).
- Meehl, G. A., A. Hu, J. M. Arblaster, J. Fasullo, and K. E. Trenberth (2013). "Externally Forced and Internally Generated Decadal Climate Variability Associated with the Interdecadal Pacific Oscillation." *Journal of Climate* 26.18, pp. 7298–7310. DOI: [10.1175/JCLI-D-12-00548.1](https://doi.org/10.1175/JCLI-D-12-00548.1).
- Meraner, K., T. Mauritsen, and A. Voigt (2013). "Robust increase in equilibrium climate sensitivity under global warming." *Geophysical Research Letters* 40.22, pp. 5944–5948. DOI: [10.1002/2013GL058118](https://doi.org/10.1002/2013GL058118).
- Morice, C. P., J. J. Kennedy, N. a. Rayner, and P. D. Jones (2012). "Quantifying uncertainties in global and regional temperature change using an ensemble of observational estimates: The Had-

- CRUT4 data set." *Journal of Geophysical Research: Atmospheres* 117.8, pp. 1–22. DOI: [10.1029/2011JD017187](https://doi.org/10.1029/2011JD017187).
- Morrison, M. (2009). "Models, measurement and computer simulation: the changing face of experimentation." *Philosophical Studies* 143.1, pp. 33–57. DOI: [10.1007/s11098-008-9317-y](https://doi.org/10.1007/s11098-008-9317-y).
- Mueller, B. and S. I. Seneviratne (2014). "Systematic land climate and evapotranspiration biases in CMIP5 simulations." *Geophysical Research Letters* 41.1, pp. 128–134. DOI: [10.1002/2013GL058055](https://doi.org/10.1002/2013GL058055).
- Myhre, G. et al. (2013). "Anthropogenic and Natural Radiative Forcing." *Climate Change 2013: The Physical Science Basis. Contribution of Working Group I to the Fifth Assessment Report of the Intergovernmental Panel on Climate Change*. Ed. by T. Stocker et al. Cambridge, United Kingdom: Cambridge University Press, pp. 659–740. DOI: [10.1017/CB09781107415324.018](https://doi.org/10.1017/CB09781107415324.018). arXiv: [arXiv:1011.1669v3](https://arxiv.org/abs/1011.1669v3).
- Nieves, V., J. K. Willis, and W. C. Patzert (2015). "Recent hiatus caused by decadal shift in Indo-Pacific heating." *Science* 349.6247, pp. 532–535. DOI: [10.1126/science.aaa4521](https://doi.org/10.1126/science.aaa4521).
- Oreskes, N., K. Shrader-Frechette, and K. Belitz (1994). "Verification, Validation, and Confirmation of Numerical Models in the Earth Sciences." *Science* 263, February, pp. 641–646. DOI: [10.1126/science.263.5147.641](https://doi.org/10.1126/science.263.5147.641).
- Otto, A. et al. (2013). "Energy budget constraints on climate response." *Nature Geoscience* 6.6, pp. 415–416. DOI: [10.1038/ngeo1836](https://doi.org/10.1038/ngeo1836).
- Palmer, M. D. and D. J. McNeall (2014). "Internal variability of Earth's energy budget simulated by CMIP5 climate models." *Environmental Research Letters* 9.3, p. 034016. DOI: [10.1088/1748-9326/9/3/034016](https://doi.org/10.1088/1748-9326/9/3/034016).
- Popp, M., H. Schmidt, and J. Marotzke (2016). "Transition to a Moist Greenhouse with CO₂ and solar forcing." *Nature Communications* 7, p. 10627. DOI: [10.1038/ncomms10627](https://doi.org/10.1038/ncomms10627).
- Power, S., T. Casey, C. Folland, A. Colman, and V. Mehta (1999). "Inter-decadal modulation of the impact of ENSO on Australia." *Climate Dynamics* 15.5, pp. 319–324. DOI: [10.1007/s003820050284](https://doi.org/10.1007/s003820050284).
- Purkey, S. G. and G. C. Johnson (2010). "Warming of global abyssal and deep Southern Ocean waters between the 1990s and 2000s: Contributions to global heat and sea level rise budgets." *Journal of Climate* 23, pp. 6336–6351. DOI: [10.1175/2010JCLI3682.1](https://doi.org/10.1175/2010JCLI3682.1).
- Ridley, D. A. et al. (2014). "Total volcanic stratospheric aerosol optical depths and implications for global climate change." *Geophysical Research Letters* 41.22, pp. 7763–7769. DOI: [10.1002/2014GL061541](https://doi.org/10.1002/2014GL061541).
- Rohling, E. et al. (2012). "Making sense of palaeoclimate sensitivity." *Nature* 491.V, pp. 0–9. DOI: [10.1038/nature11574](https://doi.org/10.1038/nature11574).
- Rose, B. E. J. and L. Rayborn (2016). "The Effects of Ocean Heat Uptake on Transient Climate Sensitivity." *Current Climate Change Reports*, pp. 1–12. DOI: [10.1007/s40641-016-0048-4](https://doi.org/10.1007/s40641-016-0048-4).

- Rose, B. E. J., K. C. Armour, D. S. Battisti, N. Feldl, and D. D. B. Koll (2014). "The dependence of transient climate sensitivity and radiative feedbacks on the spatial pattern of ocean heat uptake." *Geophysical Research Letters* 41.3, pp. 1071–1078. DOI: [10.1002/2013GL058955](https://doi.org/10.1002/2013GL058955).
- Royer, D. L. (2016). "Climate Sensitivity in the Geologic Past." *Annual Review of Earth and Planetary Sciences* 44.1, pp. 277–293. DOI: [10.1146/annurev-earth-100815-024150](https://doi.org/10.1146/annurev-earth-100815-024150).
- Rugenstein, M. A. A., K. Caldeira, and R. Knutti (2016a). "Dependence of global radiative feedbacks on evolving patterns of surface heat fluxes." *Geophysical Research Letters* 43.18, pp. 9877–9885. DOI: [10.1002/2016GL070907](https://doi.org/10.1002/2016GL070907).
- Rugenstein, M. A. A., J. M. Gregory, N. Schaller, J. Sedláček, and R. Knutti (2016b). "Multi-annual ocean-atmosphere adjustments to radiative forcing." *Journal of Climate* 29.15, pp. 5643–5659. DOI: [10.1175/JCLI-D-16-0312.1](https://doi.org/10.1175/JCLI-D-16-0312.1).
- Santer, B. D. et al. (2008). "Consistency of modelled and observed temperature trends in the tropical troposphere." *International Journal of Climatology* 28, pp. 1703–1722. DOI: [10.1002/joc.1756](https://doi.org/10.1002/joc.1756).
- Santer, B. D. et al. (2014). "Volcanic contribution to decadal changes in tropospheric temperature." *Nature Geoscience* 7.3, pp. 185–189. DOI: [10.1038/NGEO2098](https://doi.org/10.1038/NGEO2098).
- Schmidt, G. a., D. T. Shindell, and K. Tsigaridis (2014). "Reconciling warming trends." *Nature Geoscience* 7.3, pp. 158–160. DOI: [10.1038/ngeo2105](https://doi.org/10.1038/ngeo2105).
- Schuckmann, K. von et al. (2016). "An imperative to monitor Earth's energy imbalance." *Nature Climate Change* 6.2, pp. 138–144. DOI: [10.1038/nclimate2876](https://doi.org/10.1038/nclimate2876).
- Sen Gupta, A., N. C. Jourdain, J. N. Brown, and D. Monselesan (2013). "Climate drift in the CMIP5 models." *Journal of Climate* 26.21, pp. 8597–8615. DOI: [10.1175/JCLI_D_12_00521.1](https://doi.org/10.1175/JCLI_D_12_00521.1).
- Senior, C. A. and J. F. B. Mitchell (2000). "The time-dependence of climate sensitivity." *Geophysical Research Letters* 27.17, pp. 2685–2688. DOI: [10.1029/2000GL011373](https://doi.org/10.1029/2000GL011373).
- Shaffer, G., M. Huber, R. Rondanelli, and J. O. Pepke Pedersen (2016). "Deep time evidence for climate sensitivity increase with warming." *Geophysical Research Letters* 43.12, pp. 6538–6545. DOI: [10.1002/2016GL069243](https://doi.org/10.1002/2016GL069243).
- Siongco, A. C., C. Hohenegger, and B. Stevens (2014). "The Atlantic ITCZ bias in CMIP5 models." *Climate Dynamics* 45.5-6, pp. 1169–1180. DOI: [10.1007/s00382-014-2366-3](https://doi.org/10.1007/s00382-014-2366-3).
- Smith, D. M. et al. (2015). "Earth's energy imbalance since 1960 in observations and CMIP5 models." *Geophysical Research Letters* 42.4, pp. 1205–1213. DOI: [10.1002/2014GL062669](https://doi.org/10.1002/2014GL062669).

- Solomon, S et al. (2011). "The persistently variable "background" stratospheric aerosol layer and global climate change." *Science* 333.6044, pp. 866–870. DOI: [10.1126/science.1206027](https://doi.org/10.1126/science.1206027).
- Stephens, G. L. et al. (2015). "The albedo of Earth." *Reviews of Geophysics* 53.1, pp. 141–163. DOI: [10.1002/2014RG000449](https://doi.org/10.1002/2014RG000449).
- Stevens, B. et al. (2013). "Atmospheric component of the MPI-M Earth System Model: ECHAM6." *Journal of Advances in Modeling Earth Systems* 5.2, pp. 1–27. DOI: [10.1002/jame.20015](https://doi.org/10.1002/jame.20015).
- Stevens, B., S. C. Sherwood, S. Bony, and M. J. Webb (2016). "Prospects for narrowing bounds on Earth's equilibrium climate sensitivity." *Earth's Future* 4.11, pp. 512–522. DOI: [10.1002/2016EF000376](https://doi.org/10.1002/2016EF000376).
- Tan, I., T. Storelvmo, and M. D. Zelinka (2016). "Observational constraints on mixed-phase clouds imply higher climate sensitivity." *Science* 352.6282, pp. 224–227. DOI: [10.1126/science.aad5300](https://doi.org/10.1126/science.aad5300).
- Taylor, K. E., R. J. Stouffer, and G. A. Meehl (2012). "An Overview of CMIP5 and the Experiment Design." *Bulletin of the American Meteorological Society* 93.4, pp. 485–498. DOI: [10.1175/BAMS-D-11-00094.1](https://doi.org/10.1175/BAMS-D-11-00094.1).
- Thorne, P., S. Outten, I. Bethke, and Ø. Seland (2015). "Investigating the recent apparent hiatus in surface temperature increases: 2. Comparison of model ensembles to observational estimates." *Journal of Geophysical Research: Atmospheres* 120.17, pp. 8597–8620. DOI: [10.1002/2014JD022805](https://doi.org/10.1002/2014JD022805).
- Trenberth, K. et al. (2007). "Observations: surface and atmospheric climate change." *Climate Change 2007: The Physical Science Basis*. Ed. by S. Solomon et al. Vol. 164. 236 - 336. Cambridge, United Kingdom: Cambridge University Press, pp. 235–336. DOI: [10.5194/cp-6-379-2010](https://doi.org/10.5194/cp-6-379-2010). arXiv: [arXiv:1011.1669v3](https://arxiv.org/abs/1011.1669v3).
- Trenberth, K. E. and J. T. Fasullo (2013). "An apparent hiatus in global warming?" *Earth's Future* 1.1, pp. 19–32. DOI: [10.1002/2013EF000165](https://doi.org/10.1002/2013EF000165).
- Trenberth, K. E., J. T. Fasullo, and M. A. Balmaseda (2014). "Earth's Energy Imbalance." *Journal of Climate* 27.9, pp. 3129–3144. DOI: [10.1175/JCLI-D-13-00294.1](https://doi.org/10.1175/JCLI-D-13-00294.1).
- Viereck, G. S. (1929). "What Life Means to Einstein: An Interview by George Sylvester Viereck." *The Saturday Evening Post*, 1929 October 26. Indianapolis, Indiana: The Saturday Evening Post Society, p. 117. DOI: http://www.saturdayeveningpost.com/wp-content/uploads/satevepost/what_life_means_to_einstein.pdf.
- Wang, C., L. Zhang, S.-K. Lee, L. Wu, and C. R. Mechoso (2014). "A global perspective on CMIP5 climate model biases." *Nature Climate Change* 4.3, pp. 201–205. DOI: [10.1038/nclimate2118](https://doi.org/10.1038/nclimate2118).
- Watanabe, M. et al. (2013). "Strengthening of ocean heat uptake efficiency associated with the recent climate hiatus." *Geophysical Research Letters* 40.12, pp. 3175–3179. DOI: [10.1002/grl.50541](https://doi.org/10.1002/grl.50541).

- Wetherald, R. T. and S. Manabe (1988). "Cloud Feedback Processes in a General Circulation Model." *Journal of the Atmospheric Sciences* 45.8, pp. 1397–1416.
- Williams, C. N., M. J. Menne, and P. W. Thorne (2012). "Benchmarking the performance of pairwise homogenization of surface temperatures in the United States." *Journal of Geophysical Research: Atmospheres* 117.D05116, pp. 1–16. DOI: [10.1029/2011JD016761](https://doi.org/10.1029/2011JD016761).
- Williams, K. D., W. J. Ingram, and J. M. Gregory (2008). "Time variation of effective climate sensitivity in GCMs." *Journal of Climate* 21.19, pp. 5076–5090. DOI: [10.1175/2008JCLI2371.1](https://doi.org/10.1175/2008JCLI2371.1).
- Winton, M., K. Takahashi, and I. M. Held (2010). "Importance of Ocean Heat Uptake Efficacy to Transient Climate Change." *Journal of Climate* 23.9, pp. 2333–2344. DOI: [10.1175/2009JCLI3139.1](https://doi.org/10.1175/2009JCLI3139.1).
- Yan, X.-H. et al. (2016). "The global warming hiatus: Slowdown or redistribution?" *Earth's Future* 4, pp. 1–11. DOI: [10.1002/2016EF000417](https://doi.org/10.1002/2016EF000417).
- Zachos, J. C. et al. (2003). "A Transient Rise in Tropical Sea Surface Temperature during the Paleocene-Eocene Thermal Maximum." *Science* 302.5650, pp. 1551–1554. DOI: [10.1126/science.1090110](https://doi.org/10.1126/science.1090110).
- Zhou, C., M. D. Zelinka, and S. A. Klein (2016). "Impact of decadal cloud variations on the Earth's energy budget." *Nature Geoscience* 9.12, pp. 871–874. DOI: [10.1038/ngeo2828](https://doi.org/10.1038/ngeo2828).
- Zika, J. D., W. P. Sijp, and M. H. England (2013). "Vertical Heat Transport by Ocean Circulation and the Role of Mechanical and Haline Forcing." *Journal of Physical Oceanography* 43.10, pp. 2095–2112. DOI: [10.1175/JPO-D-12-0179.1](https://doi.org/10.1175/JPO-D-12-0179.1).

EIDESSTATTLICHE VERSICHERUNG
Declaration by Author

Hiermit erkläre ich an Eides statt, dass ich die vorliegende Dissertationsschrift selbst verfasst und keine anderen als die angegebenen Quellen und Hilfsmittel benutzt habe.

I hereby declare that this thesis is composed of my original work, and contains no material previously published or written by another person except where due reference has been made in the text.

Hamburg,

Christopher Hedemann